Mechanism of proteasome-mediated processing of proteins

Dissertation der
Fakultät für Biologie der
Ludwig-Maximilians-Universität
München

vorgelegt von
Diplom-Biotechnologe
Wojciech Piwko

5. März 2007

Ehrenwörtliche Erklärung

Hiermit erkläre ich, dass ich die vorliegende Dissertation selbständig und ohne unerlaubte Hilfe angefertigt habe. Ich habe weder anderweitig versucht, eine Dissertation einzureichen oder eine Doktorprüfung durchzuführen, noch habe ich diese Dissertation oder Teile derselben einer anderen Prüfungskommission vorgelegt.

München, den 5.03.2007

Promotionsgesuch eingereicht am 05.03.2007

Tag der mundlichen Prüfung: 27.04.2007

Erster Gutachter: Prof. Dr. Stefan Jentsch

Zweiter Gutachter: Prof. Dr. Peter B. Becker

Die vorliegende Arbeit wurde zwischen Dezember 2001 und November 2006 unter der Anleitung von Prof. Dr. Stefan Jentsch am Max-Planck-Institut für Biochemie, Martinsried durchgeführt.

Wesentliche Teile dieser Arbeit sind in folgender Publikation veröffentlicht:

Piwko, W., and Jentsch, S. (2006). Proteasome-mediated protein processing by bidirectional degradation initiated from an internal site. Nat Struct Mol Biol *13*, 691-697.

Table of contents

Summary 1

1. Introduction 2

1.1. The ubiquitin/proteasome proteolytic pathway 2

1.1.1. Enzymatic cascade for ubiquitin conjugation 2

1.1.2. E3 ligases determine substrate specificity 3

1.1.3. Regulation of ubiquitin conjugation to substrates 5

1.1.4. The mode of ubiquitylation determines the fate of a conjugated substrate 8

1.1.5. Composition and structure of the 26S proteasome complex 9

1.1.6. Recognition and degradation of substrates by the 26S proteasome 11

1.2. Limited proteolysis of proteins 14

1.2.1. Proteasome-independent processing of proteins 14

1.2.2. Partial degradation of proteins by the proteasome 16

1.3. The OLE pathway 20

1.4. Aim of this work 23

2. Results 24

2.1. Mechanism of Spt23/Mga2 partial degradation 24

2.1.1. Processing initiates from an internal site 24

2.1.2. Processing intermediates are trapped in proteasome mutants 27

2.1.3. Mapping of the processing initiation site 30

2.1.4. The IPT domain stops proteasome degradation progression 33

2.1.5. Complete degradation can be initiated internally 35

2.2. Regulation of Spt23/Mga2 activation by the ankyrin repeat domain 38

2.2.1. The ankyrin repeat domain interacts with the dimerization domain of Mga2 38

2.2.2. Deletion of the ankyrin repeat domain destabilizes Mga2 42

2.2.3. Deletion of the ankyrin repeat domain leads to enhanced activation of Mga2 43

2.2.4. The ankyrin repeat domain controls localization of Mga2 44

2.2.5. Degradation of Mga2 p120 and release of p90 is inhibited by the ankyrin repeat domain 46

2.2.6. The ankyrin repeat domain inhibits processing of Mga2ΔTM 50

3. Discussion **54**

3.1. Proteolytic systems for processing of proteins **54**

3.2. Mechanism of proteasomal processing of Spt23/Mga2 **56**

3.2.1. Initiation signal for processing of Spt23/Mga2 56

3.2.2. Processing of Spt23/Mga2 initiates at an internal site 57

3.2.3. Formation of a flexible loop for processing initiation 61

3.2.4. Regulation of loop formation by the ankyrin repeat domain of Mga2 62

3.2.5. Mechanism of limited proteasomal degradation 66

3.3. Regulation of the OLE pathway by the ubiquitin/proteasome system **68**

3.4. Complete degradation and processing of substrates by the proteasome **72**

4. Materials and methods **75**

References **92**

Abbreviations **101**

Acknowledgements

Curriculum vitae

Summary

The ubiquitin/proteasome system is the main cytosolic and nuclear proteolytic system of eukaryotic cells, regulating a multitude of important cellular processes by controlling protein levels. The proteasome is a highly processive enzyme that usually degrades substrates to small peptides. However, some proteins evolved mechanisms allowing them to escape complete degradation. These substrates engage the proteasome to activate intrinsic dormant functions by processing their inactive precursors.

This study focuses on the mechanisms controlling partial degradation of proteins by the ubiquitin/proteasome system using as an experimental model the activation of the yeast transcription factors Spt23 and Mga2. Previous work showed that Spt23 and Mga2 undergo regulated processing of their ER membrane-bound inactive precursors (p120) to shorter transcriptionally active forms (p90). The proteasome is believed to engage loosely folded regions at either the N- or C-termini of its substrates for initiation of degradation. However, during the processing reaction the N-terminal domains of Spt23/Mga2 are not degraded, while the C-termini are localized to the ER lumen and not accessible for the proteasome, suggesting internal initiation sites. In the first part of this work, this hypothesis was experimentally tested. Processing of Mga2 variants with their C-termini stabilized by fusion to a tightly folded domain resulted in accumulation of stable C-terminal products, which are not normally detected due to their rapid degradation. Similar results were obtained with native Spt23/Mga2 processed by functionally impaired proteasomes, confirming that their partial degradation is initiated at internal sites. Furthermore, tight dimerization of p120 molecules was shown to be crucial to halt proteasome progression, thereby preventing complete degradation of p120 and allowing p90 formation. Altogether, the data presented suggest that proteasomal processing of Spt23/Mga2 is initiated by an internal cleavage, followed by bidirectional proteolysis of the polypeptides until it is halted by a barrier, the dimerization domain. Importantly, this work shows that not only partial but also complete degradation of proteins can be initiated at polypeptide loops, suggesting a more general mechanism of proteasomal activity.

The second part of this work focused on the regulation of Spt23/Mga2 processing by intramolecular interaction between the dimerization and ankyrin repeat domains. This interaction could be shown to inhibit processing of the p120 molecule from the p120/p90 heterodimer and allow a distinct step of regulation of Mga2 activity by tightly controlled mobilization of its processed transcriptionally active p90 form.

1. Introduction

1.1. The ubiquitin/proteasome proteolytic pathway

The ubiquitin/proteasome system (UPS) is the main eukaryotic cytosolic and nuclear proteolytic pathway serving for selective degradation of cellular proteins. By influencing protein abundance, the proteasome contributes to the dynamic state of cells, which allows a tight control of many biochemical pathways and cellular responses upon changes of the environment.

The UPS was found to regulate a multitude of important cellular processes, including cell cycle progression, transcription, immune response and quality control of *de novo*-produced proteins. Since many substrates of the proteasome localize to the same cellular compartments, the system needs to select possible targets, discriminate them from other stable proteins and degrade them specifically at the proper moment. Unlike conventional site-specific proteases, which recognize substrates by specific motifs, the proteasome has no apparent preference for a substrate sequence, as it has to act on a broad spectrum of proteins. To avoid promiscuous degradation by the proteasome, a specialized system evolved that selects proteins and marks them with the small protein ubiquitin. In addition, the catalytic sites of this complex are not directly accessible for native proteins. In the proteasome, the active sites are buried inside a protein barrel-like complex and access to the proteasome is prevented by narrow openings, allowing only unfolded polypeptide chains to enter the proteolytic chamber. The combination of a highly selective and regulated recognition of substrates by the ubiquitylation machinery with broad activity of the proteasome, make the UPS exceptionally potent degradation system.

1.1.1. Enzymatic cascade for ubiquitin conjugation

Ubiquitin is a small, highly evolutionarily conserved protein found abundantly in all eukaryotic cells. The conjugation of ubiquitin to a substrate (ubiquitylation) is a three-step enzymatic reaction (Figure 1-1) that results in a covalent linkage between the C-terminus of ubiquitin and a lysine residue of the target protein. When the substrate of this conjugation reaction is a lysine residue of another ubiquitin moiety, a polyubiquitin chain is formed. The first step, which is catalyzed by the ubiquitin-

activating enzyme (UBA; E1), involves the ATP-dependent formation of a high-energy thioester bond between the C-terminal glycine residue of ubiquitin and a cysteine residue from the E1 active centre (McGrath et al., 1991). This activated ubiquitin is transferred in a similar enzymatic reaction to a cysteine residue of the ubiquitin-conjugating enzyme (UBC; E2). In a third step, ubiquitin is finally attached to the target protein usually via an isopeptide bond between the C-terminal glycine of ubiquitin and the ε-amino group of the substrate lysine residue. This reaction is mediated by a class of enzymes called ubiquitin ligases (E3). Sometimes, for efficient polyubiquitylation of a substrate, additional E4 enzymes are required (Koegl et al., 1999; Richly et al., 2005).

The involvement of three distinct steps in ubiquitylation provides the means to control substrate specificity. The first reaction of ubiquitin activation is mediated by a single E1 enzyme encoded in all eukaryotes by a single gene (Uba1) (Pickart, 2001). However, both E2 and E3 enzymes represent protein families. In the yeast *Saccharomyces cerevisiae* there are 11 ubiquitin-conjugating enzymes and a much larger number of E3 ligases. Usually, an E2 enzyme can interact with several E3 ligases and each of the E3 enzymes can selectively interact with several substrates via specific recognition motifs. This ensures the targeting of many different proteins to the proteasome in a selective and regulated way.

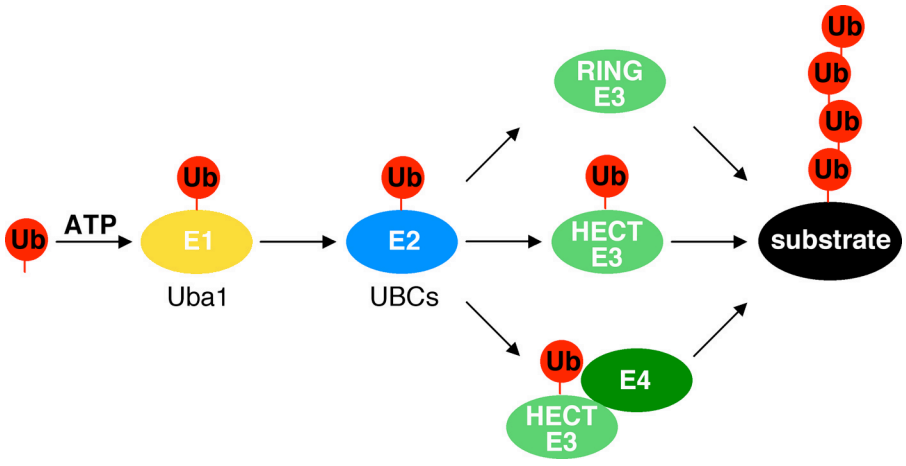

Figure 1-1. The enzymatic machinery for ubiquitylation. Ubiquitin is transferred to a substrate through a cascade of E1, E2 and E3 enzymes, and in some cases additionally an E4 enzyme.

1.1.2. E3 ligases determine substrate specificity

E3 ubiquitin ligases comprise a large group of enzymes, which mediate the attachment of ubiquitin molecules to substrates. This process must be highly specific

to avoid undesired degradation of other proteins. In addition, E3 ligases are often of modular organization in order to recognize a broad range of substrates. For efficient ubiquitylation, the substrate must possess an E3-binding site and an exposed lysine residue, which can accept the ubiquitin moiety from the E2/E3 enzyme complex.

E3 ubiquitin ligases can be divided according to the conserved catalytic domains, into two major groups: the so-called HECT enzymes and RING finger-containing enzymes, which differ greatly in their mechanism of reaction.

The HECT (homologous to E6AP C-terminus) domain family proteins harbour an evolutionarily conserved sequence of about 350-amino acids, which is responsible for the interaction with a ubiquitin-loaded E2 enzyme (Huibregtse et al., 1995; Scheffner et al., 1995). The HECT domain also contains an invariant cysteine residue to which the ubiquitin molecule is transferred from the E2 enzyme (Figure 1-2a). The N-terminal domains vary among different members of these E3 ligases and are responsible for specific interactions with ubiquitylation substrates. The first identified protein of the HECT family was E6AP (E6-associated protein), which after oncogenic papillomavirus infection in the presence of the viral E6 protein ubiquitylates and targets the tumour suppressor p53 for rapid degradation (Scheffner et al., 1993). Of the five members of HECT E3s in *Saccharomyces cerevisiae*, the best studied is Rsp5. This enzyme is essential for cell viability and implicated in the regulation of many cellular processes including fatty acids metabolism, transcription, endocytosis and protein sorting. Rsp5 contains an N-terminal lipid-interacting C2 domain responsible for its localization to endosomal membranes and three centrally located WW domains that are known to bind specific (L/P)PXY amino acid sequences (PY motifs) (Chang et al., 2000; Dunn et al., 2004).

The second class of E3 enzymes contains a short RING (“really interesting new gene”) finger motif, rich in cysteine and histidine residues that coordinate two zinc ions (Borden, 2000). Even though there is no sequence or structural similarity between the HECT and RING domains, both domains bind to the E2 enzyme at the same surface (Zheng et al., 2000). However, unlike the HECT domain, the RING finger does not form covalent linkage with ubiquitin, but rather increases the probability of the ubiquitin transfer reaction by bringing the E2 bound ubiquitin in close proximity to the lysine residue of the substrate (Figure 1-2b). The RING finger-containing E3 enzymes are composed of one or several different subunits. Single

subunit enzymes are e.g.: cytosolic Ubr1, nuclear Rad18 or the ER membrane-bound Hrd1 protein. These proteins contain the RING finger and the substrate recognition site in the same molecule. The multisubunit E3 ligases are composed of scaffold proteins, regulatory proteins and variable subunits, which recognize substrates. Examples of the multisubunit RING finger E3 ligases in yeast are the SCF (Skp1-Cul1-F-box) complex (Figure 1-2c), which is mainly involved in the degradation of phosphorylated proteins (Petroski and Deshaies, 2005), and the APC/C (anaphase promoting complex/cyclosome) complex (Figure 1-2d), which plays an essential role in the degradation of cyclins (Peters, 2006). SCF complexes belong to a group of E3 ubiquitin ligases that are assembled on the cullin (Cul1/Cdc53) scaffold, which recruits the RING finger protein Rbx1 and the Skp1 protein, which in turn interacts with variable F-box containing substrate-recruiting adaptors. Notably, APC/C exhibits a similar organization as it contains a cullin-like subunit called Apc2, a RING-finger subunit Apc11 and variable substrate-binding subunits: Cdc20, Cdh1 or Ama1 (Peters, 2006).

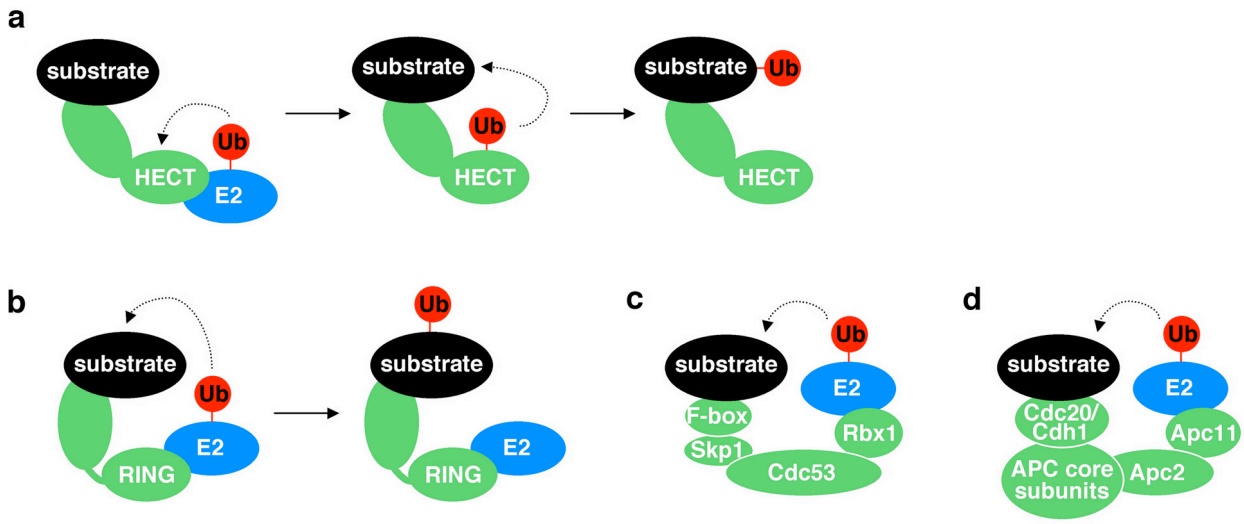

Figure 1-2. Mechanisms of ubiquitylation by E3 ubiquitin ligases. (**a**) HECT type enzymes form a thioester bond with ubiquitin via a cysteine residue in their active centre and subsequently transfer ubiquitin to a lysine residue of a substrate. (**b-d**) RING finger containing ligases: monomeric (**b**) and multi-subunit: SCF (**c**) and APC (**d**). RING finger containing enzymes facilitate transfer of ubiquitin from the E2 enzyme to a substrate.

1.1.3. Regulation of ubiquitin conjugation to substrates

Targeting of proteins for ubiquitylation needs to be tightly controlled to avoid any erroneous degradation of cellular proteins. Therefore, proteins possess specific degradation signals (degrons), which usually serve as E3 binding sites (Hochstrasser

et al., 1999). In addition, many regulatory mechanisms have evolved that assure proper timing and modulate the selectivity of ubiquitylation.

In the well established N-end rule pathway, for example, the degron signal recognized by the ubiquitin ligase Ubr1 is the N-terminal residue of certain proteins (Bachmair and Varshavsky, 1989; Johnson et al., 1995). The identity of the N-terminal residue defines the affinity for the Ubr1 ubiquitin ligase, which in turn translates into different half-lives of the substrates. Other examples of degrons are specific sequences, e.g. the destruction box and the KEN box of some cell cycle regulators recognized by the APC/C complex (Burton and Solomon, 2000; Hilioti et al., 2001; Pfleger and Kirschner, 2000) or the PXY motif found in many substrates of the Rsp5 E3 ligase (Chang et al., 2000).

One central role of the UPS is protein quality control by the removal of proteins that are aberrantly folded and therefore unable to perform their functions. In this case, the target selection is thought to be mediated by recognition of certain substructures, such as solvent-exposed hydrophobic patches, unpaired cysteines and immature glycans, rather then by specific sequences. This process involves a specialized subset of chaperones cooperating with the E3 ligases. In mammalian cells, the cytosolic E3 ligase CHIP works together with Hsp70-Hsp90 chaperones to target defective proteins for ubiquitylation (Esser et al., 2004). Another, well studied cellular quality control pathway is ERAD (ER-associated degradation), which involves E3 ligases that specifically target misfolded proteins with either lumenal and transmembrane lesions (Hrd1 E3 ligase associated complex) or cytoplasmic lesions (Doa10 E3 ligase complex) (Ismail and Ng, 2006). Specific recognition of Hrd1 substrates with misfolded luminal domains is mediated by the E3 ligase partner protein Hrd3, the ER-lumenal chaperone Kar2 and the lectin-like protein Yos9, querying the status of the substrates glycosylation (Denic et al., 2006; Gauss et al., 2006). In the case of proteins with disturbed transmembrane domains only Hrd1 and Hrd3 seem to be required (Carvalho et al., 2006). Misfolding of a protein must not necessarily be the result of mistakes in folding of newly produced proteins, but can also be done “on purpose” in order to regulate the abundance of certain proteins, as it was reported for the yeast proteins Ole1 and Hmg2 (Braun et al., 2002; Shearer and Hampton, 2005). Different mechanism, but the same principle can be applied to the regulation of degradation of **a**1 and α2 transcription factors controlling opposite

mating types in haploid yeast *S. cerevisiae* cells. The α2 factor is stable only in diploid cells due to the binding of the **a**1 partner, which masks its hydrophobic degron site Deg1, otherwise exposed to the solvent and recognized by Doa10 E3 ligase (Johnson et al., 1998; Swanson et al., 2001).

A common mechanism by which the interaction of ubiquitin ligases with their substrates is regulated involves post-translational modifications of either of them. The most common type of substrate modification used to control degradation is phosphorylation. The prerequisite for the ubiquitylation of the yeast G2 cyclins Clb2 and Clb3, the cyclin-dependent kinase inhibitor Sic1 or the mammalian IκB and NFκB transcription factors is their phosphorylation allowing an interaction with the appropriate SCF type E3 ligase (Willems et al., 2004). Another post-translational modification regulating ubiquitylation of proteins may be the conjugation of the ubiquitin-like protein SUMO (small ubiquitin-related modifier; Smt3 in yeast), termed SUMOylation. As it was show for IκBα, SUMOylation on one of the ubiquitin acceptor lysines inhibits its ubiquitylation and degradation, suggesting that SUMO can block ubiquitylation by a direct competition for the modification site (Desterro et al., 1998).

Similarly to the modification of substrates, also E3 ligases can be modified to change their activity or ability to bind a substrate. In yeast, upon DNA damage, protein kinase A (PKA) phosphorylates the APC/C subunit Cdc20, blocking thereby the degradation of cyclin Clb2 and securin and inducing cell-cycle arrest (Searle et al., 2004). Also modification of the SCF complexes subunit Cul1 by the ubiquitin like protein Nedd8 (in yeast Rub1) was shown to promote the ubiquitylation of certain substrates (Podust et al., 2000).

Since ubiquitylation is a reversible modification, the degradation of substrates can be additionally regulated by a special class of proteins termed deubiquitylating (DUB) enzymes, which cleave specifically the isopeptide bond of ubiquitin modification (Amerik and Hochstrasser, 2004). Such activity can lead to removal of ubiquitin from the substrate. This type of regulation was shown in yeast for the DUB enzymes Ubp2 or Otu1, which antagonize the E3 ligase Rsp5 and the E4 enzyme Ufd2, respectively (Kee et al., 2005; Rumpf and Jentsch, 2006).

1.1.4. The mode of ubiquitylation determines the fate of a conjugated substrate

The most extensively studied function of ubiquitylation is the targeting of proteins for degradation by the proteasome. However, in other cases ubiquitylation serves non-proteolytic functions such as regulation of protein traffic or enzymatic activity. This is reflected by the fact that different substrates can be modified by different types of ubiquitylation. Ubiquitin can be attached either as a single molecule (monoubiquitylation) or as an ubiquitin polymer (polyubiquitylation) to the substrate. The polymeric ubiquitin chains can be further divided into different types, depending on which of the seven lysine residues of ubiquitin is used to form the isopeptide bond with the next ubiquitin molecule. Monoubiquitylation and differently linked polyubiquitin chains are recognized in cells as signals that target the conjugated proteins to different fates. Recognition of these signals is mediated by a large group of ubiquitin-binding proteins, containing at least one of several classes of domains that were shown to specifically interact with monoubiquitin and/or polyubiquitin chains. Among these domains are UIM (ubiquitin interacting motif), UBA (ubiquitin associated) and CUE (coupling of ubiquitin conjugation to endoplasmic reticulum degradation) (Hicke et al., 2005).

Modification by monoubiquitin is not usually directly implicated in targeting of proteins to the proteasome for degradation. Instead, this signal is broadly used to mark proteins designated for endocytosis and intracellular trafficking. In *S. cerevisiae,* internalization of various plasma membrane permeases and transporters requires monoubiquitylation of their cytoplasmic domains by the Rsp5 ubiquitin ligase. Moreover, another step of endocytosis, sorting of proteins to the multivesicular bodies involves monoubiquitylation of cargo proteins (Welchman et al., 2005). This type of modification is also used in DNA damage signalling. In this process, replication stalled at DNA damage sites can be resumed upon PCNA monoubiquitylation catalyzed by the E2 Rad6 (Ubc2) and E3 Rad18 enzymes, which allows PCNA to associate with translesion polymerases that are able to read through the damaged site (Hoege et al., 2002). Rad6 is also implicated in the monoubiquitylation of histone H2B on the K123 residue and this modification is required for transcriptional activation (Sun and Allis, 2002).

The function of polyubiquitylation is primarily determined by the kind of ubiquitin linkage in the chain attached to the substrate. The most abundant in cells and the only essential for yeast viability are K48-linked chains, which target substrates to the proteasome for degradation (Finley et al., 1994; Pickart and Fushman, 2004). The role in proteolysis was reported also for K29-linked chains catalyzed by Ufd2, which is, however, believed to switch to K48-linkage during extension (Koegl et al., 1999; Saeki et al., 2004) and for K11-linked chains (Baboshina and Haas, 1996). Interestingly, substrates conjugated with K6-linked chains in the DNA repair foci, although targeted to the proteasome, are not degraded (Morris and Solomon, 2004; Nishikawa et al., 2004).

The second most abundant mode of polyubiquitylation assembly in cells is the conjugation of chains linked via the K63 residue of ubiquitin. This type of modification is implicated in several non-degradative regulatory functions. In DNA repair, for example, PCNA can be modified by the K63-linked chain by the activity of Rad6 and Rad18, and the heterodimeric E2 enzyme Ubc13-Mms2 and the E3 enzyme Rad5 (Hoege et al., 2002). This K63-linked polyubiquitin is a signal for the error-free pathway of DNA repair, which presumably involves a template switch to the undamaged sister chromatid. Another example is the inflammatory response pathway, where K63-linked chains function as signals for activation of the IκBα (the inhibitor of transcription factors NFκB) kinase (IKK). Phosphorylation of IκBα triggers its degradation, allowing subsequent translocation of NFκB to the nucleus and transcriptional response (Kanayama et al., 2004).

1.1.5. Composition and structure of the 26S proteasome complex

The 26S proteasome is the well known member of a family of so-called “chambered” or “self-compartmentalized” proteases found in all organisms ranging from bacteria to humans (Pickart and Cohen, 2004). Chambered proteases are large multi-subunit enzymes, which physically sequester their proteolytic sites inside their barrel-shaped structures. This structural organization determines a specific mechanism of degradation, in which the recognition of degradation signals is independent of the cleavage sites of substrates. Such mode of action gives an advantage to degrade any type of substrates over “conventional proteases” recognizing specific sequences near the cleavage sites. The 26S proteasome is a large 2.5 MDa ATP-dependent

proteolytic complex composed of a central catalytic core particle (20S proteasome) and two regulatory particles (19S caps) that sit at the top of two openings of the core particle (Figure 1-3) (Baumeister et al., 1998). The 20S particle is a cylindrically shaped complex composed of a stack of two identical inner hetero-heptameric rings (made of β1 to β7 subunits; Pre3, Pup1, Pup3, Pre1, Pre2, Pre7, Pre4 in yeast) and two identical outer hetero-heptameric rings (made of α1 to α7 subunits; Scl1, Pre8, Pre9, Pre6, Pup2, Pre5, Pre10 in yeast) (Groll et al., 1997). Three of the β subunits of each of the two rings harbour proteolytic sites of different cleavage preferences (chymotrypsin-, trypsin- and caspase-like), although the cleavage site usage by the proteasome is largely promiscuous (Kloetzel, 2004). Proteasomal substrates can only access these catalytic sites via narrow pores in the α rings at either end of the 20S cylinder. This ensures that only unfolded polypeptide chains can enter the proteasome (Groll et al., 1997). In addition, the access of substrates to the 20S particle is gated by N-terminal extensions of the α-subunits (Groll et al., 2000) The proteasomal gates open upon association with the 19S cap, allowing the passage of substrates to proteolytic sites (Kohler et al., 2001). In the architecture of the 20S proteasome certain interior compartments can be distinguished – two large axial antechambers formed by the α and β rings and a central catalytic chamber formed by

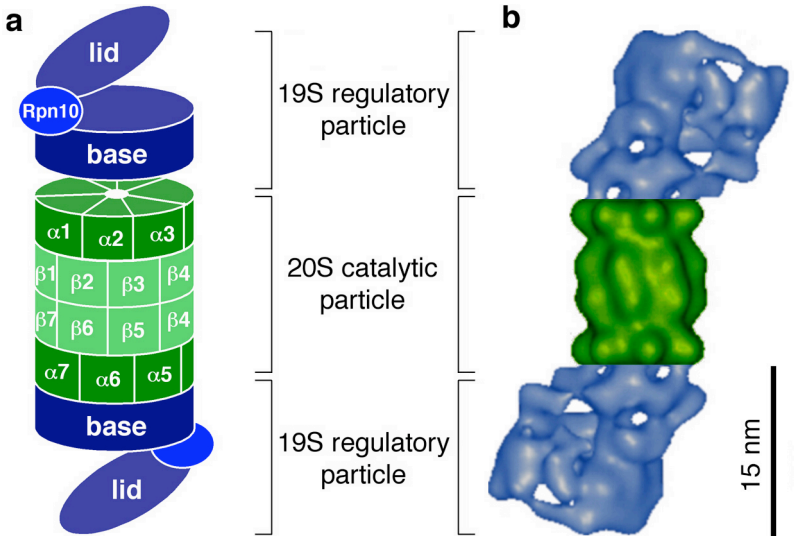

Figure 1-3. The 26S proteasome. (**a**) Schematic representation of the 26S proteasome complex. (**b**) Composite model of the three-dimensional structure of the 26S proteasome from *Drosophila* based on electron microscopy and modelled using the crystal structure of the 20S proteasome from *Thermoplasma* (Modified after Baumeister et al., 1998).

the two β rings. The role of the antechambers is still not clear, but they might store proteins in an unfolded or partially refolded state prior to degradation or store cleaved polypeptides for further digestion to smaller peptides (Sharon et al., 2006).

Each 19S regulatory particle contains at least 17 different subunits and is assembled from two subcomplexes: a base, which is composed of a hetero-hexameric ring of AAA type ATPases (Rpt1-6) and two non-ATPase subunits (Rpn1-2), and a lid that sits on the top of the base (subunits Rpn3, 5-9 and 11-12) (Figure 1-3a). Both subcomplexes are stably associated via an additional subunit Rpn10 (Glickman et al., 1998). The main functions of the 19S cap are recruiting substrates tagged with the polyubiquitin chain, and unfolding and translocating them to the catalytic particle. Polyubiquitin chains on target proteins are recognized directly by components of the 19S cap and by ubiquitin-binding factors delivering substrates to the 19S cap. Since the gates of the 20S proteasome are narrow, substrates need to be unfolded in order to enter the catalytic chamber. This is mediated by the ATPases located in the base (Braun et al., 1999). Interestingly, the 19S cap possesses also an intrinsic deubiquitylation activity residing in the Rpn11 subunit of the lid (Yao and Cohen, 2002). This enzyme is believed to take part in the recycling of ubiquitin conjugated to the substrates destined for degradation. Moreover, there is a growing list of proteins associating with the 19S cap, like the E3 ubiquitin ligases Ubr1and Ufd4, the E4 enzyme Hul5, and the deubiquitylating enzyme Ubp6, which may provide more regulatory functions for processing of substrates by the 26S proteasome (e.g. by regulating polyubiquitin chain length on a substrate) (Crosas et al., 2006; Hanna et al., 2006; Leggett et al., 2002; Xie et al., 2000).

1.1.6. Recognition and degradation of substrates by the 26S proteasome

To ensure selective degradation, several classes of proteins are involved in specific recognition of ubiquitylated substrates and their delivery to ubiquitin receptors on the proteasome. Studies on model substrates have shown that the minimal length of a polyubiquitin chain usually required for efficient targeting to the 26S proteasome encompasses four ubiquitin molecules (Thrower et al., 2000). The Rpn10 subunit of the 19S cap possessing the UIM motif was shown to bind polyubiquitin chains, and was proposed to function as a proteasomal receptor for ubiquitylated substrates (Deveraux et al., 1994). Moreover, a recent report demonstrated that two

homologous proteins Rad23 and Dsk2, both containing UBA domains and loosely associating with the proteasome, deliver polyubiquitylated substrates to the 26S proteasome (so called “escort pathway”) (Richly 2005). However, the triple knockout of these genes in yeast is not lethal, indicating that other components are also responsible for ubiquitin chain recognition (Elsasser and Finley, 2005; Richly et al., 2005). A candidate for this function is one of the ATPases of the 19S cap, Rpt5, that was also shown to bind ubiquitin chains (Lam et al., 2002). This possibility is particularly interesting since such an interaction would also bring the substrate directly to the unfolding machinery and in proximity to the proteasomal gates. In addition, these various ubiquitin receptor sites at the proteasome might also have preferential affinities to ubiquitin chains of different length and could bind substrates depending on whether they are modified with short or long chains.

The initial recruitment of a substrate is followed by the engagement of its loosely folded region (usually either of the polypeptide termini) by the ATPases ring (Figure 1-4a) (Prakash et al., 2004). The ATPases are thought not only to provide a force for sequential mechanical unfolding of the substrate and for the translocation of the unfolded polypeptide to the catalytic particle, but they might also regulate opening of the proteasomal gates (Kohler et al., 2001). Notably, not all proteins targeted to the proteasome are degraded equally well. The degradation speed seems to be determined by the unfolding efficiency by the ATPase motor, which is believed to depend on the local structure stability of the protein region engaged by ATPases for unfolding (Lee et al., 2001). Once the unfolding, translocation and degradation have started, the substrate is fixed in the proteasome (Figure 1-4b), and no longer requires the polyubiquitin tag. In fact, ubiquitin possesses an extraordinarily stable fold and by being difficult to unfold it slows down the degradation (Yao and Cohen, 2002). Therefore, and to save energy that otherwise would be used to produce ubiquitin *de novo*, the proteasome has evolved a way to recycle ubiquitin. The removal of the polyubiquitin chains is catalyzed by the 19S cap DUB enzyme Rpn11 and is coupled to the substrate translocation step to ensure that too early chain removal will not result in a release of the protein before engagement by ATPases (Figure 1-4c). Since the proteasome is a highly processive protease, it usually degrades substrates completely to small oligopeptides of about 5-20 residues in length. These degradation products leave the proteasome by diffusion, perhaps also in a gated

manner (Bajorek and Glickman, 2004; Kohler et al., 2001). The peptides generated by the proteasome can be further degraded to free amino acids by cellular peptidases, however in higher eukaryotes they are also transported via ER to the cell surface and presented to the immune system by MHC class I molecules (Kloetzel, 2004).

Although most of the proteasomal substrates need the polyubiquitin mark, some may be degraded in an ubiquitin independent manner. One such natural substrate of the proteasome is ornithine decarboxylase (ODC) acting in the biosynthetic pathway of polyamines. By a feedback mechanism, excess of polyamines leads to the production of antizyme, an interactor of ODC, which enhances the affinity of ODC to the proteasome and promotes its efficient degradation (Li and Coffino, 1992; Murakami et al., 1992). In addition, *in vitro* experiments demonstrated that certain unfolded protein segments are degraded by the 20S proteasome in an ubiquitin independent manner, which suggests that some disordered proteins might possess intrinsic features targeting them directly to the proteasome (Liu et al., 2003). This is further supported by an observation that certain hydrophobic peptides activate the peptidase activity of the proteasome, most likely by influencing opening of the gates (Kisselev et al., 2002).

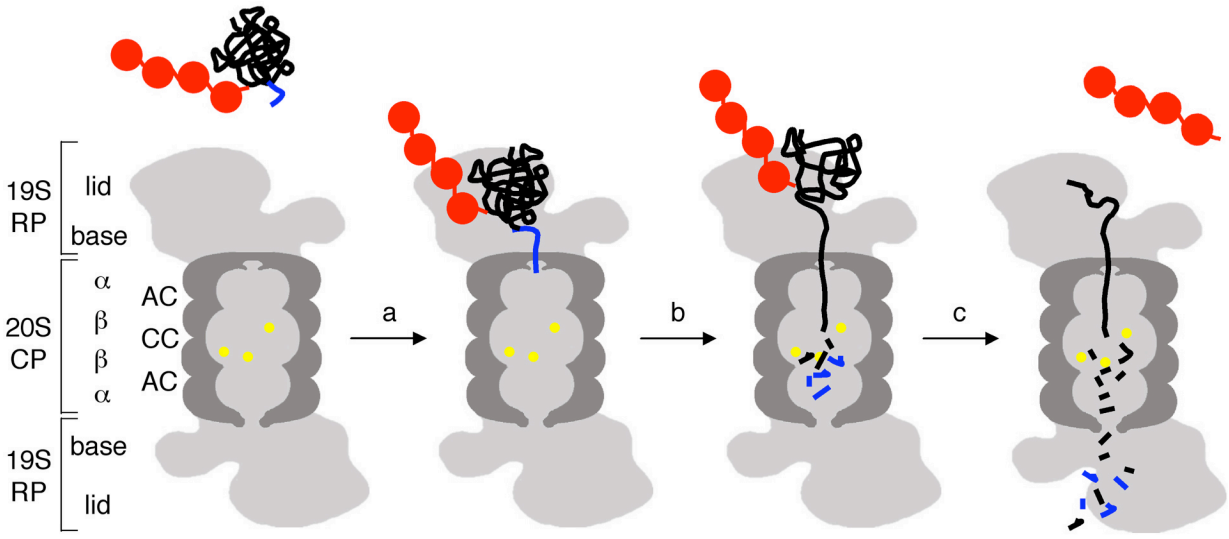

Figure 1-4. Mechanism of the ubiquitin/proteasome dependent degradation. (**a**) Polyubiquitylated (red circles) substrate (black) is recognized by the 19S regulatory particle (19S RP) components. (**b**) The ATPases of the base find a loosely folded "engagement site" (blue) of the substrate, start unfolding and translocation of the unfolded polypeptide to the antechamber (AC) and then to the catalytic chamber (CC). The substrate is degraded to small peptides by active sites (yellow dots) located in CC. (**c**) The polyubiquitin chain is removed during the degradation by the Rpn11 DUB enzyme of the 19S lid and further disassembled to free ubiquitin in the cytosol by other DUB enzymes (not shown).

1.2. Limited proteolysis of proteins

Proteolysis is employed by cells not only for the complete degradation of proteins but represents also an important step for the maturation of some proteins. Similarly to the modification of proteins by the attachment of various chemical groups, also proteolytic processing of polypeptide chains was shown to modulate protein conformation, as well as binding properties and activity. However, in contrast to chemical modifications, which are usually reversible, the proteolytic cleavage is not.

The list of physiological processes found to be regulated by limited proteolysis is large and still growing. Proteolytic processing was shown to function as early as at the level of protein translation, where it is required to remove initiator methionine or/and signal peptides from many secretory proteins. Furthermore, processing was found to be a mechanism commonly used by enzymatic systems for activating otherwise inactive precursor forms (zymogens). In many signalling pathways, limited proteolysis enables activation of signalling molecules, e.g. by cleaving membrane-bound proteins in order to release active fragments, which can be transported to the nucleus for nuclear functions. Moreover, some proteins are produced as long fusions (polyproteins) and their maturation requires specific cleavage into several active fragments.

Most of the proteases mediating partial proteolysis of proteins are characterized by a high specificity of the cleavage reaction and thus can only be employed for the processing of a limited number of substrates. However, also the proteasome, which has a broad range of substrates and is mainly implicated in the complete degradation of proteins, can mediate limited proteolysis of some of its substrates.

1.2.1. Proteasome-independent processing of proteins

The importance of proteolytic processing was first demonstrated by studies on the activation of two enzymes of the digestive system, trypsin and chymotrypsin, which are produced in the pancreas as inactive forms, trypsinogen and chymotrypsinogen, respectively (Neurath, 1989). Trypsinogen is activated upon secretion to the small intestine, where it is activated by proteolytic cleavage by the enzyme enterokinase. The resulting trypsin can further activate trypsinogen by autocleavage and in addition process chymotrypsinogen to active chymotrypsin. The strategy to activate enzymes by processing of inactive precursors is employed also in cascades of consecutive

activation of zymogens during blood coagulation or in apoptosis (activation of caspases) (Chang and Yang, 2000; Neurath, 1989).

Proteins of the ER, the Golgi apparatus and from the secretory pathway possess a signal sequence, which targets them to the ER. Processing of these proteins by the ER lumen enzyme signal peptidase occurs co-translationally and leads to the removal of the signal peptide. An example of such processing is the formation of the active form of the hormone insulin, which moreover requires a multi-step proteolytic processing (Steiner, 1998). Insulin is synthesized as a precursor polypeptide preproinsulin that contains an N-terminal signal sequence targeting the polypeptide chain to the ER. In the first cleavage step occurring during the translocation of the polypeptide to the ER lumen, proinsulin is formed by the elimination of the signal sequence by the signal peptidase. A second processing step occurs in secretory vesicles and involves a series of cleavage events mediated by specific proteases, which remove an internal peptide from proinsulin. As a result, active insulin consisting of two polypeptide chains connected by disulfide bonds is secreted.

The yeast polyubiquitin gene *UBI4* encodes for a polyprotein composed of five tandemly repeated copies of ubiquitin, which is further processed to single ubiquitin molecules by ubiquitin-specific peptidases. Production of ubiquitin by this mechanism seems to be very efficient and can provide the cell with extra ubiquitin under stress conditions, which is essential to sustain cell viability (Finley et al., 1987). Other examples of polyprotein processing are Env, Gag and Gag-Pol polyproteins of the human immunodeficiency virus (HIV) (Dunn et al., 2002). The retroviral genome is translated by the host-cell machinery into polyproteins, which are cleaved at specific sites by the viral peptidases to produce mature capsid proteins, non-structural proteins and enzymes.

Proteolysis is a hydrolytic reaction, which requires the presence of water molecules. Thus, the sites of proteolytic processing are believed to be located in the flexible inter-domain segments of proteins or surface loops that are exposed to the aqueous environment. Interestingly, a growing number of enzymes is reported to mediate also the cleavage of transmembrane segments of proteins (Brown et al., 2000). This regulated intramembrane proteolysis (RIP) is conserved from bacteria to animals and involves distinct groups of specialized membrane-bound proteases,

which are able to cleave residues inserted into the non-aqueous environment of biological membranes. One of the proteins activated by such a mechanism is sterol regulatory element binding protein (SREBP), a transcription factor that activates genes essential for the biosynthesis of sterols and fatty acids in animal cells (Brown et al., 2000). SREBP is synthesized as a transmembrane precursor protein, which is kept in the ER when cholesterol levels are high. Upon depletion of cholesterol, SREBP is transported to the Golgi apparatus where it undergoes activation upon two sequential proteolytic cleavages by the site-1 and site-2 proteases, leading to the liberation of the N-terminal active transcription factor domain. Another well known example of RIP is processing of the plasma membrane signal receptor Notch, which controls many developmental processes in animals (Fortini, 2002). Proteolysis of Notch is catalyzed by the integral membrane multi-subunit protease γ-secretase, which cleaves the transmembrane segment of Notch and allows its cytoplasmic domain to translocate into the nucleus, where it functions as a transcriptional activator. The same enzymatic complex mediates also the cleavage of amyloid precursor protein (APP), which yields the amyloid β peptide (Aβ), forming extracellular plaques in Alzheimer's disease (Fortini, 2002).

1.2.2. Partial degradation of proteins by the proteasome

The main cellular task of the proteasome is the irreversible elimination of proteins in order to regulate certain cellular processes or to remove potentially toxic misfolded proteins. Therefore, the proteasome is highly processive and usually completely degrades proteins to small peptides. Several features of the proteasome contribute to this mechanism of action: the ATPase motor mediates the unfolding of substrates, the six active sites in the proteolytic chamber efficiently cleave polypeptides and the proteasomal gates prevent premature exit of the peptides until degradation is completed. Although the proteasome is well equipped to destroy proteins, some of proteins evolved mechanisms preventing complete degradation. Instead, these substrates seem to use the proteasome system to activate certain intrinsic, but dormant biological activities by specifically eliminating inhibitory domains while leaving other domains intact. This phenomenon, termed regulated ubiquitin/proteasome-dependent processing (RUP) was first described for the mammalian transcription factor NFκB1. This protein resides in the cytosol as a

dormant precursor (p105), which upon certain cellular stimuli becomes ubiquitylated and targeted to the proteasome. Instead of the complete degradation, the proteasome eliminates only the C-terminal domain of p105, yielding a shorter active form (p50), which is subsequently translocated to the nucleus for transcriptional response (Fan and Maniatis, 1991; Orian et al., 2000; Palombella et al., 1994). Later studies identified more proteasomal substrates that are not degraded to completion, but are rather activated by RUP: the mammalian transcription factor NFκB2 (p100 precursor processed to p52 subunit) (Amir et al., 2004), the yeast NFκB-related proteins Spt23 and Mga2 (Hoppe et al., 2000; Rape and Jentsch, 2002), the transcriptional regulator of the Sonic hedgehog pathway in *Drosophila* Cubitus Interruptus (Ci) and its vertebrate homologs Gli2 and Gli3 (Jiang and Struhl, 1998; Pan et al., 2006), and the mammalian transcription factor Sp1 (Su et al., 1999). In all these cases, the substrates are apparently ubiquitylated upon certain cellular signals and subsequently processed by proteasomes. This special mode of activation suggests that they may possess specific features recognized by the proteasome as a stop signal. However, such signal seems not to be a specific sequence, as a comparison of sequences of the proteins mentioned above does not reveal one common feature.

Based on the experimental data available for NFκB p105 and Spt23/Mga2, two alternative models of processing mechanisms have been suggested that differ mainly in the way how the proteasome initiates processing. According to the “end first” model, the polypeptide chain is degraded from one end (in case of NFκB p105 the C-terminus has been proposed), but proteolysis proceeds only halfway because the proteasome encounters a “stop-transfer signal” that prevents further degradation (Figure 1-5a) (Orian et al., 1999; Palombella et al., 1994). In the alternative “loop model”, the substrate folds into a hairpin loop, which is threaded into the proteolytic chamber, thereby enabling the proteasome to attack the substrate from an internal site (Figure 1-5b-d) (Hoppe et al., 2000; Hoppe et al., 2001). In this model, complete degradation is prevented by a tightly folded domain or through a tight binding to a “life saving” partner (Lee et al., 2001; Rape et al., 2001; Rape and Jentsch, 2002; Tian et al., 2005).

Particularly controversial is the mechanism of NFκB p105 processing initiation, as in addition to the post-translational processing of the full-length precursor also a

co-translational model has been proposed, in which the incompletely synthesized nascent polypeptide chain serves as a processing substrate (Figure 1-5b). Since the C-terminal ends of such precursors are buried in the ribosome and are therefore not accessible for the proteasome, an internal initiation site has been suggested (Lin et al., 1998; Lin et al., 2000). However, this model has been questioned recently by the finding that the 20S proteasomes can process purified full-length NFκB p105 derivatives *in vitro* (Moorthy et al., 2006). The same authors suggested also that ubiquitylation of p105 might not be required for the processing initiation and proposed that certain regions in the NFκB precursor sequence could possess the ability to open the otherwise closed gates of 20S proteasome (Figure 1-5c).

The "loop model" (Figure 1-5d) has been first proposed for the processing of the *Saccharomyces cerevisiae* NFκB-related proteins Spt23 and its homolog Mga2 (Hoppe et al., 2000; Rape and Jentsch, 2002). The Spt23 precursor (p120) is mono/oligoubiquitylated by the ubiquitin ligase Rsp5 and targeted to the proteasome

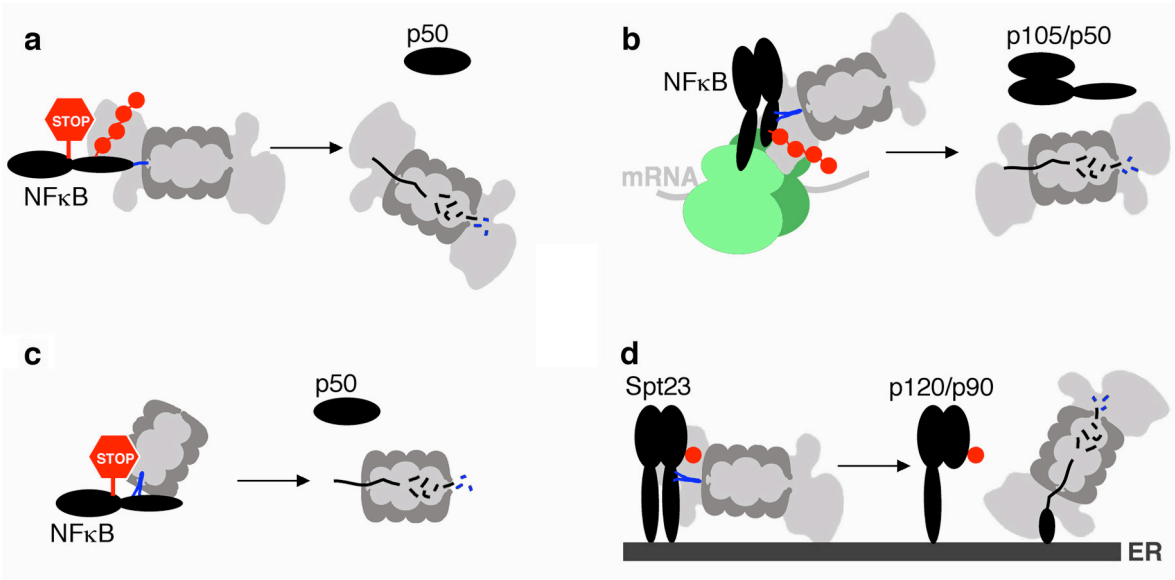

Figure 1-5. Models for proteasomal processing of NFκB p105 and Spt23 p120. (**a**) "Stop-transfer model" proposed for the processing of the full-length precursor of NFκB p105. After ubiquitylation (red circles), the 26S proteasome recognizes p105 and starts its degradation from the C-terminus (initiation sites are indicated in blue), but stops when it encounters the GRR sequence (stop sign). (**b**) Model for co-translational processing by endoproteolytic cleavage of p105 nascent polypeptide chains, which dimerize on polyribosomes (green). The tight dimerization domain prevents complete degradation of N-terminal parts of NFκB by the proteasome and leads to the formation of processed p50 form (**c**). Model for post-translational, ubiquitin-independent processing of p105 by the 20S proteasome initiated by internal cleavage. (**d**) The "loop model" for Spt23 p120 processing. The C-termini of p120 precursors is inserted into ER membrane via the transmembrane span and not accessible to the proteasome. Processing involves cleavage of the polypeptide loop by the proteasome and degradation of the C-terminal ER anchor, whereas p90 is protected from degradation by tight dimerization with p120.

for processing (the OLE pathway, see chapter 1.4) (Hoppe et al., 2000; Rape et al., 2001). Similar to the NFκB situation, this process involves complete degradation of the C-terminal domain, whereas the N-terminal part that constitutes the active transcription factor (p90) is spared from degradation. The key argument for the “loop model” stems from the fact that the C-terminus of Spt23 is buried in the ER membrane, whereas the N-terminal domain constitutes the active transcription factor and thus remains intact. It was therefore proposed that a central region of Spt23 forms a hairpin loop, allowing the proteasome to initiate processing from an internal site (Hoppe et al., 2000). Based on the crystal structure of the yeast 20S proteasome it was argued that the openings of the proteasome are wide enough to accommodate two juxtaposed polypeptide chains (Rape and Jentsch, 2002). Support for this model came from recent *in vitro* studies showing that artificial circular polypeptides and cross-linked polypeptide chains are substrates of the proteasome (Lee et al., 2002; Liu et al., 2003).

The evidence for the “stop-transfer signal” model came from observations that proteins with certain regions of low complexity amino acid composition are poor substrates for the proteasome. The sequence of the viral protein EBNA1 contains glycine-alanine repeats, which are known to inhibit its proteasomal degradation, allowing the Epstein-Barr virus to escape from the cellular immune defence (Sharipo et al., 1998). Similar sequences rich in glycine residues (GRR; glycine-rich region) were found in NFκB precursors close to their processing sites. Moreover, a deletion of this region from the p105 precursor was shown to abolish formation of the processed p50 form of the transcription factor (Lin and Ghosh, 1996; Orian et al., 1999).

Notably, efficient processing requires that Spt23 homo-dimerizes via the IPT domain (immunoglobulin-like/plexins/transcription factors) (Rape et al., 2001). The IPT domain exists also in NFκB and its mutation abolishes processing of p105 (Lin et al., 2000). This suggests that it plays the same role in the processing of mammalian and yeast proteins. Since dimerization via the IPT domains is characterized by a very stable fold and was shown to mediate a very strong interaction (Urban and Baeuerle, 1990), it was proposed to hinder the proteasome progression by being resistant to unfolding by ATPases (Rape and Jentsch, 2002). A recent report suggested a new model in which the tightly folded domains (e.g. IPT domain) work together with the

low complexity regions (e.g. GRR) to stop the proteasome (Tian et al., 2005). However, although yeast transcription factors have IPT domains, they seem not to possess low complexity regions at proper positions. Notably, studies on NFκB expressed in *S. cerevisiae* showed that p105 is efficiently processed by the yeast proteasome perhaps in an ubiquitin dependent manner, but the p50 formation does not depend on the presence of the GRR (Sears et al., 1998). This difference suggests distinct mechanisms of the proteasomal progression stop in yeast and mammals, or that the mechanism of partial degradation is more complex than previously believed.

1.3. The OLE pathway

The fluidity of biological membranes in yeast *Saccharomyces cerevisiae* is largely controlled by the activity of an ER membrane-bound Δ9-fatty acid desaturase enzyme, Ole1, which converts saturated to unsaturated fatty acids (UFAs) by introducing double bonds into their carbon chains. The importance of this process is reflected by the fact that the activity of this enzyme is essential for yeast cell viability (Zhang et al., 1999). The abundance of Ole1 in yeast is mainly controlled by the so-called OLE pathway (Figure 1-6), which is extensively regulated by the proteasome, and thus turned out to be a useful tool to study the UPS.

The first step of the OLE pathway involves the RUP-dependent activation of two homologous transcription factors Spt23 and Mga2 that are partially overlapping in activation the *OLE1* gene (Hoppe et al., 2000). Although deletion of either of the transcription factors alone has no significant phenotype in yeast, the double deletion is lethal, but can be rescued by providing an external source of UFAs (Zhang et al., 1999). Spt23/Mga2 are produced as 120 kDa precursor forms (p120), which are inserted into the ER membrane via single C-terminal TM spans. Upon unsaturated fatty acids depletion, Spt23 homodimerizes and is subsequently mono/oligoubiquitylated by the HECT type E3 ligase Rsp5 (Hoppe et al., 2000). This triggers the production of the processed form p90, which remains associated with the partner p120 molecule (“processing template”) in a dormant complex at the ER.

In a second step, p90 that retained its monoubiquitin mark is liberated from the ER for nuclear export by the chaperone $Cdc48^{Ufd1/Npl4}$ (Rape et al., 2001). This complex specifically binds ubiquitylated proteins and is thereby capable of segregating them from unmodified partners. Notably, p90 mobilization from p120 of Mga2 also depends on the segregase $Cdc48^{Ufd1/Npl4}$, however it has been reported that it involves selective Rsp5-mediated polyubiquitylation of the processing template molecule and targeting to the proteasome for complete degradation (this model however, has been refused by the same authors recently) (Shcherbik and Haines, 2007; Shcherbik et al., 2003). Rsp5 and the $Cdc48^{Ufd1/Npl4}$ complex play therefore important roles in both branches of the OLE pathway – activation of Spt23 and Mga2, but the detailed mechanisms of action are different. After mobilization from the ER membrane, p90 forms of Spt23 and Mga2 are translocated into the nucleus to activate expression of the *OLE1* gene, thereby increasing the abundance of UFAs.

Another level of regulation in the OLE pathway affects the active transcription factor. The nuclear Spt23 form is very unstable since the initial monoubiquitin on p90

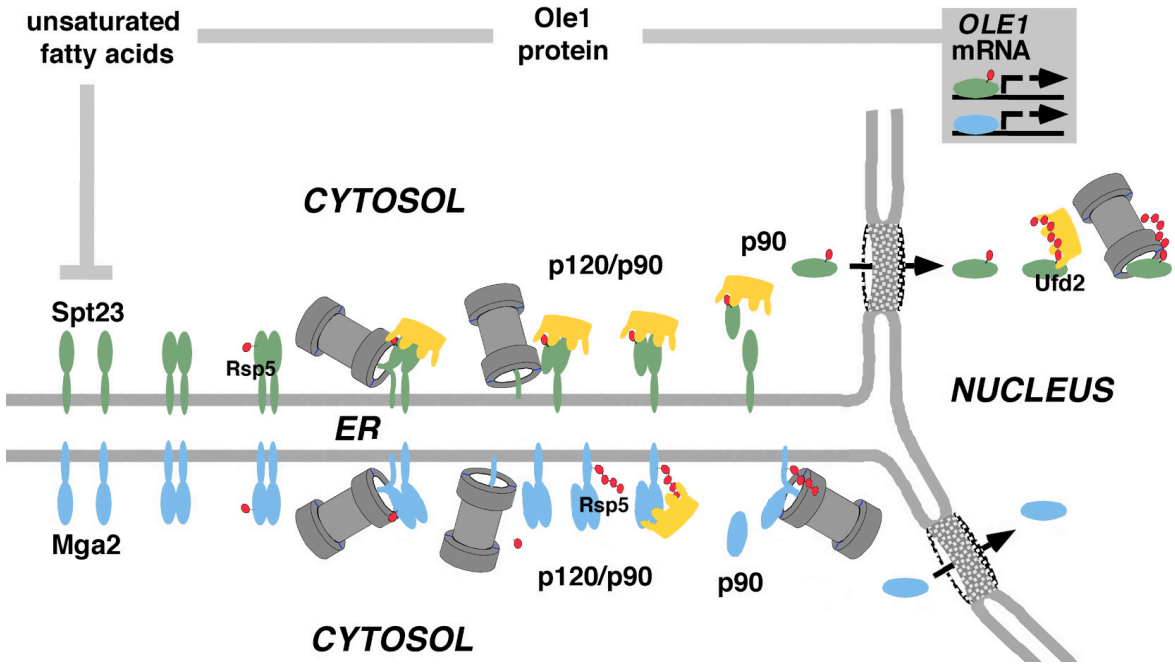

Figure 1-6. The OLE pathway. Spt23 (in green) and Mga2 (in blue) transcription factors activation by UPS. Monoubiquitylation (in red) of Spt23 by Rsp5 ubiquitin ligase is required for processing by the proteasome (gray barrel). In case of Mga2, Rsp5 is dispensable for initiation of the proteasomal processing (the E3 ligase is not known), but is responsible for liberation of p90 from processing template p120. The $Cdc48^{Ufd1/Npl4}$ complex (in yellow) plays several roles in the pathway: mobilization of Spt23 or Mga2 p90 from the ER; recruitment of E4 enzyme (Ufd2) to Spt23 p90, its polyubiquitylation and degradation; as well as ER associated degradation of Ole1 (not shown). In a feedback regulation of the pathway, production of Ole1 protein leads to increased UFAs levels that inhibit processing of Spt23.

can be further extended by the Cdc48 binding E4 enzyme Ufd2, enabling targeting of the transcription factor to the proteasome by the ubiquitin escort factor Rad23 (Richly et al., 2005). Interestingly, in yeast strains harbouring an *ufd2* deletion, Spt23 p90 is partially stabilized and apparently overactive, as these cells are hypersensitive to UFA supplement to the growth medium. This seems to be in line with the finding that certain transcription factors are activated after mono/oligoubiquitylation and transactivation is often coupled with degradation of a transcription factor (Muratani and Tansey, 2003). Degradation of p90 can also be negatively regulated, as Ufd2 action can be antagonized by other Cdc48 cofactors: Ufd3 competing directly with Ufd2 for the binding site on Cdc48 and Otu1 possessing a DUB activity (Rumpf and Jentsch, 2006).

The Ole1 enzyme itself is a short-lived protein degraded by the ERAD machinery, with its half-life negatively regulated by UFAs in a negative feedback loop (Braun et al., 2002). Interestingly, high levels of UFAs, or alteration in membrane fluidity, are also sensed by cells as signals to inhibit processing of Spt23 (Hoppe et al., 2000). Moreover, experiments with addition of UFAs to the growth medium showed that expression from the *OLE1* promoter is efficiently shut down under such conditions (Chellappa et al., 2001), despite the presence of Mga2, processing of which was reported not to be significantly influenced by high levels of UFAs (Hoppe et al., 2000). These data suggest that another mechanism could serve for inhibition of the transcriptional activity of Mga2 (e.g. regulation of p90 mobilization). A distinct regulatory mechanism was reported for activation of Mga2, which under hypoxic conditions leads to a robust expression from the *OLE1* promoter (Jiang et al., 2001). Again, this induction can be strongly inhibited by increased UFA levels as a negative feedback response (Chellappa et al., 2001). Changes of the membranes fluidity might be directly sensed by the ER membrane-inserted precursor forms of Spt23/Mga2, resulting in the regulation of their processing or mobilization of their processed p90 forms.

Notably, the ubiquitin/proteasome system is involved in the control of several consecutive steps of the OLE pathway, leading to both activation (Spt23 p120 processing, p90 mobilization, p90-mediated transcription) and inhibition (p90 and Ole1 degradation) of the pathway. This multi-step regulation assures a tight and quick response to changes of membranes fluidity in yeast cells.

1.4. Aim of this work

The proteasome is the most abundant eukaryotic proteolytic complex, which controls the half-lives of probably most intracellular proteins. Together with the selectivity of the proteasome, ubiquitylation assures a high substrate specificity. Notably, some of target proteins developed mechanisms that allow them to escape complete degradation and to undergo proteasomal processing. Activation of the yeast transcription factors Spt23 and Mga2 involves selective degradation of the C-terminal parts of their inactive precursors, leading to the release of active N-terminal domains. However, the mechanism of this non-conventional activity of the proteasome remained unclear.

The aim of this study was to understand how partial degradation of Spt23 and Mga2 by the proteasome is accomplished. To answer this question, variants of these transcription factors were created, which helped to identify the features of Spt23 and Mga2 that allow them to prevent complete degradation. Moreover, mutants of the ubiquitin/proteasome system were used, in order to determine the structural requirements for processing of the transcription factors.

2. Results

2.1. Mechanism of Spt23/Mga2 partial degradation

2.1.1. Processing initiates from an internal site

It has been proposed that the proteasome initiates degradation of its substrates from either their N- or C-termini, which are usually loosely folded (Lee et al., 2001; Prakash et al., 2004). However, the C-terminal ends of Spt23/Mga2 precursors are localized to the ER lumen and thereby not accessible to the proteasome, while the N-terminal parts encompassing the transcription activation domains are protected against proteasomal degradation. To explain how processing of this membrane bound proteins is initiated, it was proposed that central regions of Spt23/Mga2 form hairpin loops allowing the processing initiation from an internal site (Hoppe et al., 2000; Rape et al., 2001; Rape and Jentsch, 2002).

The easiest way to prove the proposed model for proteasomal processing initiation would be the isolation of processing intermediates corresponding to the N- and C- terminal parts of the protein resulting from the initial cleavage. However, C-terminal processing intermediates of Spt23/Mga2 were normally not observed, most likely due to their very rapid elimination (Hoppe et al., 2000). To circumvent this problem, Mga2 variants that have their C-terminal domains stabilized by fusion to the *Mus musculus* dihydrofolate reductase (DHFR) sequence were generated. The advantage of this experimental approach comes from the fact that DHFR is a tightly folded monomeric protein, which is strongly stabilized by binding of its ligand analogue methotrexate (MTX). This domain was shown to be resistant to unfolding and degradation by prokaryotic ATP-dependent proteases and the proteasome (Eilers and Schatz, 1986; Johnston et al., 1995; Lee et al., 2001). To allow the detection of the fusions, myc and HA epitopes were added at their N- and C-termini, respectively. In the initial experiment, the transmembrane lacking form of Mga2 (^{myc}Mga2ΔTM-DHFR^{HA}) was investigated (Figure 2-1a). This truncated protein is soluble and has in principle its C-terminus accessible for proteasomal degradation initiation. The ligand driven stabilization of DHFR in the fusion construct should thereby allow discriminating between two possible ways of processing initiation, either from an internal site or from the C-terminus.

Analogous to the findings with Spt23 (Hoppe et al., 2000), truncated Mga2 forms are processed less efficiently than the normal protein, however their processing yields similar p90 fragments (Figure 2-1b). As detected by Western blot analysis, expression of ^{myc}Mga2ΔTM-DHFR^{HA} in *S. cerevisiae* led to the generation of p90 levels similar to those of the control ^{myc}Mga2ΔTM. Addition of MTX to the growth medium did not change the processing efficiency (Figure 2-1b; anti-myc blot). Moreover, in the same experiment, additional anti-HA reactive fragments of about 35 kDa (C35; singular term “fragment” will be used for this nonhomogeneous pool of proteins) were observed, representing the truncated C-terminal part of the fusion construct that were not detectable for the WT protein (^{myc}Mga2^{HA}). Interestingly, the abundance of C35 was further increased upon MTX addition to the growth medium, indicating that the accumulation of the C-terminal fragment depends on the stability of DHFR.

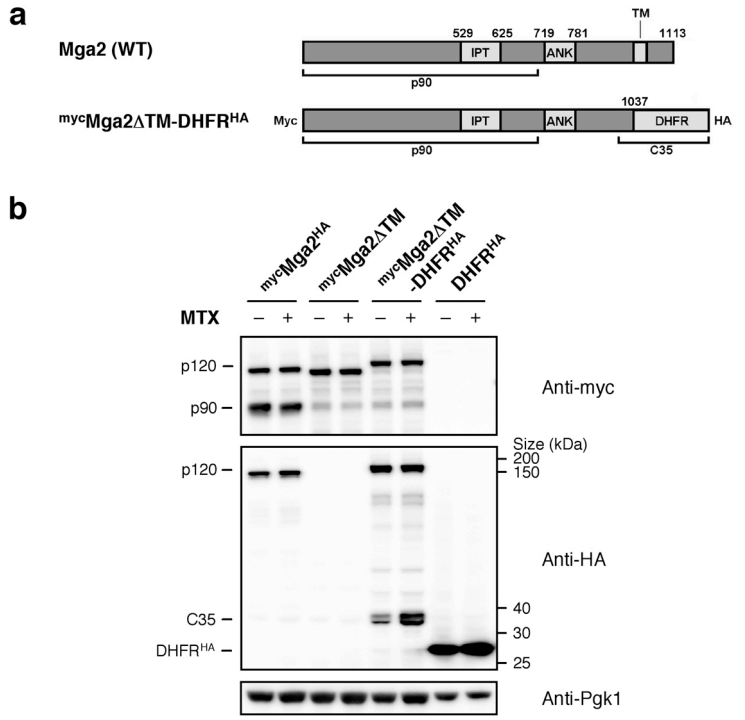

Figure 2-1. Processing of soluble Mga2 variants initiates from an internal site. (**a**) Schematic representation of Mga2ΔTM-DHFR fusion protein. Approximate fragment sizes of p90 and C35 are indicated by brackets. The position of the IPT and ankyrin repeat (ANK) domains and the transmembrane span (TM) are indicated. (**b**) Identification of N- and C-terminal processing fragments. Cell lysates were analyzed by immunoblotting with either anti-myc or anti-HA antibodies. Addition of methotrexate (MTX; “+”) stabilized the C-terminal domains of ^{myc}Mga2ΔTM-DHFR^{HA}, yielding upon processing the C-terminal fragment C35. The positions of p120, p90, C35 and tagged free DHFR (DHFR^{HA}) are indicated. Cytosolic Pgk1 protein was used as loading control.

In a similar experiment, a DHFR fusion to the full-length membrane-bound Mga2 (^{myc}Mga2-DHFR^{HA}; Figure 2-2a) was investigated. This fusion protein was inserted into the ER membrane similarly to WT Mga2 as judged by a membrane fractionation experiment and was also efficiently processed (Figure 2-2b, c). Again, processing of this construct, in addition to the N-terminal p90 fragment, gave rise to a specific C-terminal fragment of about 32 kDa (C32) that was stabilized upon addition

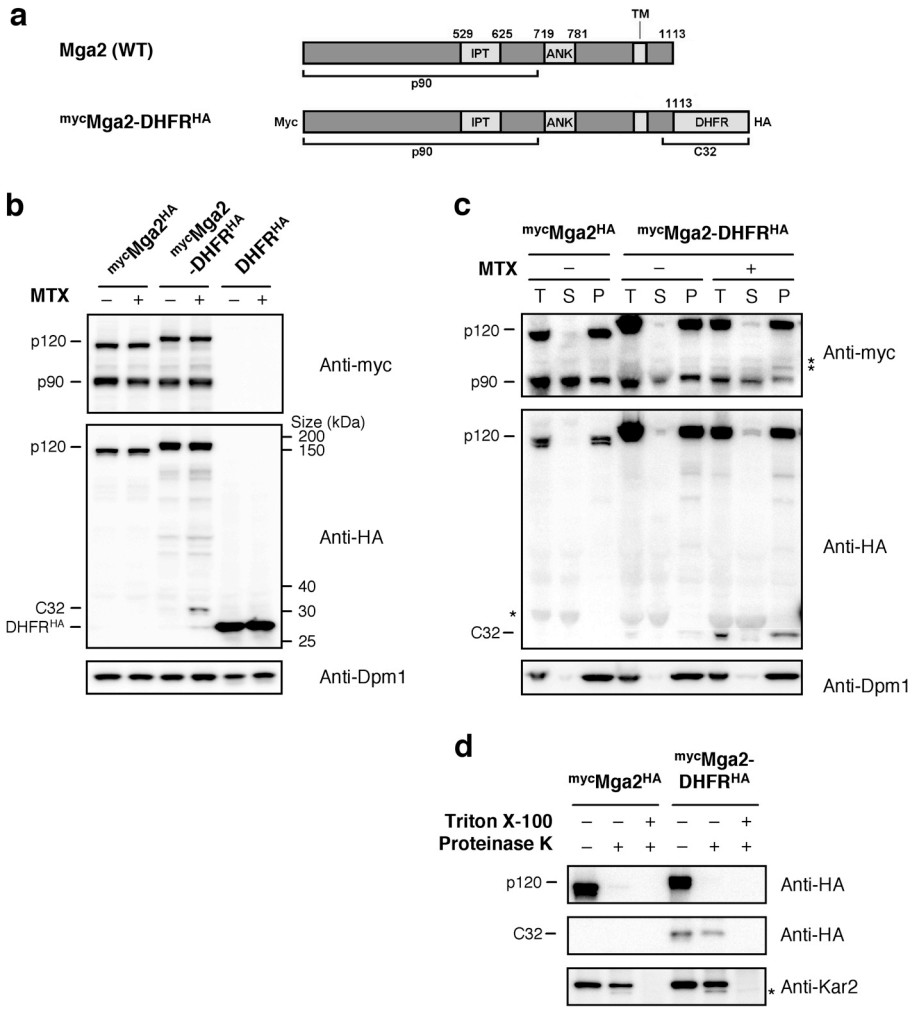

Figure 2-2. Processing of Mga2 p120 initiates from an internal site. (**a**) Schematic representation of Mga2-DHFR fusion protein. Approximate fragment sizes of p90 and C32 are indicated by brackets. (**b**) Processing of ^{myc}Mga2-DHFR^{HA} but not ^{myc}Mga2^{HA} gives rise to the C-terminal intermediate fragment (C32; anti-HA immunoblot). Addition of MTX stabilizes C32 and does not interfere with p90 production (anti-myc immunoblot). The positions of p120, p90, C32, and DHFR^{HA} are indicated. The ER integral membrane protein Dpm1 was used as loading control. (**c**,**d**) ER-lumenal localization of the C32 fragment. (**c**) Membrane fractionation experiment. Total extracts ("T") of WT cells expressing ^{myc}Mga2^{HA} or ^{myc}Mga2-DHFR^{HA} grown in the presence or absence of MTX were fractionated into pellet ("P") and soluble ("S") fractions. The Western blot was probed with anti-myc or anti-HA antibodies to detect full-length proteins (p120) and p90 and C32 fragments. The C32 fragment is found in the pellet fraction, indicating its localization to the ER. ER-membrane-bound Dpm1 was used for fractionation control. (**d**) Protease protection assay. Whole cell lysates from cells used in **(c)** were incubated with Proteinase K in the absence or presence of Triton X-100. Full-length ^{myc}Mga2-DHFR^{HA} is Proteinase K sensitive, indicating that it faces the cytosol. In contrast, C32 is largely protected against Proteinase K, analogous to the ER-lumenal protein Kar2, indicating that it localizes to the ER lumen. Asterisks denote cross-reactive bands.

of MTX and not detected for the WT protein (Figure 2-2b; anti-HA blot). Moreover, the abundance of p90 was again not influenced by MTX, indicating that the C-terminus accessibility is not important for the processing of either of the Mga2 versions. Furthermore, localization of the C32 fragment was investigated by membrane fractionation and proteinase K protection assays and C32 was found to reside in the ER lumen (Figure 2-2c, d). It therefore represents the C-terminal remnant of the ER membrane inserted p120 precursor and thus shows that the C-terminus is not required for the initiation of processing. Both investigated C-terminal fragments, C35 and C32, were slightly larger than $DHFR^{HA}$ itself and thus likely contained about 40-60 extra residues on the N-terminal side of the DHFR domain. As catalytic sites are separated spatially from the opening of the proteasome, the DHFR fragments released from the stalled proteasome contain additionally parts of the undegraded Mga2 polypeptide chain.

Altogether, the employed experimental approach allowed the detection of C-terminal intermediates of Mga2 derivatives processing in addition to the p90 fragment. These data suggest that processing of Mga2 initiates from an internal site, most likely in a polypeptide loop located in the C-terminal part of p120. Moreover, it could be shown that proteasome progression towards the C-terminus of the protein can be stopped by stable structures encountered during degradation, a mechanism, which could be similar to that employed for p90 production.

2.1.2. Processing intermediates are trapped in proteasome mutants

Further support for the finding that processing of Mga2-DHFR variants is initiated from an internal site came from experiments performed under conditions that allow to trap processing intermediates of native Spt23 and Mga2 precursors. Previously, it was reported that yeast cells carrying point mutations in the proteasome, such as *pre1-1* or *cim3-1* (point mutations in the genes for a β-subunit of the 20S barrel and an ATPase subunit of the 19S cap, respectively; (Ghislain et al., 1993; Heinemeyer et al., 1991; Seufert and Jentsch, 1992), accumulate proteolytic intermediates of some short-lived ERAD substrates due to inefficient proteasomal activities (Mayer et al., 1998). Specifically, these cells have difficulty in extracting and degrading ER membrane-inserted parts of the proteins.

This suggested that after initiation of processing of Spt23/Mga2 in proteasomal mutants, degradation of the C-terminal part of the precursor might be inefficient, leading to an accumulation of C-terminal cleavage fragments. It was previously described, the processing of Spt23 can be only partially blocked in these leaky mutants, while inhibition of Mga2 processing was much stronger (Hoppe et al., 2000). As shown in Figure 2-3a,b, experiments with proteasome mutants expressing doubly tagged $^{myc}Spt23^{HA}$ or $^{myc}Mga2^{HA}$ grown at the non-permissive temperature revealed that they accumulate proteolytic fragments of about 50 kDa (termed C50 fragment; detected by anti-HA immunoblot for the C-terminal epitope), which were completely absent in the WT control. Since the same Spt23 C50 fragment accumulated in two distinct proteasome mutants, the C50 formation seems to be specific for the attenuated proteasomes activity. Further investigation of this fragment by a membrane fractionation experiment revealed its exclusive localization to the microsomal pellet fraction (Figure 2-3c). In line with previously published data (Hoppe et al., 2000; Rape et al., 2001), this finding indicates that proteasomal processing of Spt23 occurs directly at the ER membrane and does not require membrane extraction prior to processing initiation.

Spt23 is the key regulator of membrane fluidity in yeast cells, and its processing is negatively regulated by unsaturated fatty acid pools. It was reported previously that palmitoleic acid (16:1) added to the yeast growth medium at high concentration is

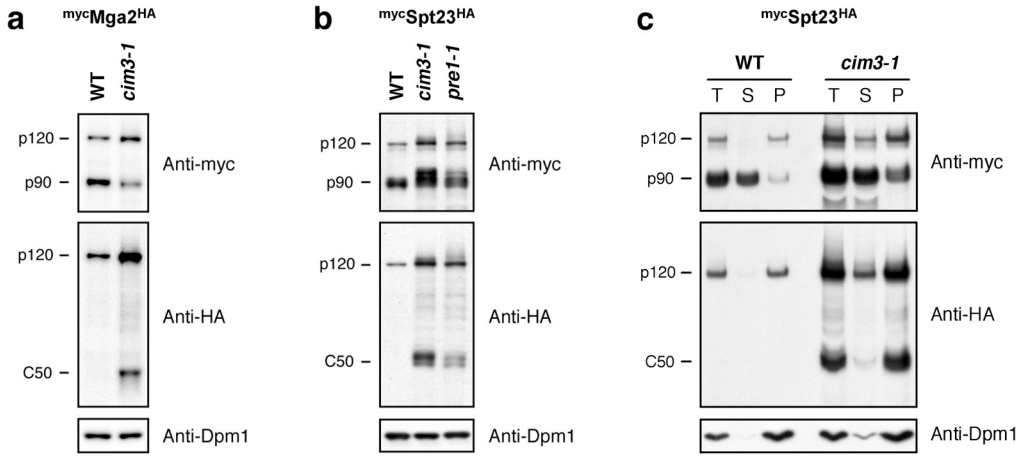

Figure 2-3. Accumulation of proteolytic intermediates of Spt23 and Mga2 in proteasome mutants. (**a**) Mga2 processing and (**b**) Spt23 processing in proteasome mutants gown at 37°C gives rise to an additional C-terminal C50 fragment. Note that Spt23 p90, a short-lived protein (Hoppe et al., 2000; Richly et al., 2005), is stabilized in the proteasome mutant (**c**) The C-terminal C50 fragment of Spt23 localizes to the ER membrane. Total extracts ("T") of WT or *cim3-1* cells expressing $^{myc}Spt23^{HA}$ were fractionated into pellet ("P") and soluble ("S") fractions. ER membrane protein Dpm1 was used as fractionation control.

able to block processing of Spt23 (Hoppe et al., 2000). This physiological regulation could therefore be used to demonstrate that C50 is indeed an intermediate of p120 processing by the proteasome, as UFAs abundances should influence C50 fragment formation in proteasome mutant cells. As expected, addition of palmitoleic acid to the growth medium of cells expressing ^{myc}Spt23^{HA}, led to the stabilization of the p120 precursor, inhibiting thereby the production of the N-terminal p90, and in *cim3-1* cells also the formation of the C-terminal C50 fragment (Figure 2-4a). This indicates that the production of both N- and C-terminal Spt23 fragments is controlled by the same physiological trigger.

To further demonstrate that the C50 fragment is formed from the Spt23 p120 precursor, a processing time-course experiment was performed. Mutant *cim3-1* cells expressing ^{myc}Spt23^{HA} were first grown in the presence of palmitoleic acid to inhibit processing of Spt23 and then transferred to a medium that lacks UFAs. After cycloheximide addition, samples were withdrawn at various time points and protein levels were determined by Western blot analysis. As shown in Figure 2-4b, both p90 and C50 accumulated over time *in vivo* with similar kinetics, and the fragment

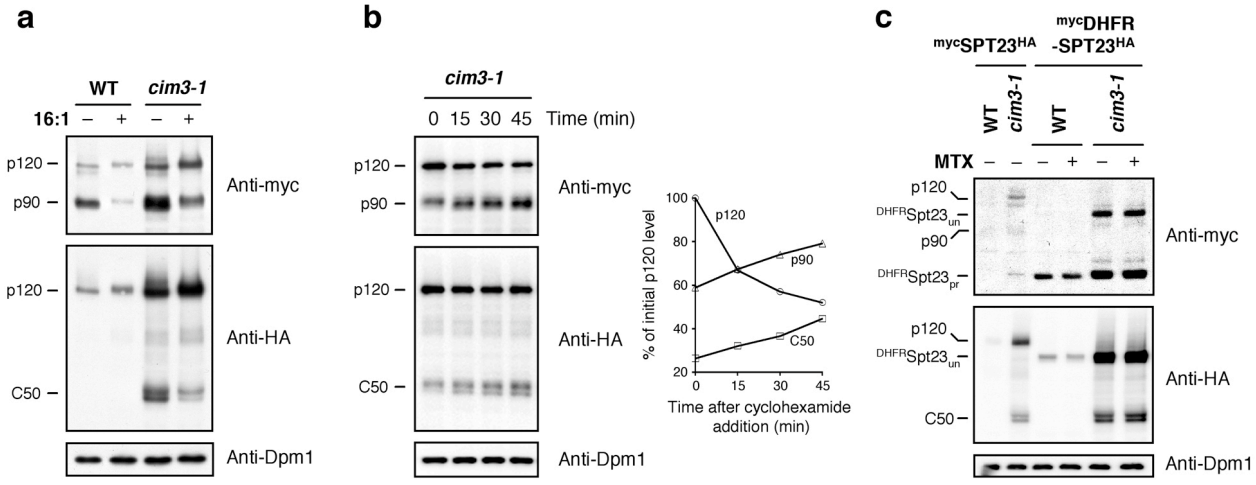

Figure 2-4. The C50 fragment is an intermediate of Spt23 proteasomal processing (**a**) Inhibition of processing of Spt23 by addition of palmitoleic acid (16:1) at 37°C for 90 min leads to reduced production of p90 and C50. (**b**) N- and C-terminal fragments (p90 and C50) of Spt23 are generated with similar kinetics and on expense of the full-length p120. Proteasome mutant cells (*cim3-1*) were grown at room temperature in palmitoleic acid-containing medium to block processing of ^{myc}Spt23^{HA} and were subsequently shifted to 37°C to induce proteasome defects. Cells were transferred to palmitoleic acid-free medium and cycloheximide was added to the culture to block translation. Samples were withdrawn after indicated times and subjected to Western analysis. The graph shows the quantification of the data. Detected signals were normalized to the loading control and to the level of p120 at the 0 time point. (**c**) The C50 fragment is not produced by degradation of Spt23 initiated from N-terminus. DHFR fusion to N-terminus of Spt23 lacking residues 1-446 (^{myc}DHFR-Spt23^{HA}) does not interfere with C50 formation in *cim3-1* cells grown at 37° C in presence of MTX ("+"). Precursor (^{DHFR}Spt23$_{un}$), processed form (^{DHFR}Spt23$_{pr}$) of the fusion protein and C50 fragments are indicated.

accumulation was on expense of the p120 precursor. This finding confirmed that p90 and C50 are derived from the p120 precursor and that both fragments were produced concurrently in the proteasomal processing reaction.

To confirm that the C50 fragment resulted entirely from internally initiated processing reaction, an N-terminal DHFR fusion to Spt23 was created. In this construct, the N-terminal transcription factor domain (residues 1 to 446) was replaced by the DHFR protein (^{myc}DHFR-Spt23^{HA}). The fusion protein was efficiently processed and, when tested in *cim3-1* mutant cells, showed the same C50 fragment as observed previously (Figure 2-4c). Formation of this product was not changed by the addition of MTX, which stabilizes the N-terminus against initiation of proteasomal degradation. Thus, the obtained result demonstrates that the C50 fragment does not derive from N-terminally initiated degradation of Spt23 but only from internally initiated processing.

Altogether, the above findings show that proteasome mutants are useful tools to detect the otherwise short-lived C-terminal intermediates of Spt23 and Mga2 processing, which is initiated by endoproteolytic cleavage of the polypeptide chains.

2.1.3. Mapping of the processing initiation site

The results presented above suggested that the processing initiation site might be located in the region between the p90 and C50 fragments. Deletion of this part of the protein, supposedly forming a putative hairpin loop engaging the proteasome, should therefore interfere with the processing of Spt23. As both p90 and C50 migrate as a collection of bands, only a rough estimation of the sizes was possible. By creating truncation forms of Spt23, p90 was found to be composed of about 680 N-terminal residues, whereas C50 of the 300 C-terminal residues of Spt23 (Figure 2-5b). This indicated that the initial cleavage site should be located in the region between amino acids 680 and 782, containing the ankyrin repeats in the central part. Based on the yeast proteasome crystal structure, Rape and Jentsch deduced that the distance from the outside of the 20S proteasome to the active sites equals approximately 20 amino acids of an extended polypeptide chain and proposed that a stretched hairpin loop should be at least 40 amino acids in size (Groll et al., 1997; Rape and Jentsch, 2002). Hence, the central ankyrin repeat-containing region fulfils the length criteria for building up the proposed hairpin loop. However, deletion of the ankyrin repeat

domain alone (Spt23Δ709-771) did not abolish processing (Figure 2-5c; in fact it moderately induced processing), indicating that the ankyrin repeat itself is not the crucial processing signal. Interestingly, also deletions of sequences that directly flank the ankyrin repeats (Spt23Δ651-708, Spt23Δ775-814), or even of the entire 164 amino acids ankyrin repeat-containing region, only moderately interfered with Spt23 p90 formation (Figure 2-5a,c).

These findings suggest that the elements that promote processing from an internal site may be redundant and do not seem to be equivalent to specific amino acid sequences. In fact, the observation that the fragments produced by proteasomal processing are not homogenous in size is consistent with this observation. These

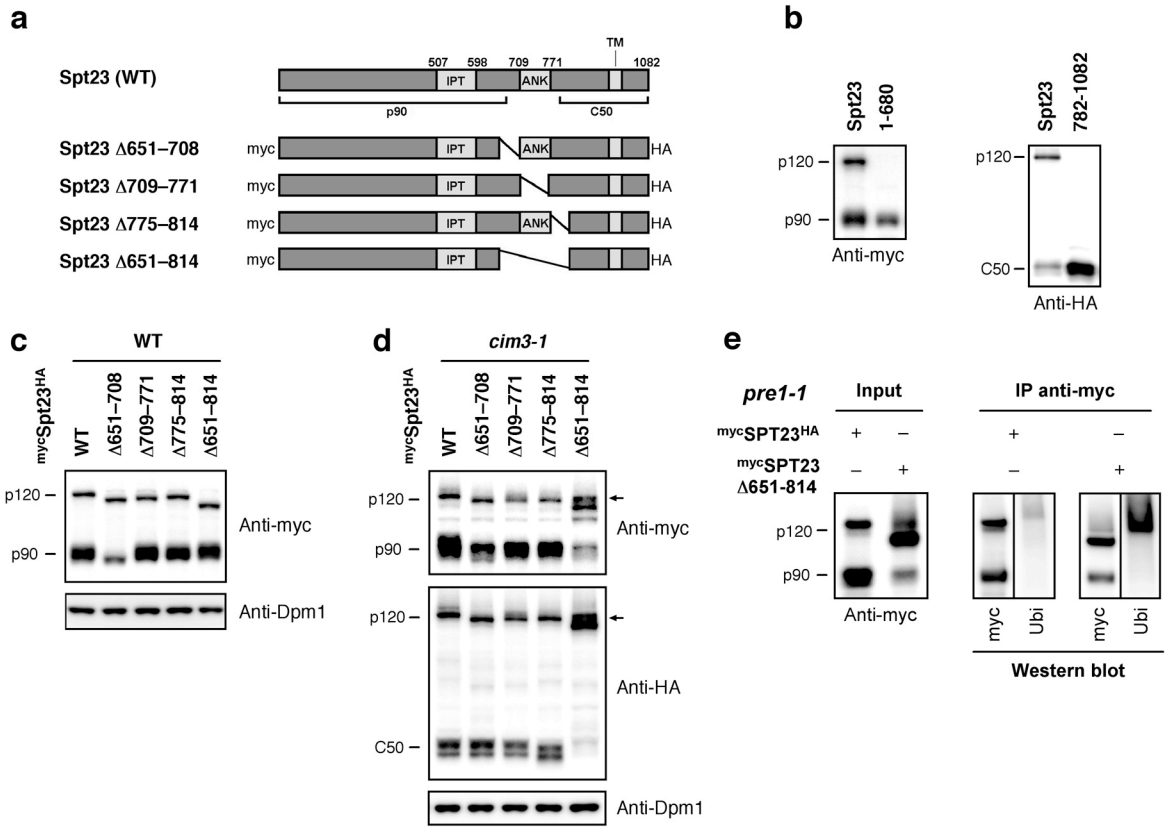

Figure 2-5. Mapping of the processing initiation site. (**a**) Schematic representation of Spt23 deletion mutants used for processing initiation site mapping. (**b**) Size estimation of p90 and C50 fragments. Constructs composed of N-terminal 680 and C-terminal 302 residues were found to migrate in SDS-PAGE similarly to p90 and C50, respectively. Epitopes used for detection are the same as in ^{myc}Spt23^{HA} (control lanes). (**c**,**d**) Processing of ^{myc}Spt23^{HA} deletion mutants. Various deletion mutants of Spt23 within the ankyrin repeat-containing region were assayed for processing in WT cells (**c**) and *cim3-1* mutant cells (**d**). None of the introduced deletions was able to abolish processing of Spt23 in WT cells. However, deletion of the entire ankyrin-containing region (Δ651-814) leads to inhibition of the processing in *cim3-1* mutant cells grown at 37 °C, as p120Δ651-814 and its monoubiquitylated form (indicated by an arrow) are strongly stabilized and p90 and C50 fragments are diminished. (**e**) Anti-myc immunoprecipitation under denaturing conditions of ^{myc}Spt23^{HA} or ^{myc}Spt23Δ651-814 proteins expressed from *GAL1-10* promoter in *pre1-1* cells grown at 37 °C. The crude extract input is shown in left panel. The immunoprecipitated material (right panel) was analyzed by immunoblots with anti-myc (left lines) and anti-ubiquitin (right lines) antibodies.

results implicate also that the nature of the defects in *cim3-1* and *pre1-1* mutants is a loss of processivity of the enzymatic reaction, as the proteasomes are able to initiate and continue degradation of short fragments, but cannot complete the degradation (e.g. due to diminished substrate unfolding activity of the 19S ATPases).

Interestingly, in *cim3-1* cells grown at the non-permissive temperature, expression of the ^{myc}Spt23Δ651-814^{HA} construct did not result in formation of the C50 fragment and the p120 form was strongly stabilized (Figure 2-5d). Since the abundance of p90 was also diminished, this was likely due to processing inhibition of this Spt23 mutant. Moreover, a band migrating slower than p120Δ651-814 accumulated strongly and could represent a monoubiquitylated precursor form. To confirm the identity of this modification, lysates from proteasome mutants cells grown at the non-permissive temperature and overexpressing ^{myc}Spt23^{HA} or ^{myc}Spt23Δ651-814 were subjected to anti-myc immunoprecipitation under denaturing conditions and the precipitated material was analyzed by Western blot against ubiquitin (Figure 2-5e). This experiment revealed that indeed short ubiquitin conjugates are formed on the p120 precursor of normal and mutant Spt23, and the p120 monoubiquitylation signal co-migrates with the previously detected slower migrating band (compare anti-myc and anti-ubiquitin blots). This result suggests that although p120Δ651-814 is ubiquitylated, it is not a good substrate for processing by functionally impaired proteasomes. As processing of Spt23Δ651-814 could only be inhibited in the *cim3-1* mutant but not in WT cells, this suggests that the removed region serves as a primary processing initiation site, and that the engagement of an alternative site requires full proteasomal activity. Efficient processing of Spt23Δ651-814 may require generation of a loop by local unfolding of the sequence neighbouring the yet

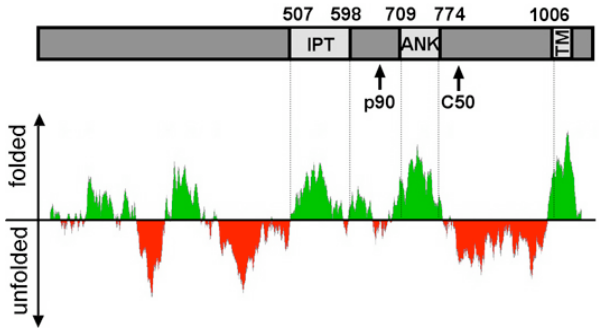

Figure 2-6. Folding prediction for Spt23. FoldIndex graph shows tendency for folding of Spt23. Folded (green) and unfolded (red) regions, p90 and C50 approximate sizes are indicated. The C-terminus of Spt23 is largely unfolded, indicating that it may serve as the initiation site for processing.

unidentified ubiquitylation site. This result suggests also that the *cim3-1* mutation most likely impairs the unfolding activity of the proteasome and therefore creation of an alternative initiation site.

Analysis of the Spt23 amino acid sequence with the protein folding prediction program FoldIndex (Prilusky et al., 2005) revealed a tendency for an unfolded conformation of the whole C-terminal region of Spt23, starting with the sequence following ankyrin repeats up to the TM span (Figure 2-6). This suggests that this region might be able to form the initiation loop/loops. In addition, also the region located between the IPT domain and ankyrin repeats contains an unfolded stretch, which could serve as an initiation site. The folding prediction may explain as well why the proteasome removes the C-terminal part of Spt23 p120 so rapidly, since it may lack any structured regions that might be difficult to unfold and translocate into the proteasomal cavity. Moreover, after the initial recruitment by the ubiquitin signal, the proteasome may easier remodel this loosely folded part of Spt23 and therefore create the alternative processing initiation loop.

2.1.4. The IPT domain stops proteasome degradation progression

As shown above, the production of stable Spt23/Mga2 C-terminal fragments by 26S proteasomes can be observed either when complete degradation is prevented by tightly folded barriers (e.g. DHFR), or if the proteasome is functionally impaired by mutation. It was previously reported that some tightly folded proteins are more resistant to unfolding by ATPases (Lee et al., 2001). It was therefore interesting to investigate whether formation of the p90 fragments of Spt23/Mga2 involves a stable structure resistant to proteasome action. A good candidate for such a barrier is the IPT domain, since crystallographic studies showed that dimerized NFκB IPT domains exhibit very stable immunoglobulin-like folds (Ghosh et al., 1995; Huang et al., 1997; Muller et al., 1995). Moreover, deletion of the IPT domain from NFκB or Spt23/Mga2 abolishes their processing (Lin et al., 2000; Rape et al., 2001; Shcherbik et al., 2004). This suggests that the IPT domain may be specifically required for the generation of the processing products, or it is necessary to define these proteins as proteasome substrates.

To address this question, Spt23WT or Spt23ΔIPT variants (Figure 2-7a) were expressed in the *cim3-1* proteasome mutant cells. Interestingly, the C-terminal C50 fragment that is specific for cells expressing functionally impaired proteasomes was produced regardless whether the IPT domain was present or not (Figure 2-7b). This indicates that the IPT domain itself is not essential for Spt23 proteolysis. However, expression of Spt23ΔIPT in this mutant led to the accumulation of novel N-terminal fragments (N75). This suggests that certain more stably folded regions within the N-

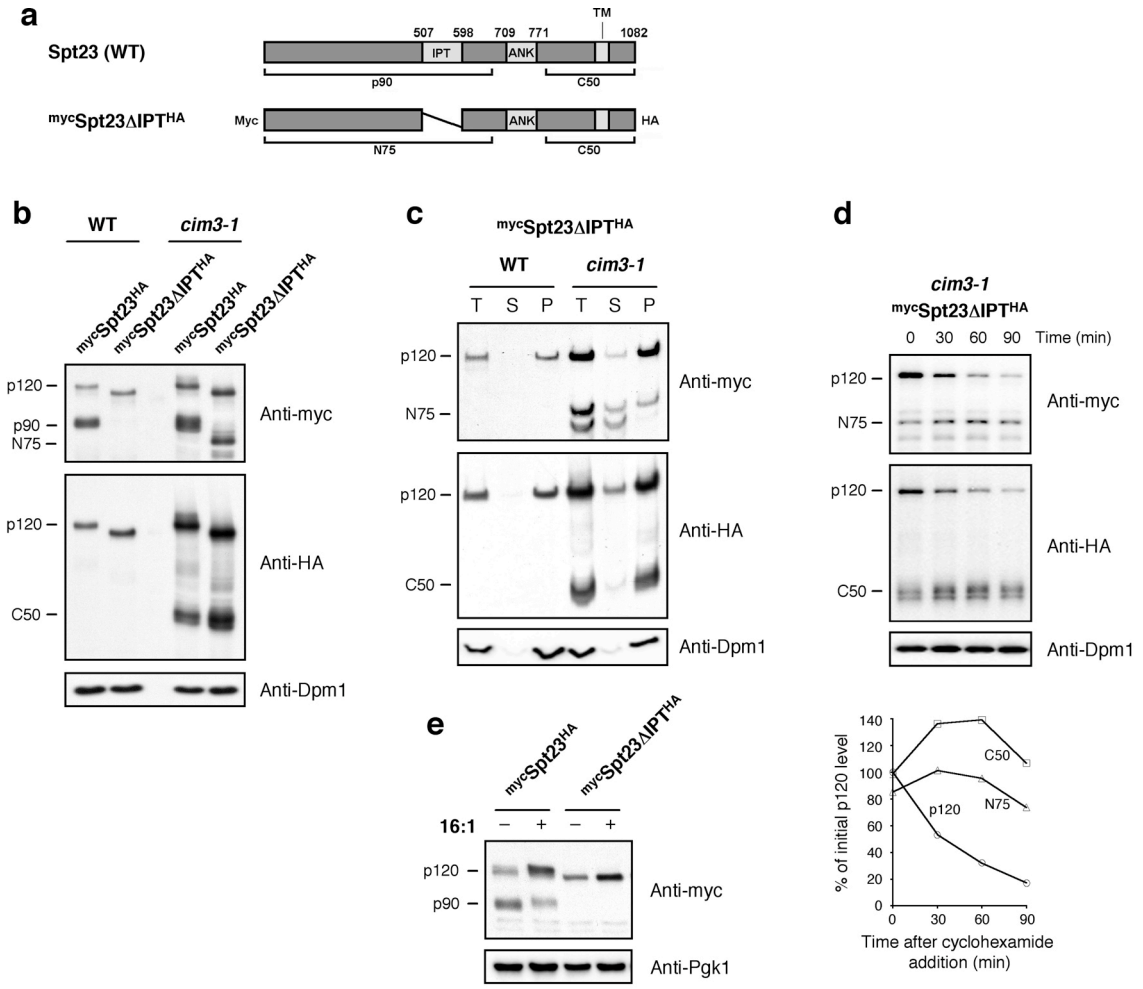

Figure 2-7. The alternative to Spt23 processing is complete degradation. (**a**) Schematic representation of Spt23 WT and an Spt23 variant that lacks the IPT domain (Spt23ΔIPT), and of the corresponding N- and C-terminal fragments (brackets) observed in the *cim3-1* proteasome mutant (p90, N75, C50). (**b**) Detection of Spt23 WT and Spt23ΔIPT-derived fragments in WT and *cim3-1* mutant cells. The level of total protein of Spt23ΔIPT is reduced to about 40% of WT Spt23 (quantification not shown). Note that the full-length Spt23 is stabilized in the *cim3-1* mutant, indicating that WT proteasomes completely degrade Spt23 if the IPT domain is absent. (**c**) ER membrane localization of the C50 fragment. Lysates from WT and *cim3-1* cells expressing Spt23ΔIPT, grown at 37 °C were subjected to membrane fractionation. Dpm1 was used as the fractionation control. (**d**) Kinetics of N75 and C50 formation from Spt23ΔIPT precursor in *cim3-1* cells. The experiment was performed as in Figure 2-4b. (**e**) Addition of palmitoleic acid (16:1) not only inhibits processing of WT Spt23, but also inhibits complete degradation of the Spt23ΔIPT variant.

terminal domain of Spt23 (besides the IPT domain) hinder complete degradation, but only in cells that express functionally impaired proteasomes. In addition, fractionation experiment showed that the C50 fragment was exclusively localized to the ER membranes, while most of N75 was soluble (Figure 2-7c). Interestingly, the most abundant fragment from N75 was partially localized to the pellet fraction, indicating that there are additional regions besides the IPT domain that mediate or stabilize Spt23 dimers. In addition, when the dimerization mutant turnover was investigated in *cim3-1*, it showed concomitant formation of both the N75 and C50 fragments from the precursor form (Figure 2-7d). These results suggest that the N75 form is an equivalent to Spt23 p90, since its formation is initiated by the same way, although it differs by the mechanism by which proteasomal progression is halted (proteasome defect versus stable IPT domain, respectively).

All these data support the hypothesis that the alternative to Spt23 processing is complete degradation. Indeed, in Spt23ΔIPT-expressing cells not only p90 was absent, but the total amount of the Spt23 protein was concurrently reduced to less than 40% (Figure 2-7b). Intriguingly, addition of palmitoleic acid to the growth medium not only down-regulated Spt23 WT processing, but also led to a significant stabilization of the unprocessed Spt23ΔIPT variant (Figure 2-7e). Together, these data suggest that the cellular signal (low concentration of unsaturated fatty acids) triggers proteasomal degradation of Spt23, which normally leads to processing due to the presence of the IPT domain. However, the same conditions will cause complete Spt23 degradation, if the IPT domain has been experimentally removed.

2.1.5. Complete degradation can be initiated internally

Given the finding that *in vivo* proteasomes can initiate processing of Spt23/Mga2 from a centrally located polypeptide loop, it was tempting to speculate that this mechanism can be applied more generally also for the complete proteasomal degradation of substrates. One of the proteins that undergoes rapid, regulated degradation by UPS is an integral ER-membrane protein Hmg2, which is one of two isozymes of yeast HMG-CoA reductases (HMGR), the rate-limiting enzymes in cholesterol biosynthesis (Hampton and Rine, 1994). Degradation of Hmg2 involves key players of the ERAD (ER-associated degradation) machinery and was shown to be tightly regulated by certain physiological cues, with its half-life varying between 5-

10 min and 6h (Bays et al., 2001; Hampton and Rine, 1994). Hmg2 is composed of a large N-terminal transmembrane region and a C-terminal cytosolic catalytic domain, both connected by a not conserved linker region. Interestingly, the individual transmembrane spans that are connected by polypeptide loops facing the cytosol, as well as the flexible linker region between the transmembrane and catalytic domains, could serve as possible internal initiation sites for proteasomal degradation.

To test the hypothesis that degradation of Hmg2 can be initiated from an internal site, the turnover of the short-lived variant of Hmg2 that carries a myc epitope tag close to the N-terminus (^{6myc}Hmg2; Hampton et al., 1996) was investigated. In order to detect also C-terminal proteolytic fragments, an HA-tag was added to its C-terminus (^{6myc}Hmg2^{HA}). As expected, also this doubly tagged Hmg2 variant was rapidly degraded in WT and strongly stabilized in the *cim3-1* proteasome mutant strain (Figure 2-8a). Yet, concomitant with the slow decay of the full-length protein in the proteasome mutant, several anti-myc and anti-HA-reactive fragments appeared during the chase period. Notably, both N- and C-terminal fragments accumulated with similar kinetics, suggesting that the degradation of Hmg2 via ERAD is most likely initiated from an internal site (or several internal sites). Moreover, since many of these N- and C-terminal fragments localized to the microsomal pellet fraction (Figure 2-8b), these findings also indicate that the observed proteasomal ERAD mechanism takes place directly at the ER membrane prior to the substrate retrotranslocation.

It was reported that he half-life of Hmg2 is regulated by ubiquitylation catalyzed by the integral ER membrane ubiquitin ligase Hrd1. Since this enzyme is not essential for yeast viability, it was possible to directly investigate how ubiquitylation of Hmg2 influences the appearance of degradation intermediates. The experiment with *cim3-1* Δ*hrd1* cells expressing ^{6myc}Hmg2^{HA} grown at 37 °C revealed that the full-length protein was stabilized and the formation of both the N- and C-terminal degradation intermediates was strongly reduced, as compared to *cim3-1* cells (Figure 2-8c). These degradation products were not completely absent, suggesting that additional pathways may contribute to the degradation of ^{6myc}Hmg2^{HA}.

Together these results demonstrated that the degradation of Hmg2 induced by the E3 ligase responsible for its natural regulation *in vivo* is initiated from an internal site. This suggests a more general mechanism by which flexible polypeptide loops flanked by folded regions may often serve as internal initiation sites for degradation.

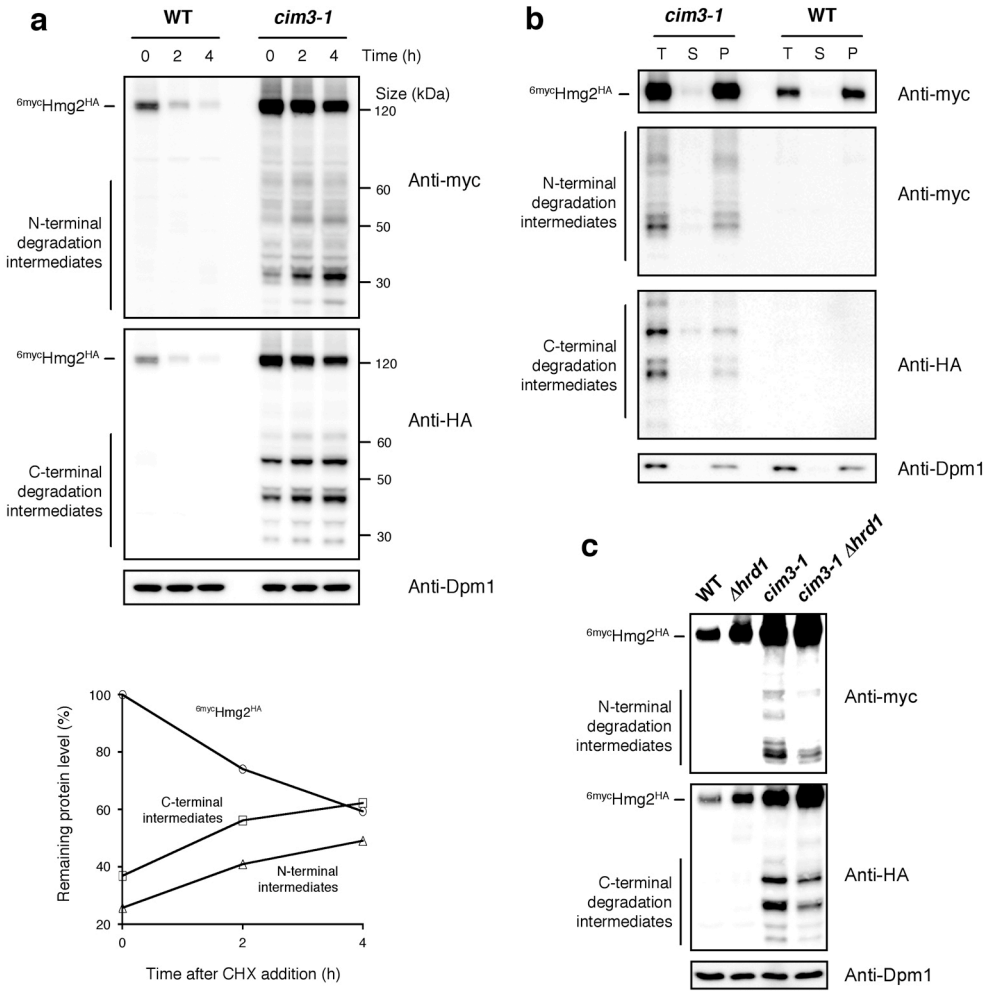

Figure 2-8. Degradation of Hmg2 by ERAD gives rise to both N- and C-terminal fragments in proteasome mutants. (**a**) WT and *cim3-1* cells expressing doubly tagged $^{6myc}Hmg2^{HA}$ were grown at 37 °C to induce proteasomal activity defects in *cim3-1*. CHX was added to the cultures to inhibit translation and samples were withdrawn after indicated time points. N- and C-terminal fragments were detected using anti-myc and anti-HA-specific antibodies, respectively. Dpm1 levels were monitored for loading control. The decay of the full-length Hmg2 protein and the production of the degradation fragments were quantified (bottom panel). (**b**) N- and C-terminal degradation intermediates of $^{6myc}Hmg2^{HA}$ localize to the ER membrane. Membrane fractionation was performed for WT and *cim3-1* cells expressing $^{6myc}Hmg2^{HA}$ grown at 37 °C. Degradation intermediates formed in *cim3-1* are found in the pellet. ER-membrane-bound Dpm1 was used for fractionation control. (**c**) Formation of Hmg2 degradation intermediates is reduced in cells lacking Hrd1.

2.2. Regulation of Spt23/Mga2 activation by the ankyrin repeat domain

The processing of Spt23/Mga2 is strikingly similar to that of the mammalian NFκB precursors. In both cases, it requires ubiquitylation and the proteasome to eliminate C-terminal parts of the proteins, whereas the N-terminal transcription factor domains are spared from degradation. Further comparison of their domain compositions reveals more similarities (Figure 2-9). Precursors of all of these transcription factors posses centrally located IPT domains mediating dimerization and C-terminally located ankyrin repeat domains, which are completely degraded during the processing reaction. The conserved topology of these domains may reflect their similar functional relationship and suggest similar modes of processing regulation for yeast and mammalian transcription factors.

The ankyrin repeat is a 33-residue sequence motif and is one of most common structural constituents of proteins. It folds into two antiparallel α-helices followed by a β-hairpin or a long loop. In most cases, ankyrin repeats are found as tandem repeats and they are responsible for mediating various specific protein-protein interactions (Mosavi et al., 2004; Sedgwick and Smerdon, 1999).

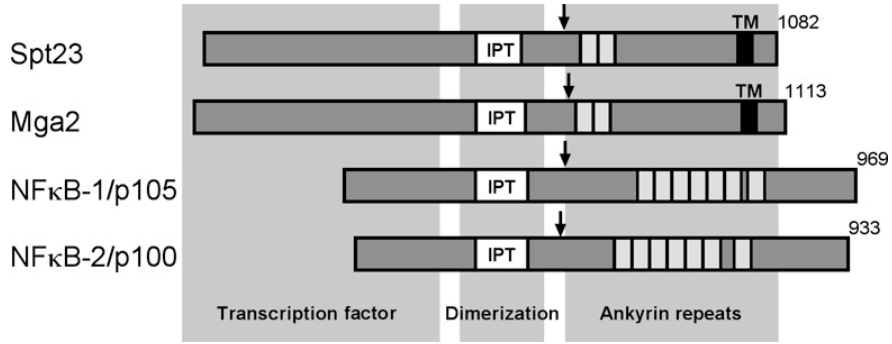

Figure 2-9. Yeast Spt23/Mga2 and mammalian NFκB transcription factors share domain homology. Transcription factor domains and dimerization domains (IPT) are located in the N-terminal and central parts of the proteins that are protected from proteasomal degradation. Ankyrin repeats (grey boxes) are located in the C-terminal parts of the proteins, which are completely removed upon proteasomal processing (processing sites are indicated by arrows). Spt23/Mga2 possess additionally a C-terminal transmembrane span (TM) anchoring the proteins in the ER membrane.

2.2.1. The ankyrin repeat domain interacts with the dimerization domain of Mga2

It was reported that p50, the processed form of the NFκB p105 subunit, binds ankyrin repeats of the p105 precursor and inhibits its processing (Cohen et al., 2001). In

addition, crystal structure data provide evidence for an interaction of NFκB dimers with ankyrin repeats of IκB molecules that are homologous to the C-terminal ankyrin repeat domains of NFκB precursors (Huxford et al., 1998; Jacobs and Harrison, 1998). Interestingly, this interaction involves extensive contacts of ankyrin repeat domain with the dimerization surface formed by IPT domains and in addition extends to a downstream located NLS signal, masking it and preventing translocation of the protein to the nucleus (at least in case of the p65 subunit). As both the IPT and ankyrin repeat domains are present also in the p120 precursor of Spt23/Mga2 and are both highly conserved between most of their fungal orthologs, this suggests a common mechanism of interaction and perhaps regulation of processing.

To test whether the ankyrin repeat and dimerization domains of the yeast transcription factors can interact, an Mga2 variant with the TEV protease site introduced between the IPT domain and the ankyrin repeats (amino acids 671-678 of Mga2 replaced with the ENLYFQG sequence) was generated. The construct was additionally tagged with myc and HA epitopes at the N- and C-terminus, respectively (^{myc}Mga2(TEV)^{HA}; Figure 2-10a). This experimental approach allows separation of the N- and C- terminal parts of Mga2 upon cleavage of the specific site by the TEV protease, in a proteasome-independent way (that would normally lead to a complete elimination of the C-terminus) and assaying if they are still associated. As shown in Figure 2-10b, the introduced TEV site did not interfere with the processing reaction as compared to the WT protein. Lysates from Δ*mga2* cells overexpressing ^{myc}Mga2(TEV)^{HA} under the control of *GAL1-10* promoter were incubated with 0.2% dodecyl maltoside to extract Mga2 from membranes and subsequently subjected to immunoprecipitation with anti-HA antibodies to pull down precursor forms of ^{myc}Mga2(TEV)^{HA}. Beads containing immunoprecipitated material were split into two parts, which were then incubated with or without the TEV protease. The beads were subsequently washed and bound proteins were analyzed by Western blots against N- or C-terminal tags (Figure 2-10c). In this experiment, Mga2(TEV) p120 was pulled down together with a minor pool of the associated p90 form. Immunoprecipitated proteins were efficiently cleaved by the TEV protease and a significant pool of the N-terminal cleavage fragment remained associated with the C-terminal part immobilized on the beads. In a similar experiment with microsomes isolated from cells expressing ^{myc}Mga2(TEV)^{HA} and treated with or without the TEV protease, analogous results

were obtained (Figure 2-10d). After centrifugation and separation of the soluble material, both N-terminal and C-terminal cleavage products were found to be associated with the membrane fraction. These data demonstrate that the N- and C-terminal domains of Mga2 can interact, possibly via the IPT and ankyrin repeat domains.

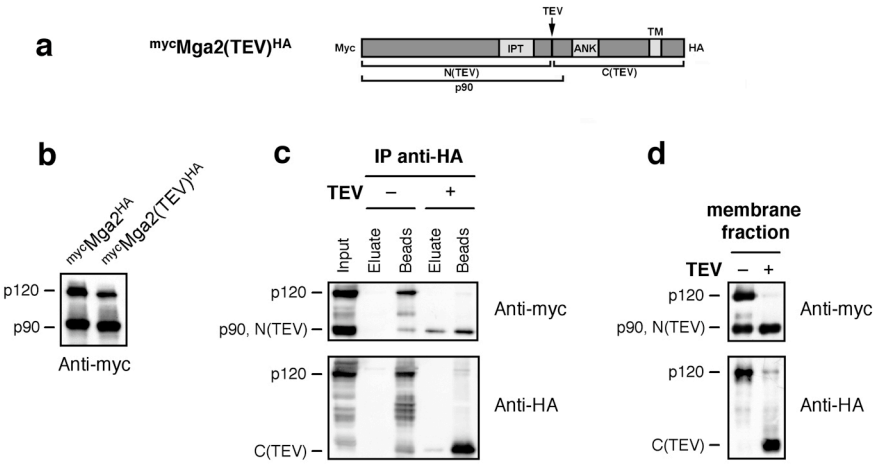

Figure 2-10. N- and C-terminal parts of Mga2 can interact. (**a**) Schematic representation of the Mga2 construct with introduced TEV protease cleavage site (TEV). Approximate sizes of N- and C-terminal cleavage products (N(TEV) and C(TEV), respectively) and p90 are indicated by brackets. Note the roughly similar size of N(TEV) and p90 fragments. (**b**) Introduction of TEV site does not interfere with the processing. Lysates of Δ*mga2* cells expressing ^{myc}Mga2(TEV)^{HA} under the control of *GAL1-10* promoter were analyzed by Western blotting. (**c**) Beads with anti-HA immunoprecipitated ^{myc}Mga2(TEV)^{HA} were incubated in buffer without ("–") or with TEV protease ("+"). The material bound to beads ("Beads") and the released soluble proteins ("Eluate") were analyzed by immunoblots against N- and C-terminal tags (myc and HA, respectively) (**d**) Membrane fraction containing Mga2(TEV) protein was prepared by high spin centrifugation, incubated in the absence or presence of TEV protease and subjected to Western analysis. (**c**,**d**) Input lane (**c**) contains lysate of cells used for the experiments. Investigated protein fragments are indicated. Note that p90 co-migrates in SDS-PAGE with the N(TEV) fragment.

To test whether the ankyrin repeat and dimerization domains are able to interact directly, the yeast two-hybrid system was employed. Mga2 domain composition (Figure 2-11) was predicted using the protein domains architecture program SMART (Letunic et al., 2006). In all of the created constructs, the transcription activation domain (TAD) was omitted in order to avoid previously reported autoactivation (Zhang et al., 1997). Even though, Mga2 and some of its truncations exhibited strong activation of reporter promoters, which for some of the constructs could be blocked by addition of various concentrations of 3-aminotriazole (see Materials and Methods). Also the TM span and the ER-lumenal domain were not included in any of the constructs to avoid membrane insertion and permit nuclear localization. Truncations of Mga2 that contained the IPT domain were used as baits for testing interactions with constructs containing the ankyrin repeat domain. The results of this experiment

confirmed that the ankyrin repeat and IPT domains interact (Figure 2-11). All baits interacted with the ankyrin repeat-containing constructs, however, not with the ankyrin repeats alone. This suggests that the two isolated ankyrin repeats may form only part of the interaction surface and do not bind to the IPT domain strong enough to activate the reporter system. Interestingly, it has been reported that terminal ankyrin repeats are difficult to detect by protein domain architecture analysis programs, as they often vary in many otherwise well-conserved hydrophobic residues from the consensus sequence (Mosavi et al., 2004). It is therefore conceivable that perhaps another not predicted ankyrin repeat stabilizes the structure and binding to the IPT domain of Mga2. In any case, binding of the C-terminal region of Mga2 to the IPT domain clearly depends on all ankyrin repeats as a point mutation in the second repeat (*ANK**; consensus site LHFA mutated to AAFP; according to Mosavi et al., 2002) abolished the interaction (Figure 2-11). The results presented above strongly suggest that the interactions mediated by the ankyrin repeats are conserved between the yeast Mga2/Spt23 and the mammalian NFκB transcription factors.

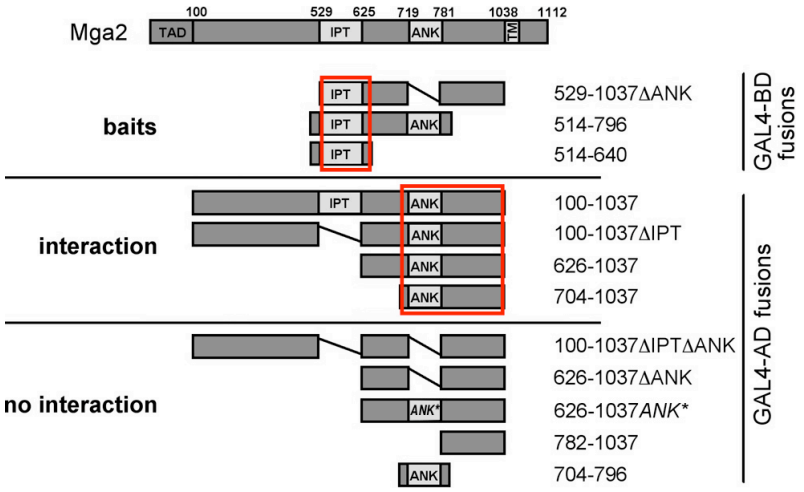

Figure 2-11. Ankyrin repeat and dimerization domains of Mga2 interact. Schematic representation of the yeast two-hybrid interactions between Mga2 ankyrin repeat (ANK) and dimerization (IPT) domains containing constructs. Truncations used for the assay, fused to GAL4 activation (AD) or DNA binding (BD) domains, are described by the respective numbers of residues from Mga2 (right panel). Additional mutations are indicated. The minimal fragments of Mga2 required for the interaction are highlighted by red boxes. The observed interaction with IPT domain depends strictly on the presence of ankyrin repeats, seems however to be additionally stabilized by downstream regions, as the isolated ANK truncation does not sustain the interaction.

2.2.2. Deletion of the ankyrin repeat domain destabilizes Mga2

To investigate the functional importance of the ankyrin repeats of Mga2, constructs that lack this domain (Mga2ΔANK) were created and compared with full-length forms of the protein. Western blot analysis of lysates from WT cells expressing normal ^{myc}Mga2 or mutant ^{myc}Mga2ΔANK constructs under the control of endogenous or *GAL1-10* promoters revealed that although both forms are efficiently processed, the total abundance of the protein lacking the ankyrin repeat domain was reduced to about 65% (Figure 2-12a). This indicates that the deletion of the ankyrin repeats destabilizes the protein. In fact, quantification of p120 and p90 abundances showed that the precursor form is stronger influenced by the deletion, so that the processing efficiency (ratio of p90 to p120 abundances) increases. This suggests that this mutation may affect the turnover of the precursor protein by increasing the processing of Mga2.

To test this hypothesis, the half-life kinetics of Mga2WT and Mga2ΔANK were investigated by the *GAL1-10* promoter shut-off experiment. This experiment revealed that WT Mga2 p120 and p90 forms are very stable with half-lives of a few hours (Figure 2-12b; upper panel). In contrast, when the ^{myc}Mga2ΔANK variant was

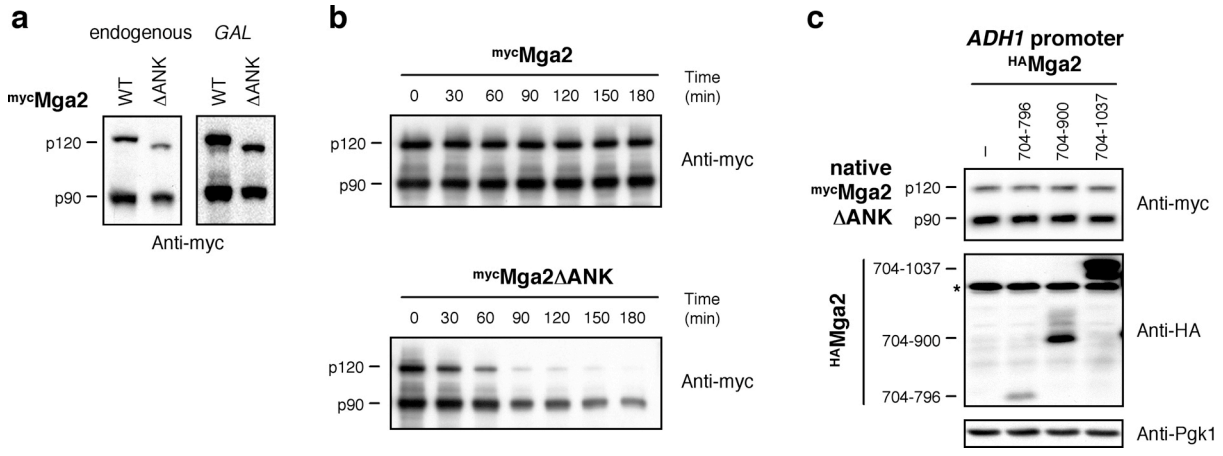

Figure 2-12. Deletion of the ankyrin repeat domain influences the stability of Mga2 p120 and p90. (**a**) Expression of WT and ΔANK forms of Mga2 from endogenous or the *GAL* promoters was investigated by Western blot analysis. (**b**) *GAL* promoter shut-off experiment for WT cells expressing Mga2 and Mga2ΔANK grown at RT. The ankyrin repeats mutation destabilized, the otherwise very stable, p120 and p90 forms. (**c**) Overexpression of the ankyrin repeats does not lead to the stabilization of the p120 form of the endogenously expressed ^{myc}Mga2ΔANK. The constructs 704-1037 and 704-900 containing the ankyrin repeat domain are truncations of Mga2 that were previously identified in YTH assay (Figure 2-11) to be sufficient to interact with the IPT domain. All truncation constructs are tagged with the HA epitope at their N-termini and are expressed under the control of the *ADH1* promoter. "-" denotes empty vector control; an asterisk indicates a crossreactive band. Pgk1 was used as a loading control.

examined, both p120 and p90 became unstable with half-lives of about 45 min and 2.5 h, respectively (Figure 2-12b; lower panel). The reason for the observed destabilization of p90 must be caused indirectly by the ankyrin repeats deletion, as the p90 fragment seems not to contain the ankyrin repeats (note that p90 expressed from the Mga2WT protein migrates at the same height on the SDS gel as p90 from the Mga2ΔANK variant; Figure 2-12). Interestingly, overexpression of various Mga2 constructs containing ankyrin repeats did not cause a stabilization of the p120 precursor of the Mga2ΔANK mutant protein (Fig2-12c). This may suggest that the interaction between the ankyrin repeat and the IPT domain is functional only if it occurs in the same p120 molecule (intramolecular interaction).

2.2.3. Deletion of the ankyrin repeat domain leads to enhanced activation of Mga2

Decreased stability of the Mga2ΔANK variant suggests that its activity may be compromised as well. The Mga2ΔANK mutant protein was therefore tested for its ability to rescue the synthetically lethal mutant Δ*spt23* Δ*mga2*. This mutant strain is inviable due to the absence of the Ole1 protein and therefore insufficient levels of UFAs. However, the viability of Δ*spt23* Δ*mga2* can be restored by heterologous expression of *OLE1* or by addition of oleic acid (the product of the Ole1 enzymatic activity) to the growth medium (Zhang et al., 1999). Δ*spt23* Δ*mga2* mutant cells were transformed with low copy vectors expressing ^{myc}Mga2 or ^{myc}Mga2ΔANK from their endogenous promoters and tested in serial dilutions for their ability to grow on plates with or without oleic acid supplement (Figure 2-13a). Both Mga2WT and Mga2ΔANK were able to restore the viability of Δ*spt23* Δ*mga2* cells equally well, suggesting that the transcriptional activity of the Mga2ΔANK mutant protein is sufficient to maintain yeast cell viability.

The transcriptional activity of Mga2 and Mga2ΔANK was further assessed in a transcription reporter assay, in which the β-galactosidase-encoding gene placed under the control of the *OLE1* promoter is used as a reporter gene. To exclude activation of the reporter by the endogenous Spt23 and Mga2 proteins, the assay was performed in Δ*spt23* Δ*mga2* cells, whose viability was restored by heterologous expression of *OLE1* from the *ADH1* promoter. Subsequently, this reporter strain was transformed with ^{myc}Mga2 or ^{myc}Mga2ΔANK expressed from the endogenous

promoter. Finally, equal amounts of cells were plated and incubated at 30 °C. After 36 hours of growth, an X-Gal overlay assay was performed and the results were examined 90 min later. Surprisingly, the ^{myc}Mga2ΔANK mutant, although less abundant in cells, turned out to be stronger activator of transcription than the Mga2WT protein (Figure 2-13b). This result suggests that the ankyrin repeat domain might be a negative regulator of Mga2 activity. As the ankyrin repeats are not present in the p90 protein, this function may be achieved either by inhibition of p120 processing or translocation of p90 to the nucleus.

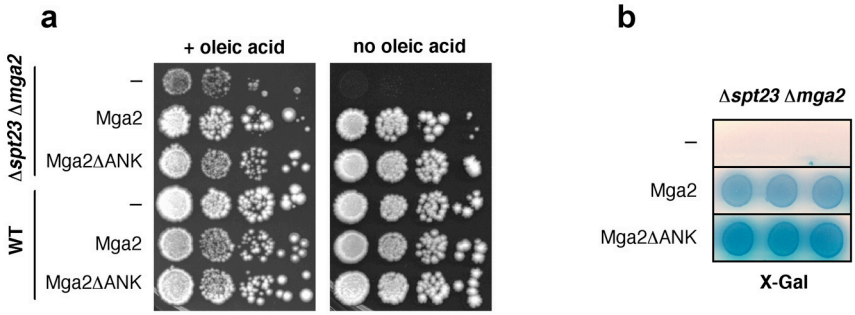

Figure 2-13. The ankyrin repeat domain is not required for the Mga2 essential function and negatively regulates its activity. (**a**) Mga2ΔANK is able to rescue Δ*mga2* Δ*spt23* cells indicating that this mutation does not interfere with Mga2 essential functions in yeast cells. WT and Δ*mga2* Δ*spt23* cells expressing normal or ΔANK form of Mga2, or transformed with empty vector as a control ("-"), were plated in 10-fold dilutions on synthetic media with or without oleic acid (18:1) supplement. Plates were incubated at 30 °C for 3 days. (**b**) Mga2ΔANK is a more potent transcription factor as compared to Mga2WT. Δ*mga2* Δ*spt23* cells rescued by the overexpression of Ole1 protein from the *ADH1* promoter and carrying the reporter gene under the control of *OLE1* promoter were transformed with Mga2, Mga2ΔANK or empty vector as a control. Equal amounts of cells (3 independent clones from each transformation) were plated on selective medium and after 36h of incubation at 30°C the X-Gal overlay assay was performed. After 90 minutes of incubation with the substrate at 30°C plates were scanned.

2.2.4. The ankyrin repeat domain controls localization of Mga2

Increased transcriptional activity of the Mga2ΔANK mutant protein in comparison with the Mga2WT protein suggests that the ankyrin repeats may influence the nuclear localization of the transcription factor Mga2 p90. To test whether deletion of ankyrin repeats changes the intracellular localization of Mga2, immunofluorescence microscopy was employed. Cells expressing ^{myc}Mga2 or ^{myc}Mga2ΔANK from the *GAL1-10* promoter were harvested in the exponential phase of growth, fixed with formaldehyde, and analyzed by indirect anti-myc deconvolution immunofluorescence microscopy (Figure 2-14a). Since the myc epitope of the investigated variants was fused to the N-terminus of Mga2, it allowed detection of both p120 and p90 forms.

This experiment revealed a striking difference in the localization of the investigated proteins. While Mga2WT showed predominantly ER and perinuclear staining, Mga2ΔANK was mainly nuclear. These results suggest that although the WT form of Mga2 is efficiently processed, only a minor pool of p90 is translocated into the nucleus. In contrast, the processed form of the Mga2ΔANK mutant protein is transported efficiently to the nucleus. This is in line with an earlier experiment (Figure 2-13b) showing that the transcriptional activity of the Mga2ΔANK mutant is increased in comparison to the WT protein. These findings suggest that the ankyrin repeat domain may be crucial for regulating Mga2 intracellular localization and function.

It was previously demonstrated that Mga2 p90 is kept in a dormant form at the ER membrane, presumably by association with the p120 partner molecule (Shcherbik et al., 2003). To test whether the ankyrin repeat domain-mediated interaction may directly contribute to the stability of the Mga2 p120/p90 complex, a membrane fractionation experiment was performed with extracts from cells expressing either the Mga2WT or the Mga2ΔANK mutant protein. Both Mga2 and Mga2ΔANK p90 forms were found in the soluble fraction and in the membrane bound p120/p90 heterodimeric complex (Figure 2-14b). The p120/p90 association could not be resolved by treatment with high salt, indicating a strong interaction. However, incubation of the membrane fraction with a high pH buffer led to a significant release of p90, confirming a peripheral membrane association. On the other hand, the p120 form proved to be an integral membrane protein, as it could only be extracted by

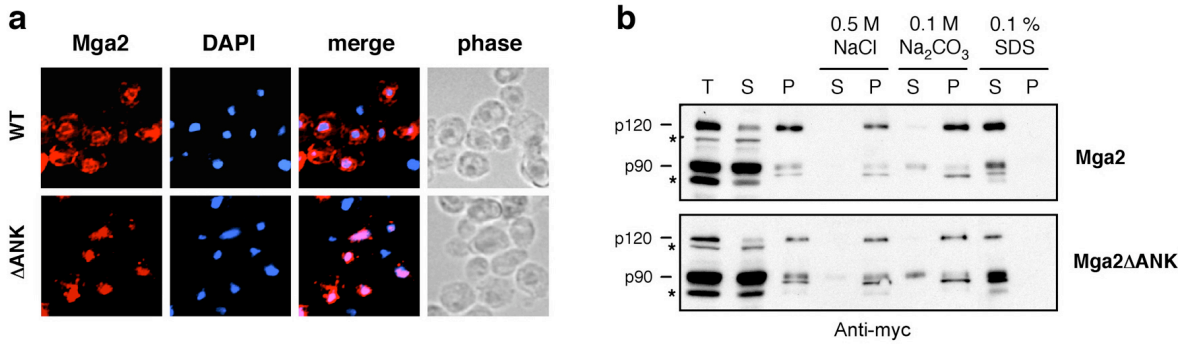

Figure 2-14. Ankyrin repeats inhibit nuclear localization of Mga2. (**a**) Intracellular localization of ^{myc}Mga2 and ^{myc}Mga2ΔANK was investigated by indirect anti-myc deconvolution immunofluorescence microscopy. WT form of Mga2 localizes to the ER and nuclear envelope, while the ΔANK mutant accumulates strongly in the nucleus. (**b**) Deletion of the ankyrin repeat domain does not change p120/p90 interaction strength. Membrane fraction from WT cells expressing Mga2 or Mga2ΔANK was treated with high salt buffer, high pH buffer or 0.1% SDS. "T" indicates whole cell extracts, "S" – soluble and "P" – membrane fractions. Asterisks denote crossreactive bands.

detergent treatment. Deletion of the ankyrin repeats did not significantly change the localization and interaction strength, suggesting that this domain is not crucial for stabilizing the association of p90 with the precursor molecule.

2.2.5. Degradation of Mga2 p120 and release of p90 is inhibited by the ankyrin repeat domain

Mga2 p120 seems to be degraded by an ERAD-related reaction involving the ubiquitin ligase Rsp5 and the $Cdc48^{Ufd1/Npl4}$ complex (Shcherbik et al., 2003). This process was proposed to liberate Mga2 p90 from the ER membrane. The deletion of the ankyrin repeats strongly destabilized Mga2 (Figure 2-12b), suggesting that this domain may regulate the ERAD of p120.

To test the involvement of Rsp5 and the $Cdc48^{Ufd1/Npl4}$ complex in the destabilization of Mga2ΔANK, expression shut-off assays in *rsp5-1* and *ufd1-2* (Ufd1 is an essential component of the $Cdc48^{Ufd1/Npl4}$ complex; Meyer et al., 2000) yeast mutants grown at the non-permissive temperature were performed. These experiments revealed that both Rsp5 and Ufd1 contribute to the enhanced degradation of p120ΔANK, as this deletion construct was stabilized in both *rsp5-1* and *ufd1-2* mutants when compared to WT cells (Figure 2-15a). Also the slow turnover of the p120WT protein was influenced in both mutant cells. Moreover, similar to the data reported for some ERAD substrates examined in *cdc48*, *ufd1* and *npl4* mutants (Bays et al., 2001; Jarosch et al., 2002), the ubiquitylated forms of p120 Mga2 and p120 Mga2ΔANK accumulated in *ufd1-2* cells. This suggests that both proteins are recognized and modified by the ubiquitin ligase Rsp5, and that the ankyrin repeats-mediated interaction might therefore inhibit a downstream step during the engagement of ubiquitylated substrates by the proteasome. This is further supported by a preliminary co-immunoprecipitation experiment showing that there is no enhanced binding of Rsp5 to Mga2ΔANK if compared to Mga2WT (data not shown).

Both *rsp5-1* and *ufd1-2* mutant cells strongly stabilized not only p120 but also the p90 form of Mga2ΔANK (Figure 2-15a). It is therefore possible that, similar to certain transcription factors that are controlled by degradation after transcription initiation (Muratani and Tansey, 2003), p90 is degraded once it has reached the nucleus and turned on the expression of *OLE1*. As shown by expression shut-off

(Figure 2-15a) and immunofluorescence (Figure 2-14a) experiments with the Mga2WT protein, the mobilization of p90 is slow, presumably because it is kept at the ER membrane in an inactive complex with the p120 form and thus remains stable. However, in case of the ankyrin repeats mutant protein, p90 is rapidly released from the ER and translocated to the nucleus where it can be degraded. In addition, degradation of p90 in the nucleus could also depend on Rsp5 and the Cdc48$^{Ufd1/Npl4}$ complex, similarly to the situation for Spt23 (Richly et al., 2005).

In the next experiment, the half-life of the Mga2ΔIPT mutant protein, whose dimerization and therefore the formation of p90 form is abolished (Figure 2-15b), was investigated. The expression shut-off experiments showed that Mga2ΔIPT is a short-

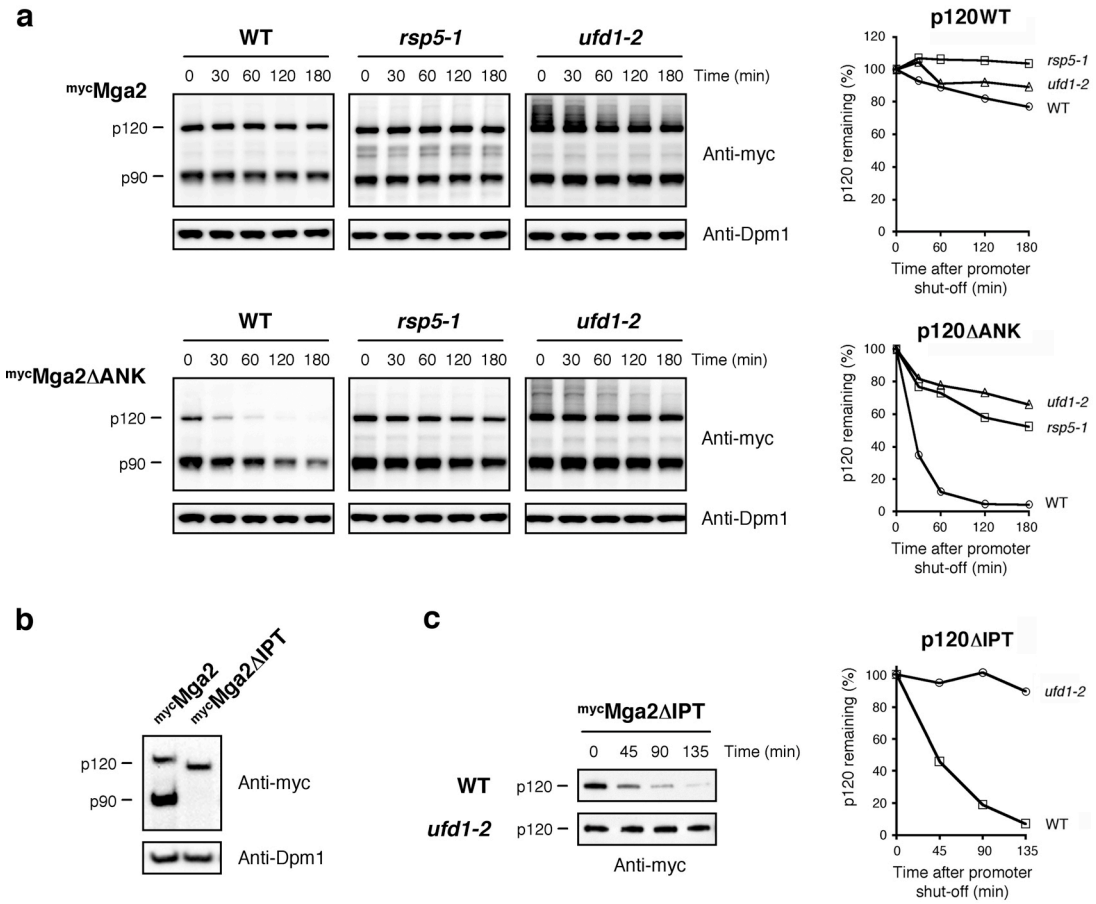

Figure 2-15. Ankyrin repeat domain of Mga2 inhibits Rsp5 and Cdc48$^{Ufd1/Npl4}$ mediated degradation of p120. (**a**) Increased degradation/processing of p120ΔANK can be significantly blocked in *rsp5-1* and *ufd1-2* mutants. *GAL* promoter shut-off experiments were performed for Mga2 and Mga2ΔANK expressed in WT, *rsp5-1* and *ufd1-2* mutants. The cells were grown in galactose containing medium at 30 °C to reach logarithmic phase of growth. Prior to glucose and CHX addition, the cells were incubated for 3h at non-permissive temperature (37 °C). Graph (right panel) shows quantification of p120WT or p120ΔANK decay under the investigated conditions. (**b**) Mga2ΔIPT mutant does not form the processed p90 fragment. (**c**) Mga2ΔIPT p120 form is unstable in WT, but strongly stabilized in *ufd1-2* mutant cells. *GAL* promoter shut-off experiment for Mga2ΔIPT expressed in WT or *ufd1-2* cells at 37 °C. Quantified data is presented on the graph (right panel).

lived protein in WT cells, but is stabilized in *ufd1-2* mutant cells (Figure 2-15c). The finding that deletion of the IPT domain causes destabilization of the Mga2 precursor, similarly to the deletion of the ankyrin repeats, supports the hypothesis that the intramolecular interaction between these two domains is responsible for the high stability of the Mga2WT precursor (compare Figure 2-15a and c). The fact that Mga2ΔIPT is stabilized in *ufd1-2* cells suggests that its degradation might involve the same machinery that is used to liberate the processed transcription factor from the processing template molecule.

Since the Mga2ΔANK variant is characterized by increased mobilization of p90, this deletion construct might be able to rescue yeast mutant phenotypes associated with reduced levels of the Ole1 protein. It was reported that the phenotype of the *ufd1-2* yeast mutant strain can be suppressed by addition of oleic acid to the growth medium (Hoppe et al., 2000), suggesting that the primary defect in these cells is associated with the OLE pathway. The Mga2ΔANK variant was tested in temperature sensitive *ufd1-2* mutant cells for the ability to promote their growth at non-permissive temperatures. Indeed, expression of the Mga2ΔANK but not the Mga2WT protein in this strain partially rescued its lethality at 34 °C (Figure 2-16a). To investigate how the deletion of the ankyrin repeats influences association of Mga2 p90 with ER membranes in the *ufd1-2* mutant, a membrane fractionation experiment was performed. While in WT cells about 60 % of Mga2WT p90 and 70 % of Mga2ΔANK p90 were found in the soluble fraction, in *ufd1-2* cells mobilization of Mga2WT p90 was impaired (about 40% of soluble p90). In contrast, the mobilization efficiency of Mga2ΔANK p90 in the *ufd1-2* background (70%) was comparable to that of WT cells (Figure 2-16b). These results suggest that, the mobilization of Mga2ΔANK p90 is at least partially independent of the $Cdc48^{Ufd1/Npl4}$ complex.

The deletion of the gene for the ubiquitin ligase Rsp5 in *S. cerevisiae* is lethal as it blocks processing of Spt23 and mobilization of Mga2 p90 and therefore the expression of *OLE1* (Hoppe et al., 2000; Shcherbik et al., 2003). However, the viability of the Δ*rsp5* strain can be restored by addition of oleic acid to the growth medium (Hoppe et al., 2000). To test whether Mga2ΔANK can also rescue the lethality of the Δ*rsp5* strain, cells were transformed with plasmids expressing either the Mga2WT or Mga2ΔANK protein under the control of the endogenous promoter. Interestingly, expression of the Mga2ΔANK but not of the Mga2WT protein could

restore the viability of Δ*rsp5* cells (Figure 2-16c), suggesting that the mobilization of p90 from p120ΔANK is mediated by an additional, Rsp5-independent mechanism. Next, the Mga2WT and Mga2ΔANK proteins expressed in the Δ*rsp5* strain (in the presence of oleic acid in the growth medium) were analyzed by immunoblotting, which revealed that the p90/p120 ratio of Mga2ΔANK was increased as compared to Mga2WT (Figure 2-16c; right panel). While the p90 form of the WT protein is less abundant than p120 and might therefore be part of the ER-bound heterodimeric complex, the p90 form of the Mga2ΔANK variant is more abundant than p120, indicating that a significant fraction of the protein is most likely soluble. Since degradation of Mga2 p120 requires Rsp5-mediated polyubiquitylation, it is tempting to speculate that the increased p90 mobilization of Mga2ΔANK in Δ*rsp5* strain could result from an action of the ubiquitin ligase responsible for targeting of Mga2 for processing. In the case of the Mga2ΔANK mutant protein, the p120 molecule from

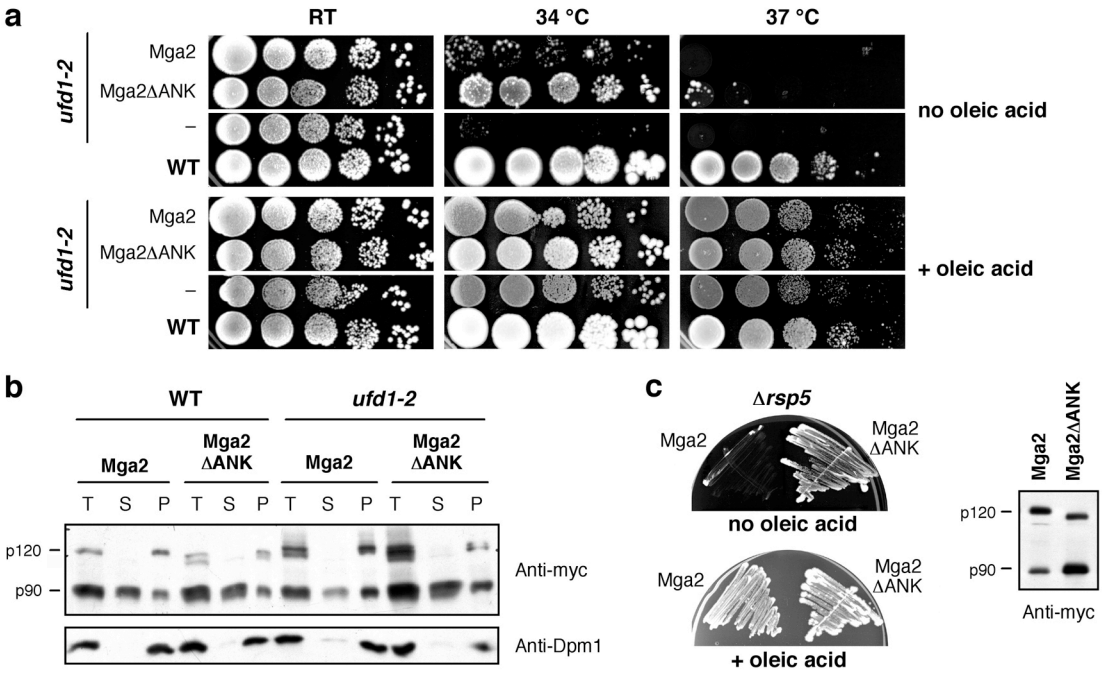

Figure 2-16. Mga2ΔANK expression can partially rescue *ufd1-2* cells grown at 34°C (**a**) **and rescue Δ*rsp5* mutant cells grown at RT** (**c**). (**a**) Equal amounts of *ufd1-2* cells expressing Mga2WT or ΔANK mutant constructs were plated in 10-fold dilution on YPD plates with or without oleic acid supplement and incubated at different temperatures for 3 days; "-" indicates empty vector control. (**b**) Mobilization of p90 is inhibited in *ufd1-2* strain for Mga2WT but not for the Mga2ΔANK protein. Membrane fractionation experiment for WT and *ufd1-2* cells expressing ^{myc}Mga2 and ^{myc}Mga2ΔANK grown at 37 °C. "T" indicates whole cell extracts, "S" – soluble and "P" – membrane fractions. Dpm1 was used as the fractionation control. (**c**) Δ*rsp5* cells were transformed with ^{myc}Mga2 or ^{myc}Mga2ΔANK constructs in the presence of oleic acid in the selection medium. Positive clones were further tested on plates with or without oleic acid for their ability to grow at RT. Cells from the rescue experiment were grown in YPD medium supplemented with oleic acid and analyzed by Western blotting (right panel).

the p120/p90 complex might be targeted for the proteasomal processing, which would lead to the formation of two soluble p90 fragments. Since the E3 ligase, which induces the processing of Mga2, has not been identified so far, this hypothesis could not be tested experimentally.

In conclusion, the results presented above suggest that the ankyrin repeat domain of Mga2 inhibits ERAD of the processing template molecule and thus mobilization of the active transcription factor p90 from the ER.

2.2.6. The ankyrin repeat domain inhibits processing of Mga2ΔTM

The finding that deletion of the ankyrin repeats of Mga2 influences mobilization of p90 by both Rsp5-dependent and -independent processes raised the question whether the latter mechanism may involve processing of the precursor from the p120/p90 complex. This would be in line with the observation that processing ratio of Mga2ΔANK was slightly increased in comparison to Mga2WT (Figure 2-12a).

Support for this hypothesis came from experiments with the Mga2ΔTM variant, which is soluble and in principle does not need the mobilization step in order to be translocated to the nucleus. This form is not efficiently processed, however, when the ankyrin repeats were mutated in the ^{myc}Mga2ΔTM variant (^{myc}Mga2ΔANKΔTM), the processing defect was suppressed (Figure 2-17a) and this effect was independent of the Rsp5 ubiquitin ligase (Figure 2-17b). Similar results were obtained for the ^{myc}Mga2ΔANKΔTM-DHFR^{HA} variant regardless of whether the C-terminus of the construct was stabilized by MTX or not. As shown earlier for the weak processing of ^{myc}Mga2ΔTM-DHFR^{HA} (Figure 2-1b), also the processing of the ^{myc}Mga2ΔANKΔTM-DHFR^{HA} variant resulted in the C35 intermediate that could be induced by stabilization of the DHFR domain (Figure 2-17c), suggesting that it is initiated at an internal site of the precursor. Moreover, the C35 fragment was more abundant in the case of the protein harbouring the ankyrin repeats mutation and correlated well with the enhanced processing, implicating an increased turnover of this protein. Similar results were obtained for the ^{myc}Spt23ΔTM-DHFR^{HA} and ^{myc}Spt23ΔANKΔTM-DHFR^{HA} fusion constructs (Figure 2-17d), suggesting that the function of the ankyrin repeats is conserved between the Spt23 and Mga2 proteins.

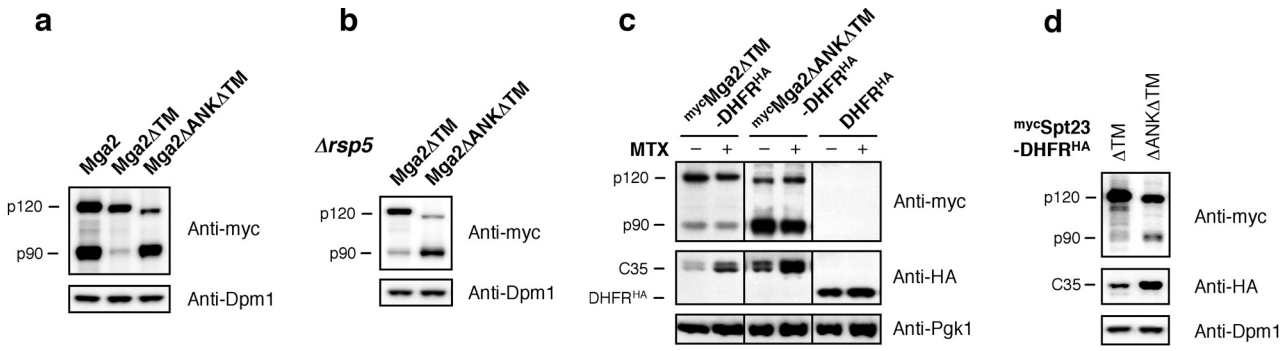

Figure 2-17. Ankyrin repeats inhibit processing of Mga2ΔTM and Spt23ΔTM. (**a**) Deletion of the ankyrin repeat domain can rescue processing defects of Mga2ΔTM. WT cells grown at RT expressing ^{myc}Mga2WT, ΔTM or ΔANKΔTM forms were harvested and lysates were analyzed by Western blots. (**b**) Processing of Mga2ΔANKΔTM does not depend on Rsp5. Δ*rsp5* cells (rescued by Ole1 under the control of *ADH1* promoter) expressing ^{myc}Mga2ΔTM and ^{myc}Mga2ΔANKΔTM forms were grown at RT. (**c**) Processing of ^{myc}Mga2ΔANKΔTM-DHFR^{HA} is initiated from an internal site. WT cells expressing ^{myc}Mga2ΔTM-DHFR^{HA}, ^{myc}Mga2ΔANKΔTM-DHFR^{HA} or DHFR^{HA} were grown for 3 hours in the presence or absence of MTX. Note that the C-terminal processing intermediate (C35) abundance correlates with the processing efficiency. (**d**) Processing of the TM span lacking form of Spt23 is inhibited by ankyrin repeat domain. Lysates from cells expressing ^{myc}Spt23ΔTM-DHFR^{HA} or ^{myc}Spt23ΔANKΔTM-DHFR^{HA} were analyzed by anti-myc and anti-HA immunoblots. Increased processing of the ΔANK variant correlates with higher abundance of the C35 intermediate. Dpm1 and Pgk1 were used as loading controls.

When the turnover of Mga2ΔTM and Mga2ΔANKΔTM proteins was investigated it turned out that, in contrast to the stable Mga2WT protein, Mga2ΔTM was short-lived, and its half-life was further diminished by deletion of the ankyrin repeats, as a result of increased processing (Figure 2-18a). In addition, deletion of the ankyrin repeat or the IPT domains in the soluble Mga2ΔTM-DHFR variant led to a drastic destabilization of the protein (Figure 2-18b). As expected for the IPT-lacking form of Mga2, its degradation does not yield the p90 fragment. These results show that removal of either of the partner interaction domains, i.e. the ankyrin repeats or the IPT domain, results in the same effect on the half-life of the Mga2ΔTM precursor form. Moreover, the finding that Mga2ΔTM form is unstable in comparison to Mga2WT suggests that displacement of p120 from the membrane not only inhibits the processing but also targets Mga2 for complete degradation. The complete degradation of the Mga2ΔTM-DHFR fusion protein was not changed in comparison to Mga2ΔTM (compare Figure 2-18a and b), suggesting that it is either initiated from the same internal site as processing (but processing is not achieved, e.g. due to impaired dimerization), or it is initiated from another N-terminal site.

Since the deletion of the transmembrane span does not include the Rsp5-binding site located in the C-terminal part of Mga2 (Shcherbik et al., 2004), it is

possible that this E3 ligase could be responsible for the observed instability of the Mga2ΔTM variant. Therefore, Mga2ΔTM stability was investigated in Δ*rsp5* and *ufd1-2* mutant cells. This experiment showed that the p120ΔTM turnover is independent of both Rsp5 and Ufd1 (Figure 2-18c,d). Moreover, the *ufd1-2* rescue experiment revealed that Mga2ΔANKΔTM but not Mga2ΔTM expression can fully restore viability of the mutant strain at 37 °C (Figure 2-18e). This result suggests that not only displacement from the ER but also the removal of the C-terminal parts of p120 by processing is required for transcription factor activation. However, the inability to rescue the OLE pathway defects by the Mga2ΔTM form (also in case of the Δ*spt23* Δ*mga2* double knockout cells) seems to be dose dependent (Hoppe et al., 2000 and data not shown), implying that it may also be the result of the increased instability of the Mga2ΔTM variant.

One possible scenario is that the E3 ligase, which normally mediates complete degradation of p90 in the nucleus, is also responsible for the observed instability of the Mga2ΔTM mutant. Such degradation may be initiated from a site (e.g. the N-terminus), which would not lead to the formation of p90. Since proteasomes of the *cim3-1* mutant strain seem to be able to initiate degradation/processing, but are impaired in proteolytic processivity, various Mga2ΔTM variants were tested in these cells for accumulation of degradation intermediates. All constructs were strongly stabilized in these mutant cells, and additionally several degradation byproducts, which are only slightly smaller than the precursor forms accumulated in cells as detected by the immunoblot against the C-terminal tag (Figure 2-18f). This result demonstrates that degradation of some molecules initiates from the N-terminus or a site close to the N-terminus. Interestingly, proteolysis of a fraction of the Mga2ΔANKΔTM and Mga2ΔIPTΔTM proteins, but not of the Mga2ΔTM variant, seem to be initiated at an internal site (most likely the processing initiation site), as both variants accumulated C-terminal degradation intermediates of about 75 kDa in *cim3-1* cells (Figure 2-18f; C75 fragments). Moreover, the Mga2ΔIPTΔTM variant accumulated also N-terminal proteolytic fragments in *cim3-1* cells (Figure 2-18f; NΔIPT fragment), supporting the interpretation that proteolysis of this protein is initiated additionally at an internal site. These results suggest that the interaction between the ankyrin repeats and the IPT domain inhibits initiation of Mga2ΔTM processing,

possibly by stabilizing a conformation that prevents formation of the polypeptide loop in the centre of the precursor.

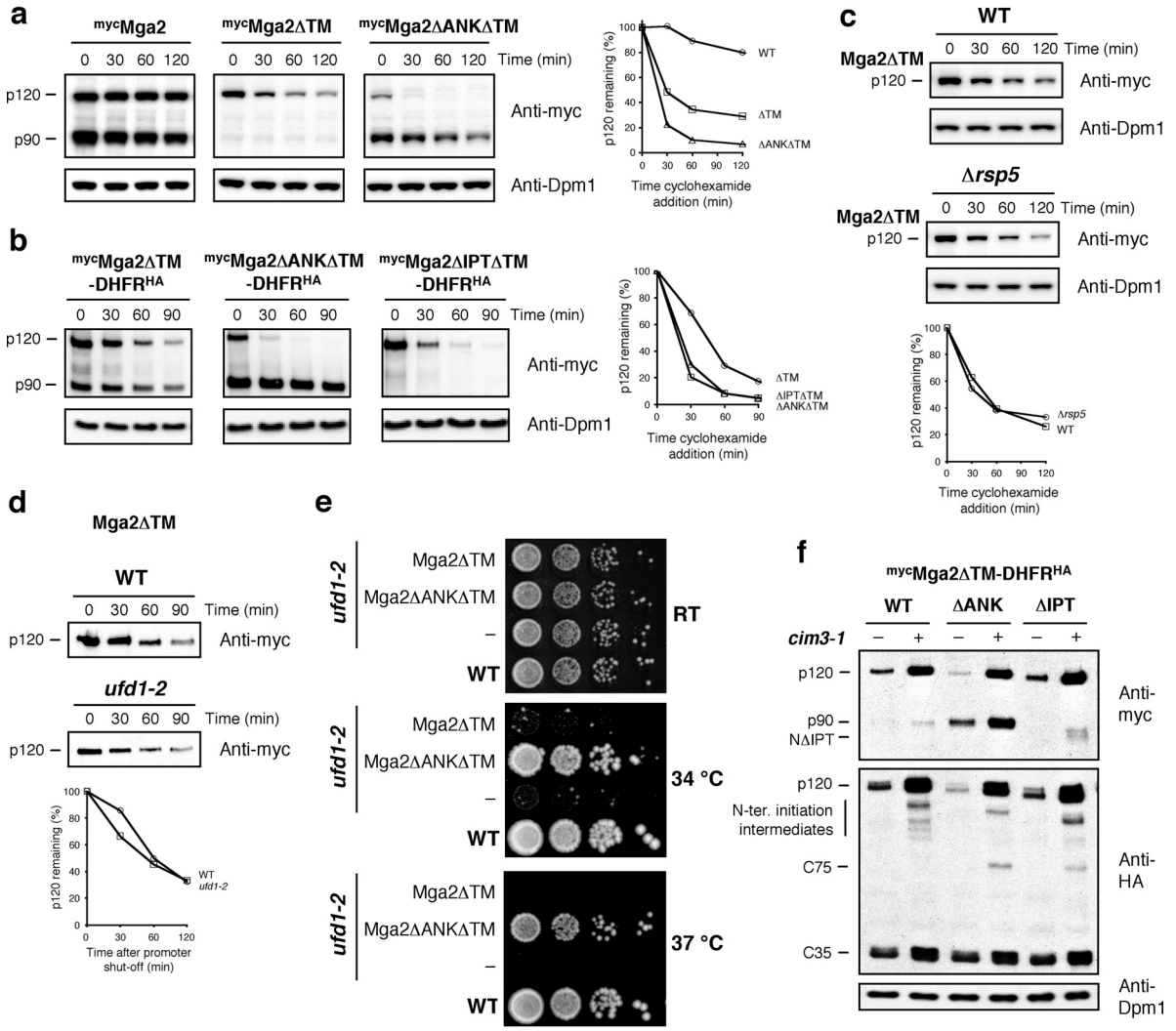

Figure 2-18. Ankyrin repeats-mediated interaction inhibits the processing of Mga2. (**a**,**b**) Loss of ANK-IPT interaction destabilizes soluble forms of Mga2. (**a**) Mga2ΔTM p120 form is a short-lived protein and can be further destabilized by ankyrin repeats mutation (Mga2ΔANKΔTM). Cycloheximide chase experiment for WT cells expressing ^{myc}Mga2WT, ΔTM or ΔANKΔTM proteins under the control of endogenous promoter, grown at RT. (**b**) Cycloheximide chase experiments in the presence of MTX in the growth medium for WT cells expressing ^{myc}Mga2ΔTM, ΔANKΔTM or ΔIPTΔTM mutants possessing C-terminal fusion of DHFR^{HA}. (**c**,**d**) Turnover of Mga2ΔTM p120 form does not depend on Rsp5 and Ufd1. *GAL* promoter shut off experiments were performed at RT for WT and Δ*rsp5* (**c**) or at 37 °C for WT and *ufd1-2* (**d**) cells expressing ^{myc}Mga2ΔTM. (**a**-**d**) Graphs (right panels) show quantification of p120 decay of different constructs of Mga2 in indicated strains and conditions. (**e**) Expression of Mga2ΔANKΔTM protein rescues *ufd1-2* mutant cells grown at 34 °C and 37 °C. The experiment was performed as described for **Figure 2-16**a. (**f**) Ankyrin repeats-mediated interaction masks the processing initiation loop. Degradation of Mga2ΔTM is initiated from the N-terminus. WT and *cim3-1* cells expressing ^{myc}Mga2ΔTM, ΔANKΔTM or ΔIPTΔTM proteins with DHFR^{HA} fused to the C-terminus were grown at 37 °C for 3h. p120, p90, NΔIPT (N-terminal processed form of ΔIPT variant), C35 fragment, intermediates of N-terminally initiated and internally initiated proteolysis (C75) are indicated. Dpm1 is used as a loading control.

3. Discussion

Since the proteasome was discovered in the early 1990's, numerous reports have proven its importance for the complete elimination of cellular proteins. However, a growing number of recent studies show that besides this function, the proteasome acts also in unconventional ways in regulated ubiquitin/proteasome-dependent processing or even non-proteolytic processes. These diverse activities of the proteasome raise the question how the fate of different proteasomal substrates is determined.

This study focuses on the understanding of the mechanism and regulation of unconventional activities of the proteasome in partial protein degradation using as an experimental system the activation of the yeast transcription factors Spt23 and Mga2. In addition, the understanding of this process provides implications to general mechanisms of protein degradation by the proteasome.

3.1. Proteolytic systems for processing of proteins

Limited proteolysis is an important cellular mechanism commonly employed for the generation of biologically active proteins by processing of their inactive precursors. Next to the broad array of site-specific proteases, which by the nature of their enzymatic reaction mediate partial proteolysis, the proteasome was found to be involved in processing of many substrates as well. Why the proteolytic system that was designed for complete destruction of proteins is also utilized for partial proteolysis seems to be an intriguing and open question. Perhaps the possibility to choose between complete or partial degradation might contribute to a more dynamic regulation of protein activity, and might be advantageous over processing by the conventional proteases.

Hydrolysis of peptide bonds requires an aqueous environment and therefore the sites for initiation of cleavage by the proteases need to be located in exposed parts of substrates, such as flexible inter-domain segments or surface exposed loops. This requirement appears to be omitted by RIP substrates, such as SREBP, APP or Notch, which are cleaved at transmembrane segments (Brown et al., 2000). It is believed, however, that enzymes mediating RIP are able to create an aqueous microenvironment around the catalytic site by a unique arrangement of their transmembrane domains (Wolfe and Kopan, 2004). Site-specific proteases seem to

recognize their substrates by short sequences near (or within) the cleavage sites, or by a unique conformation of substrates (Neurath, 1989; Wolfe and Kopan, 2004). In contrast, the proteasome seems to cleave virtually any sequence. Interestingly, some sequences were reported to stop proteasomal degradation (e.g. the glycine-alanine repeats of EBNA1 protein), but they rather seem to affect engagement of the substrates with the proteasome (Sharipo et al., 1998). Specificity of the proteasome is mainly brought about by the covalent attachment of the ubiquitin mark to the substrates, a process mediated by numerous specialized enzymes. This seems to provide a powerful step ensuring tight regulation of the fates of a broad range of different proteins. Moreover, the substrates also require an exposed unfolded region that can be translocated into the degradation tunnel to initiate sequential unfolding and degradation of the polypeptide chain.

At a first glance, the high processivity of the proteasome seems not to be suitable for processing of proteins, but as discussed below, it can also have clear advantages. It demands from the precursor proteins that they possess tightly folded barrier domains (e.g. the IPT domain of Spt23/Mga2), which allow restricted proteolysis and thus the accumulation of processed fragments. Notably, the folding of the barrier domains can be regulated (e.g. DHFR is stabilized by MTX) and may be characterized by a different local stability of N- and C-termini. This offers a way to control substrate fate by either processing or complete degradation, depending on the folding state or the direction of the proteasome-mediated proteolysis (see below). Since protein folding is a dynamic process, also the cleavage fragments produced by the proteasome vary from those produced by site-specific proteases. Products of proteasomal processing seem not to be constant in size, but rather appear as a collection of fragments (Spt23 p90 and C50 forms, Mga2 C35 cleavage intermediate), indicating several different cleavage sites. In contrast, conventional proteases seem not to rely on the presence of tightly folded regions in their substrates, but rather such domains, which stop proteolysis due to their limited availability for the active sites.

In principle, single cleavage by site-specific peptidases produces two polypeptides. Processing of precursors by these enzymes are commonly employed to separate a sterically hindering (zymogens activation) or an anchoring domain (SREBP activation) from active parts of the precursor. In contrast, the known

examples of RUP suggest that the proteasome usually degrades only one part of the precursor protein (an inhibitory domain) to small peptides, thereby yielding only one polypeptide fragment. This mechanism allows a unique regulation of proteins, whose inhibitory domains must be completely degraded, since they could bind and inhibit the active domains. Such mechanism is required for the processing of NFκB proteins, which possess inhibitory ankyrin repeat domains that, if isolated from the precursors, can still bind and inhibit the transcription factor (Moorthy and Ghosh, 2003). Analogous interaction appears to take place with the Mga2 precursor domains, suggesting that complete elimination of the C-terminal ankyrin repeats is indeed required.

Interestingly, limited proteasomal proteolysis might also yield two fragments. As demonstrated in this study, proteasomal processing can be initiated from an internal site of the precursor molecule. Therefore, if the substrate possesses two tightly folded domains located N- and C-terminally from the initiation loop, proteasomal activity can separate two polypeptide chains, both of which might have biological functions.

3.2. Mechanism of proteasomal processing of Spt23/Mga2

3.2.1. Initiation signal for processing of Spt23/Mga2

The proteasome recognizes and binds the ubiquitin modification of its substrates. Proteins degraded by the proteasome are usually modified by polyubiquitin chains and most monoubiquitylated proteins are not targeted to the proteasome. However, it was demonstrated that mono/oligoubiquitylation of the Spt23 precursor by the ubiquitin ligase Rsp5 is essential for processing initiation (Hoppe et al., 2000). Interestingly, Rsp5 was shown to efficiently catalyse polyubiquitylation of its substrates *in vitro*. However, in cells this polyubiquitylation activity seems to be counteracted by the deubiquitylating enzyme Ubp2 (Kee et al., 2005; Kee et al., 2006). Ubp2 and the UBA domain containing protein Rup1 form a complex with Rsp5, and may lead to the generation of mono/oligoubiquitylation instead of the polyubiquitin chain. This suggests that short ubiquitin chain on Spt23 may represent a signal specific for limited degradation. Since the 19S cap possesses multiple subunits that are involved in binding of ubiquitin, it is tempting to speculate that they are not equivalent in recruiting substrates modified by ubiquitin chains of different

lengths. Therefore, different binding sites on the proteasome might contribute to the regulation of the fate of substrates. Interestingly, the processed Spt23 p90 protein seems to retain the ubiquitin modification after the release from the proteasome, suggesting a difference between recognition of a signal for processing and degradation. Sites recognizing polyubiquitin chains may be located in close proximity to the Rpn11 deubiquitylating enzyme, which removes the ubiquitin mark from substrates, while sites for mono/oligoubiquitylated substrates may be spatially separated from Rpn11. Notably, the binding of single ubiquitin molecule may also be weaker than that of polyubiquitin chain and facilitate early release of monoubiquitylated substrate from the proteasome. This could have implications for the termination of the processing reaction and the release of p90. Moreover, it is possible that for efficient engagement of Spt23 precursor by the proteasome not only the monoubiquitin mark, but also an additional binding site is needed (e.g. the processing initiation loop, which is supposed to bind to the ATPases ring).

Importantly, shorter ubiquitin chains on the proteasomal substrates may offer an additional step in the regulation of their fates. The 19S cap of the proteasome was proposed to act as a “molecular gearbox”, which by remodelling of ubiquitin chains of substrates bound to the proteasome might shift their fates (Jentsch and Rumpf, 2007). Indeed, it was recently demonstrated that the deubiquitylating enzyme Ubp6 and the E4 enzyme Hul5 associated with the 19S cap could regulate the half-life of certain substrates by controlling their ubiquitin chain length (Crosas et al., 2006; Hanna et al., 2006). In addition, trimming of ubiquitin chains by Ubp6 may act as a timer for unfolding and degradation, and facilitate release of proteins from the proteasome. Interestingly, since Rsp5 is also responsible for the complete degradation of Mga2 p120, which apparently requires the formation of longer ubiquitin chains, it is possible that the molecular gearbox mechanism in this case shifts the fate of the substrate towards complete degradation. Alternatively, an additional, yet unknown factor might be involved in modulating the ubiquitylation efficiency of the Rsp5 enzyme.

3.2.2. Processing of Spt23/Mga2 initiates at an internal site

Proteasomal degradation relies on the activity of the hexameric ring of AAA ATPases that guard the entry to the catalytic particle. Narrow openings of the proteasome do

not allow globular domains to be efficiently degraded, unless they become sequentially unfolded and translocated into the proteasome. In the last years it became more evident that proteins in addition to the ubiquitin signal need to possess an unstructured region near the ubiquitylation site, which facilitates unfolding by the ATPases (Lee et al., 2001; Prakash et al., 2004). After this step, processivity of the proteasome assures that the whole substrate is degraded to small peptides. However, some proteins evolved mechanisms to interfere with the continuous degradation mediated by the proteasome, resulting in their processing and activation of their dormant activities. The first protein reported to undergo proteasomal processing was the mammalian transcription factor NFκB1, whose inactive precursor p105 is trimmed by the proteasome to give a rise to an active N-terminal p50 fragment (Fan and Maniatis, 1991; Palombella et al., 1994). Since the C-terminal domain of p105 is completely degraded by this reaction, it was proposed that the proteasome initiates the degradation from the C-terminus of p105. A “stop-transfer sequence” was suggested to interfere with proteasomal progression, leading to the release of the processed p50 fragment (Orian et al., 1999). However, later reports suggested that processing of NFκB might be more complicated, since p105 appears to undergo processing already at the ribosome before the full-length protein is synthesized, and it seems to require precursors dimerization (Lin et al., 1998; Lin et al., 2000). In this proposed “co-translational” mechanism of processing, the C-terminal part of p105 nascent polypeptide chain is buried in the ribosome, suggesting that processing could be initiated from an internal site in the p105 sequence. Support for this hypothesis came from an *in vitro* study on circular variants of natively disordered proteins, which showed that the proteasome initiates degradation in unstructured regions by an “endoproteolytic” cleavage (Liu et al., 2003). Since after synthesis polypeptides do not immediately adopt native ternary structures, they could serve as unfolded regions for the proteasomal cut, explaining the results observed for p105. However, the idea that the proteasome can initiate processing from internal sites also posttranslationally came from the work on the yeast transcription factor Spt23. This protein undergoes proteasomal processing of a full-length precursor p120, which results in the formation of a shorter N-terminal fragment p90 (Hoppe et al., 2000). Since the C-terminus of Spt23 is localized to the ER lumen, it is not accessible for the proteasome. This is reminiscent of the proposed co-translational

processing of p105 and suggests that the proteasome initiates processing of p120 from a flexible polypeptide loop (the “loop model”) located in the middle of the Spt23 sequence (Rape and Jentsch, 2002). Moreover, Spt23 (and its homolog Mga2) shares domain organization with NFκB, and requires dimerization and ubiquitylation for processing, suggesting similar mechanisms. However, a direct evidence for the initiation of proteasomal processing from internal sites was lacking due to the rapid elimination of C-terminal sequences of the transcription factor precursors in the processing reaction (Hoppe et al., 2000).

Two experimental approaches applied in this study provided the final confirmation of the “loop model”. The first series of experiments demonstrated that a fusion of a stably folded DHFR domain to the C-terminus of soluble (ΔTM) or membrane bound Mga2 precursors do not interfere with their processing (Figure 2-1 and Figure 2-2). DHFR was previously shown to be resistant to unfolding and degradation by the proteasome, especially if its structure was stabilized by binding of the ligand MTX (Johnston et al., 1995; Lee et al., 2001). Moreover, in addition to the N-terminal p90 fragment, processing of these fusion proteins yielded stable fragments corresponding to the undegraded C-terminal domains. This strongly supports the hypothesis of an internal initiation site for the proteolysis. After degradation initiated from a polypeptide loop, the proteasome starts concurrent bidirectional degradation of two N- and C-terminal parts of the polypeptide, which is however not completed due to the hindrance by stable folds encountered by the proteasome (Figure 3-1b-d). Moreover, as soluble and ER membrane-bound Mga2 precursors are apparently processed in a similar manner, precursor processing according to the loop model is not limited to membrane proteins. Since Spt23/Mga2 and NFκB precursors are homologous proteins, it seems likely that also processing of NFκB transcription factors is initiated at a flexible loop in the centre of the p105 polypeptide.

In the second experimental approach, residual processing of native forms of both transcription factors Spt23 and Mga2 by leaky proteasome mutants led to an accumulation of C-terminal byproducts of p120 processing (Figure 2-3), again supporting the “loop model” for partial degradation. Since these processing intermediates are fragments of about 300 amino acids and are localized to ER membranes (Figure 2-4), this implies that processing initiates in a region near the

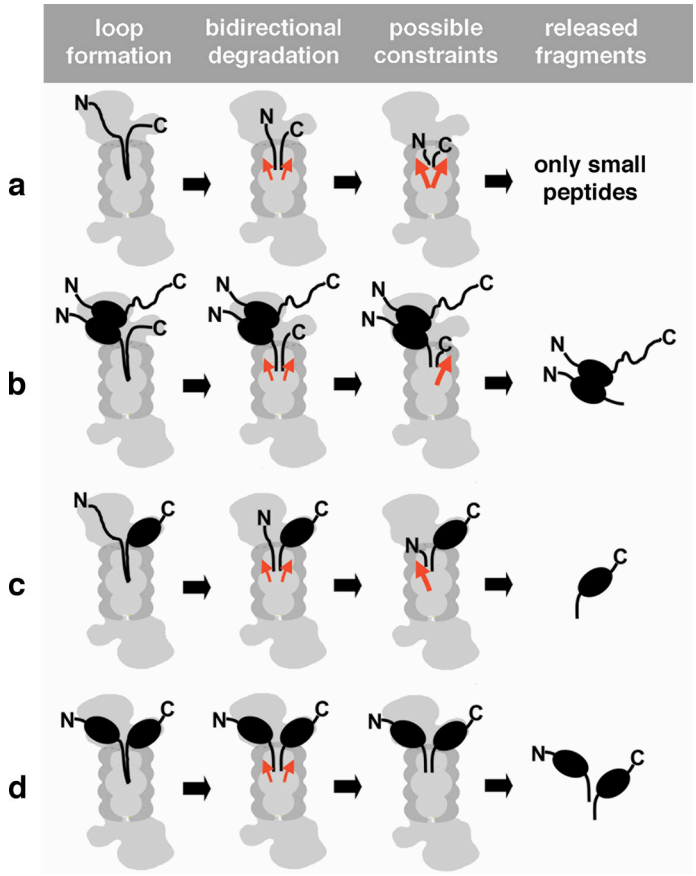

Figure 3-1. Hypothetical model for proteasome-mediated degradation and processing. The proteasome (grey) harbours within its 20S particle (dark grey) a central catalytic cavity and two antechambers. Substrate (black) recruitment is usually mediated by the ubiquitin modification of the substrate (not shown). (**a**) Complete substrate degradation may commence by the insertion of an internal polypeptide loop through the openings of the proteasome into the proteolytic chamber. The inserted polypeptide chain may partially re-fold in the antechambers and thereby prevent it from slipping back into the cytosol (not shown). Degradation initiates by a cut within the loop and continues bidirectionally (red arrows) towards both the N- and C-terminal ends of the polypeptide (middle column). If there are no steric constraints (first row), degradation continues in both directions (red bold arrows) until the polypeptide is completely degraded to small peptides, which exit the proteasome by diffusion (not shown). (**b-d**) Protein processing occurs if the polypeptide contains tightly folded dimerization domains (e.g. the IPT domain of Spt23; **b**) or other tightly folded domains (e.g. MTX-stabilized DHFR; **c,d**). These domains cannot enter the central cavity and therefore cause incomplete degradation, i.e. degradation proceeds only towards the end that is not hindered by barriers (red bold arrows). The processing product contains the tightly folded (or dimerization) domain, and additionally segments distal from these domains and a short polypeptide stretch that reflects the distance from the proteasome openings to the active sites. (**d**) Degradation of substrates that contain tightly folded domains both N- and C-terminally of the inserted loop yield two processing products. Only the authentic N- and C-termini are labelled.

ankyrin repeats of Spt23/Mga2 and that this step takes place directly at the ER membrane. Moreover, the finding that degradation of the ERAD model substrate Hmg2 is also initiated from internal site/sites (Figure 2-8) suggests that such mode of action may be employed more often by the proteasome, also for the complete elimination of proteins (Figure 3-1a).

3.2.3. Formation of a flexible loop for processing initiation

It is believed that the proteasome starts degradation of substrates in unstructured regions close to ubiquitylation sites (Prakash et al., 2004). The finding that the initiation of Spt23/Mga2 processing occurs by a cleavage at the internal site of p120 suggests that such a region exists in the centre of the p120 precursor. However, it is not clear how such regions are formed. It was speculated that these sites should be able to adopt hairpin loop conformations, which would allow their grabbing by ATPases of the 19S cap and translocation through the narrow proteasomal gates to reach the active centres of the proteasome for initial cleavage. Indeed, analysis of the crystal structure of the yeast 20S proteasome showed that its openings are wide enough to accommodate two juxtaposed polypeptide chains (Rape and Jentsch, 2002). Furthermore, it was experimentally demonstrated with substrates cross-linked by disulfide bonds that even up to three chains can enter the proteasome simultaneously (Lee et al., 2002).

It has been proposed for the glycine rich region (GRR) located in the centre of the p105 precursor that it could serve as the initiation site for processing, since it is necessary for p50 formation (Lin and Ghosh, 1996; Rape and Jentsch, 2002). This site seems to be highly flexible and loosely folded, and therefore it could form the loop accessible for initial cleavage by the proteasome. However, a recent study demonstrated that the p105 protein lacking GRR, still undergoes complete degradation suggesting that possibly additional regions might contribute to the formation of a loop as well (Tian et al., 2005).

In this study, identification of the C-terminal processing intermediate C50 resulting from aberrant processing of Spt23 in proteasome mutants cells (Figure 2-3b), combined with the size estimation of p90 and C50 fragments (Figure 2-5b) allowed the finding of the region where the initial cleavage of Spt23 occurred. This site is located within the ankyrin repeat-containing region, but since the ankyrin repeats are well-folded structures, this rather suggests the flanking sequences as candidate sites. Analysis of the potential folding of this region by the FoldIndex program (Figure 2-6) supports this idea, as the ankyrin repeat-flanking segments exhibit a tendency to adopt unfolded conformations. Interestingly, none of the tested deletions in this region could abolish processing (Figure 2-5c), suggesting that other sites may compensate for the absence of the primary site. However, processing

initiated from this alternative site/sites seems to involve local unfolding of the p120 C-terminal region, since an Spt23 mutant protein harbouring a deletion of the whole investigated ankyrin repeat-containing region could not be processed by attenuated proteasomes (Figure 2-5d). Moreover, it seems attractive to speculate that the loops that first enter the proteasome might not always be identical to the regions that are first degraded by the proteasome. Given the fact that the proteasome possesses two large antechambers that border the central catalytic chamber, it seems possible that substrates will partially re-fold within the antechambers (perhaps preventing thereby the substrate to slip back to the cytosol), thus allowing flanking polypeptide segments to slip into the catalytic chamber for the initial cut. This is in agreement with the notion that undegraded tails from different DHFR fusions released from the proteasome show variable sizes (see chapter 2.1.1; C35 and C32 fragments; also (Lee et al., 2001), suggesting that their polypeptide chains partly re-folded inside the proteasome.

Interestingly, the initial cleavage site of Spt23/Mga2 is located near the ankyrin repeats, which are responsible for the inhibition of processing, suggesting that the interaction mediated by this domain could lead to masking or re-structuring of the processing initiation loop. This could be mediated either by docking of the processed p90 form to the region of the initiation site and sterically masking it, or by intramolecular interaction involving changes in the conformation of the C-terminal region of p120 (see below).

3.2.4. Regulation of loop formation by the ankyrin repeat domain of Mga2

Analysis of the Spt23/Mga2 and NFκB precursor sequences shows similarity in the IPT and ankyrin repeat domain organization, suggesting a conserved function for both regions (Figure 2-9). Since the ankyrin repeats, which are usually protein-protein interaction motifs, are located in the putative region of initial cleavage of Mga2 by the proteasome, it is possible that they could influence formation of the processing initiation loop. Indeed, in experiments with the soluble Mga2ΔTM variant that cannot be efficiently processed, the precise deletion of the ankyrin repeats restored the formation of the p90 form (Figure 2-17). Moreover, in *cim3-1* mutant cells the Mga2ΔANKΔTM variant accumulated proteolytic fragments, indicating that processing is initiated at an internal site (Figure 2-18f; C75 fragments). This strongly

suggests that the ankyrin repeat domain may be an inhibitory element for formation of the processing initiation loop. Similarly, deletion of the ankyrin repeats from the NFκB precursor p105 leads to increased processing, but apparently does not change the efficiency of polyubiquitylation of the precursor (Cohen et al., 2001). In addition, the mutation of the ankyrin repeat domain in the native Mga2 protein variant strongly destabilized the p120 molecule (Figure 2-12b) and led to an accumulation of the active transcription factor p90 in the nucleus (Figure 2-14a). Thus, the ankyrin repeats inhibit degradation or/and processing of the Mga2 precursors.

Interestingly, the ankyrin repeats can interact with the IPT domain of Mga2 and the mutation of either of the domains led to similar effect on the Mga2 precursor half-life. This strongly argues for a model in which the interaction of these domains results in the inhibition of both processing and complete degradation of the Mga2 precursor, most likely by the same mechanism, namely by masking the site for initiation of proteolysis.

Notably, the interaction between the ankyrin repeat and the dimerization domains seems to be conserved evolutionarily. The intracellular localization of transcription factors from the NFκB family is controlled by a group of IκB proteins, which associate with NFκB dimers and thereby sequester them in the cytoplasm, and also directly interfere with their ability to bind to DNA (Baldwin, 1996). The structural hallmark of various IκB proteins is the ankyrin repeat domain, containing six or seven closely adjacent repeats mediating their interactions with the transcription factors. Importantly, this domain is very similar to the C-terminal region of the NFκB precursors and both seem to be equivalent. In fact, it was reported that the p105 precursor could also mediate IκB-like functions depending on its ankyrin repeat domain (Fu et al., 2004; Moorthy and Ghosh, 2003; Rice et al., 1992). Interestingly, a close homolog of Spt23 from yeast *Candida albicans* (CaSpt23) does not contain the ankyrin repeat domain. However, an inspection of the *C. albicans* as well as the *S. cerevisiae* genome database revealed the presence of several ankyrin repeat-containing proteins of unknown function, which could act similarly to IκB molecules to regulate CaSpt23 or ScSpt23.

What might be the mechanism of ankyrin repeat-mediated inhibition? A model proposed for the processing of the p105 protein seems attractive, which suggests that the ankyrin repeat domain of p105 could serve as a docking site for the processed p50 fragment, preventing thereby proteolysis of the precursor molecule (Cohen et al., 2001). A similar feedback mechanism could be also applied to Mga2, where the product of the processing reaction p90 would mask the processing initiation loop of the p120 precursor (Figure 3-2a). A variation of this model, involving a ternary interaction between the two IPT domains of the p120/p90 complex and the ankyrin repeats of the p120 molecule seems also plausible (Figure 3-2b). In this latter mechanism, an intramolecular interaction between the N- and C-terminally located domains of the same p120 molecule might cause the polypeptide chain to fold back and result in a “closed conformation”. Such conformational change of the Mga2 precursor could influence the putative processing initiation loop, which resides near the ankyrin repeats. This mode of the interaction is supported by crystal structure studies on NFκB-IκB complexes, which show that the ankyrin repeats of IκB bind to the cleft between the two dimerized IPT domains of NFκB proteins (Huxford et al.,

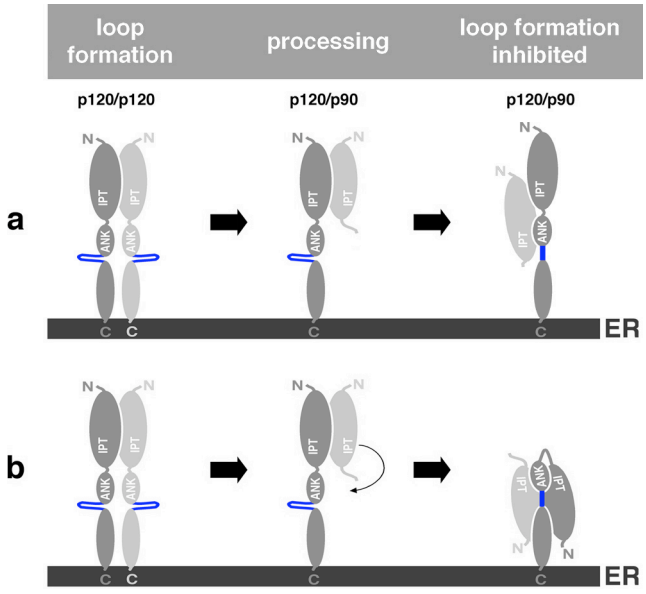

Figure 3-2. Hypothetical models for the ankyrin repeat domain-mediated inhibition of the Mga2 precursor processing. (**a**) Processed p90 fragment docks via the IPT domain to the precursor molecule and masks the processing initiation site. (**b**) C-terminal domains of the Mga2 p120 dimer are immobilized due to the insertion into the ER membrane, hindering the intramolecular rearrangements. After processing one of the p120 molecules, the C-terminal anchor is removed, which allows folding back of the polypeptide chain. Conformational change masks the processing initiation loop. Mga2 molecules are shown in gray and dark gray, the flexible processing initiation sites – in blue. Only the original N- and C-termini are indicated. The putative initiation loop could be also located in a flexible region between the IPT and ankyrin repeat (ANK) domains (not shown).

1998; Jacobs and Harrison, 1998).

Interestingly, as shown in this study, the ankyrin repeat domain is also an inhibitory element for the translocation of the processed active transcription factor p90 to the nucleus. It seems that prevention of processing of the processing template molecule may allow a separate, most likely tightly regulated step of p90 mobilization from the dormant membrane-bound p120/p90 complex. This may involve ERAD of the processing template molecule (Shcherbik et al., 2003). Under normal conditions, mobilization of Mga2 p90 is slow, which is reflected by the high stability of p120 in expression shut-off experiments (Figure 2-12b and Figure 2-15a). Interestingly, deletion of the ankyrin repeats of Mga2 led to an Rsp5-dependent drastic destabilization of p120 and release of p90, resulting in strong activation of *OLE1* expression (Figure 2-15a and Figure 2-13b). This suggests that physiological

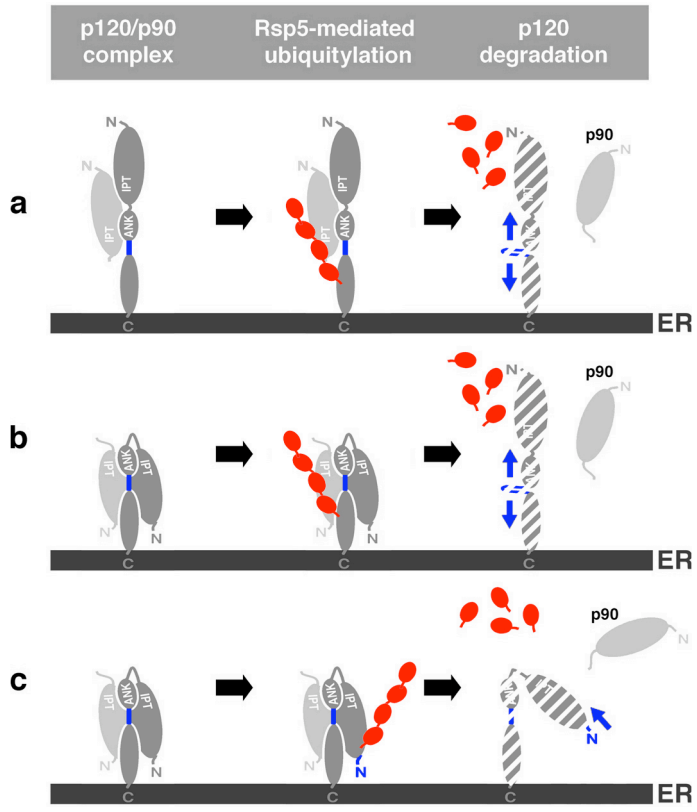

Figure 3-3. Hypothetical models for the ankyrin repeats-mediated inhibition of the Mga2 p90 mobilization from the p120/p90 complex. (**a**) The p120 molecule from the p120/p90 complex is polyubiquitylated by the Rsp5 enzyme and the interaction between the ankyrin repeats and the IPT domain is resolved (probably additional factor is involved). This leads to complete elimination of the processing template molecule. (**b**) The closed conformation of the p120/p90 complex is resolved upon polyubiquitylation by the Rsp5 enzyme. Internal degradation initiation site is used for complete elimination or processing (not shown) of the processing template. (**c**) Complete degradation of the processing template is initiated from the N-terminal site. Blue arrows show direction of degradation initiated from internal or terminal sites.

regulation of p90 mobilization might occur by dissociation of the ankyrin repeats-mediated intramolecular interaction, which would then lead to a conformational change and expose the loop for initiation of complete degradation or even processing of the processing template molecule from the p120/p90 dimer (Figure 3-3a,b). However, how this regulation is achieved is not clear yet. Possibly, additional factors are involved, which upon binding to Mga2 allow to change its conformation or to dissociate the interaction between the ankyrin repeats and the IPT domain (e.g. ATPase function of Cdc48). Also another model is possible in which complete degradation of p120 is initiated from the N-terminal site of the protein. Since the intramolecular interaction between the ankyrin repeats and the IPT domain might lead to a folding back of the precursor molecule, it could present certain N-terminal regions of Mga2 for ubiquitylation by the C-terminally bound Rsp5 enzyme and allow initiation of degradation from the N-terminus of p120 (Figure 3-3c). As demonstrated in this study, IPT dimerization does not block proteasomal progression initiated form the N-terminus (Figure 2-18f), therefore such proteolysis may lead to complete degradation of p120.

3.2.5. Mechanism of limited proteasomal degradation

The proteasome usually degrades proteins to short peptides. Thus, the identification of RUP substrates raised the question how these proteins escape from complete destruction. The GRR residing in a central region of p105 has been proposed to be a “stop-transfer signal”, as deletion of these residues abolished processing in mammalian cells (Ciechanover et al., 2001; Orian et al., 1999). Later reports suggested that rather the stability of the dimerization domain of NFκB may play a role in resisting the proteasomal unfolding activity (Lin et al., 2000; Lin and Kobayashi, 2003). Strong support for this hypothesis came from studies showing that certain stably folded domains cannot be degraded by the proteasome and moreover can protect other downstream regions against the degradation (Johnston et al., 1995; Lee et al., 2001). The IPT domain of NFκB precursors is characterized by a stable immunoglobulin-like fold and upon dimerization the polypeptide chain is difficult to unravel from the structure, because it is buried in the dimerization surface (Ghosh et al., 1995; Muller et al., 1995). Therefore, this domain is a good candidate for a barrier for complete proteasomal degradation. Furthermore, it was demonstrated that

prokaryotic ATP-dependent proteases, which are distantly related to the proteasome, can release substrates that are difficult to unfold (Kenniston et al., 2005). This indicates that processivity of chambered proteases can be influenced by tightly folded structures. A recent report combines both proposed models and suggests that the IPT domain of NFκB works in combination with a downstream low-complexity region (the GRR sequence) to block proteasome progression and to protect the N-terminal parts of the proteins from degradation (Tian et al., 2005). In this model, the dimerization domain of p105 interferes with the unfolding activity of the proteasome and the GRR reduces affinity of the engaged substrate to the proteasome, thereby facilitating the release of the processed form (p50). Although the yeast Spt23/Mga2 precursors possess centrally located IPT domains as well, they lack low-complexity sequences at positions similar to those found in NFκB. Moreover, Spt23 and Mga2 precursors harbouring deletions in sequences located downstream of the IPT domain at the position occupied by the GRR in p105, are still processed by the proteasome (data not shown). However, deletion of the IPT domain of Spt23/Mga2 was shown to completely abolish processing (Rape et al., 2001; Shcherbik et al., 2004), indicating that dimerization may be the only requirement for efficient proteasome progression stop in yeast.

Data presented in this study suggest that the alternative to precursor processing in cells is the complete degradation of the molecule. The Spt23ΔIPT mutant protein is completely degraded in WT cells, however, when the same variant is a substrate for attenuated proteasomes, it is processed to the N-terminal fragment (N75) analogously to p90 and the C-terminal C50 fragment (Figure 2-7b). This result demonstrates that the IPT domain forms a barrier for the proteasome, since processing seems to be normally initiated in the Spt23ΔIPT mutant, but it does not yield a p90 fragment. This is because bidirectional proteolysis initiated from the internal site of this mutant is not stopped, and thus leads to the complete degradation of the protein. In addition, the tightly folded DHFR domain fused to the C-termini of Spt23/Mga2 variants was able to stop proteasome progression independently of low-complexity sequences (Figure 2-1, Figure 2-2 and Figure 2-17). This suggests that (at least for yeast proteasomes) stable folds may be sufficient for degradation termination. This is in line with a report demonstrating that p105 is also processed in yeast cells independently on the GRR presence (Sears et al., 1998). Conversely,

Spt23 was shown to be efficiently processed in mammalian cells after ubiquitylation by the Rsp5 homologue Nedd4 (Shcherbik et al., 2002), suggesting that low-complexity sequences may also not be absolutely required for processing of all proteins by mammalian proteasomes. It seems possible that depending on the substrate the strength of the proteasome is regulated by additional factors. In the case of the yeast transcription factors the signal for processing could be weaker than in the mammalian counterparts and could involve a lower unfolding force of the proteasome.

It is important to note that the folding of the degradation barriers might be regulated. This idea is suggested by the fact that DHFR itself possesses a tight fold and can inefficiently stop the proteasomal progression, but when it is further stabilized upon binding of its ligand MTX, it becomes more effective in inhibiting the degradation (Figure 2-1b). A similar mode of regulation may exist for the dimerization strength of Spt23/Mga2, which might be modulated by ER membrane fluidity. Interestingly, also the direction of degradation seems to be crucial for the function of the barrier domains, since the IPT domain of Mga2 is efficiently degraded if the initiation site is within the N-terminal region of Mga2 (Figure 2-18f).

3.3. Regulation of the OLE pathway by the ubiquitin/proteasome system

UFAs are essential components of membrane lipids that determine the optimal fluidity of biological membranes and are thus essential for cell viability. Not only depletion (Zhang et al., 1999), but also too high levels of UFAs can be deleterious for cell growth (Stukey et al., 1989). Therefore, the level of *OLE1* expression is tightly controlled by the content of fatty acids in the cell (Choi et al., 1996). Expression of the *OLE1* gene is also regulated during the cell cycle with highest mRNA levels in the late G1 or early S phase (McConnell et al., 1990; Spellman et al., 1998). This increased expression might be needed to provide the daughter cell with sufficient UFAs levels. As crucial for cell viability, the activity of the OLE pathway is precisely adjusted by several mechanisms, among them proteasome-mediated processes, the majority of which deals with the activation of Spt23 and Mga2 proteins. Interestingly, although both of the transcription factors are highly homologous and both activate *OLE1* gene expression, they seem to be differentially regulated. It seems as if the

activity of Spt23 is regulated mainly at the level of processing (negatively by UFAs and positively by elevated temperatures), while the activity of Mga2 is rather controlled at the level of p90 mobilization (negatively by the ankyrin repeat domain and positively under hypoxic conditions) (see below).

Under normal growth conditions, the major transcription factor for constitutive mild activation of the *OLE1* promoter seems to be the Spt23 protein, rather than Mga2. This is suggested by some experimental evidence. In immunofluorescence microscopy experiments, Spt23 protein shows mainly nuclear localization (Hoppe et al., 2000), whereas Mga2 gives ER and nuclear envelope staining, suggesting that Mga2 p90 is inefficiently liberated from the dormant p120/p90 complex (Figure 2-14a). This seems to correlate well with the notion that Spt23 is a high-turnover protein due to the rapid processing of p120 form and the rapid degradation of p90 (probably in the nucleus after transcription activation) (Richly et al., 2005), while both p120 and p90 forms of Mga2 are stable (Figure 2-12b). Moreover, Mga2 was shown to be a more potent activator of the *OLE1* transcription than Spt23 (Chellappa et al., 2001), raising the possibility that Mga2 is utilized by cells upon stress conditions that require enhanced levels of UFAs, whereas Spt23 ensures normal *OLE1* gene expression.

The situation may be drastically different under conditions of depletion of UFAs or enhanced cellular requirements for UFAs. The processed p90 form of Mga2 might be rapidly mobilized from the dormant complex at the ER and contribute to the enhanced *OLE1* expression. In line with this model, it was reported that the transcriptional activity of Mga2 is strongly induced under hypoxic conditions (Jiang et al., 2001). Since the enzymatic reaction catalyzed by Ole1 requires molecular oxygen as an electron acceptor, upregulation of Ole1 protein in hypoxic conditions may help to sustain sufficient levels of its enzymatic activity. This regulation may also be important to turn on other target genes of Mga2 (Auld et al., 2006). It was demonstrated that under this conditions the processing ratio (p90/p120) of Mga2 increased (Jiang et al., 2002), which was rather an effect of the enhanced degradation but not processing of the Mga2 p120 molecule, as p120 levels decreased and p90 levels were not changed. This strengthens the hypothesis that Mga2 is activated upon certain conditions by p90 release from the dormant ER-localized complex. It was proposed that this process involves complete degradation

of the p120 molecule (Shcherbik et al., 2003). Moreover, as shown in this work, the mobilization of p90 seems to be regulated by the interaction between the ankyrin repeats and the IPT domain of Mga2 (see above).

Interestingly, also in cells grown at elevated temperatures the *OLE1* gene might be strongly activated by a mechanism involving the enhanced processing of the Spt23 transcription factor (Hoppe et al., 2000). High temperature-stress alters protein folding processes in cells, which may therefore require more fatty acids in order to increase the capacity of ER, the cellular compartment where the protein folding and quality control occurs.

Additional mechanisms that possibly induce the expression of *OLE1* gene under certain conditions might rely on a stabilization of the active transcription factor. Two recent reports identified factors that regulate degradation of Spt23 p90 in the nucleus (Richly et al., 2005; Rumpf and Jentsch, 2006). Notably, these factors have opposite functions: the E4 enzyme Ufd2 promotes degradation of p90, while the deubiquitylating enzyme Otu1 cooperates with the Ufd3 protein to stabilize p90. Therefore, it is possible that under conditions of increased needs for the Spt23 transcription factor, the activity of Otu1 and Ufd3 proteins is higher than that of Ufd2, leading to stabilization of the transcription factor and high expression from *OLE1* promoter.

A third mode of the OLE pathway regulation might operate to prevent expression of the *OLE1* gene under conditions of increased membrane fluidity. Indeed, the OLE pathway is strongly influenced by high levels of UFAs as it is completely turned off under such conditions (Choi et al., 1996). It was reported that processing of Spt23 but not of the Mga2 protein could be inhibited by high levels of UFAs (Hoppe et al., 2000). It was proposed that the Spt23 precursor might directly sense fluidity or thickness of the lipid bilayer. Upon changes in membrane fluidity, the Spt23 molecule might undergo a conformational change, which could regulate either the formation of the processing initiation loop (possibly involving the ankyrin repeats), the folding of degradation barrier (the IPT dimerization strength might be regulated by membrane fluidity), or the association with the Rsp5 ubiquitin ligase. It is interesting to note that while prevention of either the loop formation or the interaction with the ubiquitin ligase will exclude proteasomal degradation and processing, a prevention of the barrier formation will promote the complete elimination of p120. The latter

mechanism could be employed for the regulation of Mga2 protein abundance upon conditions of increased membrane fluidity. Although Mga2 processing was only moderately inhibited by high levels of UFAs, its abundance diminished significantly, suggesting that p120 might undergo enhanced degradation (data not shown). Moreover, results presented in this study demonstrate that selection of the initiation site and the direction of proteolysis may be critical for the fate of substrates. Therefore, an additional way to control the activity of the OLE pathway might rely on the selection of either the internal or the N-terminal site for initiation of proteolysis, and thus the decision to process or degrade Spt23/Mga2, respectively. Finally, another mechanism most likely employed to reduce *OLE1* expression may involve enhanced polyubiquitylation of the p90 fragment by the E4 enzyme Ufd2 and its subsequent degradation (Richly et al., 2005).

It seems likely that combination of all of these regulatory mechanisms could be valuable for the fine-tuning of Spt23/Mga2 activity (Table 3-1), ensuring a fast and accurate adaptation to cellular needs. Moreover, since there are certain similarities between the Spt23/Mga2 and the NFκB proteins, similar mechanisms could also be operating for the control of these mammalian transcription factors and, perhaps more generally, to control the fates of numerous other proteins.

OFF	STAND-BY	ON
p120 is short-lived	p120 is stable	p120 is stable
p120 processing is blocked	p120 processing is blocked	p120 is processed
p90 mobilization is blocked	p90 is short-lived	p90 is mobilized
p90 is short-lived		p90 is stable

Table 3-1. Hypothetical regulatory modes for the OLE pathway. The interplay between processing and complete degradation of the Spt23/Mga2 precursors (p120), and the active transcription factor (p90) mobilization and degradation decides on the activity of the OLE pathway. In the “OFF” mode, both the p120 and p90 proteins are eliminated, thus the OLE pathway is turned off. In the “STAND-BY” mode, p120 is present but not processed; the OLE pathway is turned off. In the “ON” mode, p120 is stable and efficiently processed, producing high levels of p90 (in addition p90 is stabilized); the OLE pathway is turned on.

3.4. Complete degradation and processing of substrates by the proteasome

The main way to control the fates of the proteasomal substrates seems to rely on regulating their ubiquitylation. Interestingly, not all ubiquitylated substrates are efficiently degraded by the proteasome. Results presented in this study demonstrate that the availability of a flexible region for initiation of degradation is crucial for its engagement by the proteasome (see above). Moreover, the selection of one of more available flexible degradation initiation sites of the target proteins seems to be critical for regulation of their fates as well. Findings that certain stable domains can hinder degradation depending on the direction of the proteasomal proteolysis seem to explain well how such regulation may decide on the fate of a substrate. Interestingly, when degradation of Mga2ΔTM is initiated from the N-terminus, the IPT domain seems not to hinder the proteasomal progression, as no stable C-terminal proteolytic fragments of expected molecular weight are formed (Figure 2-18f). Work on circular permutants of DHFR demonstrated that efficient unfolding and degradation by the proteasome depends on the local stability of the structure engaged first by the ATPase machinery, rather than the global stability of the domain (Lee et al., 2001). Therefore, if the local stability of the N-terminal part of the IPT domain is lower than that of the C-terminal part, the proteasome can unfold and degrade completely the IPT domain during proteolysis initiated at the N-terminal site of p120. However, in the opposite situation, when the C-terminally located initiation site is chosen, the proteasome stops degradation after it reaches the C-terminal stable part of the IPT domain, which is resistant to unfolding by the ATPase motor and thus releases the partially degraded substrate, the p90 form. In addition, masking of the unstructured initiation region may decide whether the ubiquitylated protein is stably engaged by the degradation machinery or not.

The finding that during the degradation of the ERAD substrate Hmg2 both N- and C-terminal fragments accumulate transiently during the process (as shown in *cim3-1* mutants; Figure 2-8), strongly argues that also complete proteasomal degradation may be initiated internally. Selection and cleavage of cytosolic loops of this substrate may allow a separate extraction of TM spans and thus might help to degrade a large transmembrane region composed of eight TM spans. It seems possible that the proteasomal ATPases may be involved in the extraction of Hmg2

TM segments from the membrane, similarly to the previously described situation for certain short-lived artificial ERAD substrates (Mayer et al., 1998). Interestingly, not only the N-terminal transmembrane part-derived fragments were found in the pellet fraction, but the C-terminal intermediates as well. This suggests that the fragments might be kept at the ER membrane associated with the proteasome and other ERAD components, most likely in repetitive inefficient degradation attempts.

It is likely that proteasomes in general might commence degradation from internal sites, or even that the same substrates may be degraded from various internal or terminal initiation sites, depending on position of the ubiquitin chain. If selection of the degradation initiation site is regulated, this may have interesting implications for the fate of the target protein. In line with this idea, the attachment site of polyubiquitin chain may select the initiation site. Indeed, experiments with IκBα showed that it is ubiquitylated at two N-terminally located lysines (Scherer et al., 1995) and that its degradation initiates from the N-terminus, since an N-terminal fusion of a glycine-alanine repeat region does not interfere with IκBα ubiquitylation, but blocks its degradation (Sharipo et al., 1998). In addition, the N-end rule substrate ubiquitin-X-β-galactosidase is ubiquitylated at N-terminal sites and degraded from the N-terminus (Bachmair et al., 1986; Bachmair and Varshavsky, 1989). Moreover, it was shown for the Sic1 protein that different sites for the attachment of the polyubiquitin chain to the substrate are not equivalent in promoting degradation (Petroski and Deshaies, 2003), most likely due to the different distance to the unstructured initiation site for proteolysis.

Identification of stable proteolytic fragments of Hmg2 in proteasome mutant cells raises the question whether they might also accumulate naturally in WT cells. It seems likely that the activity of the proteasome can be regulated in cells by certain physiological cues. In such hypothetical situation, proteolytic fragments could be formed and they might have physiological function. For example, incompletely degraded parts of proteins containing functional degron site might compete with the full-length substrate for the ubiquitin ligase and therefore contribute to a negative feedback loop in regulating degradation. Another possibility could be an inactivation of certain substrates by partial degradation. For example, complete degradation of polytopic proteins seems to require a long time of engagement of the proteasome and a high consumption of energy due to the need to extract the TM spans. Upon

conditions of diminished activity of the proteasome, it could be advantageous to remove only a fragment crucial for the biological function of the protein. Such processed non-functional product could be further completely degraded under normal conditions.

Interestingly, even the short peptides produced by the proteasomal degradation have other functions, than to serve as molecular bricks to build new proteins after further decomposition to amino acids. It is clear that even low concentrations of a single peptide can have biological functions. One well known case are the peptides derived from proteasomal or lysosomal proteolysis, which are bound by the major histocompatibility complexes (MHC) (Kloetzel, 2004). Although yeast cells do not possess MHC molecules, other proteins possessing peptide-binding pockets may be regulated by the proteasome mediated-proteolysis of certain substrates. Indeed, small peptides are employed by yeast, for example in the signalling of mating. When a yeast cell encounter the mating pheromones produced by the cell of the opposite cell type, it induces the expression of mating genes and thus prepares the two cells to form a diploid cell (Marsh et al., 1991). Moreover, some peptides produced by cleavage of longer precursors have functions that are independent of their precursors. It was demonstrated that peptides produced by cleavage of signal sequences from certain substrates by the signal peptide peptidase can be released to the cytosol and bind to calmodulin, a protein involved in the regulation of many cellular processes (Martoglio and Dobberstein, 1998). Also the signal peptide of the glycoprotein of the lymphocytic choriomeningitis virus (LCMV) is first utilized to target the protein to the ER, but after cleavage it has an additional functions in the virus life cycle (Froeschke et al., 2003).

Therefore, degradation of proteins or rather processing of polypeptides to smaller peptides, could serve to produce fragments that might act as “intracellular hormones” or signalling molecules. These functions may be generally overlooked in studies on degradation of proteins by the proteasome, due to a technical difficulty in detection of short peptides, but could have a high impact on the regulation of many cellular processes.

4. Materials and methods

4.1. Materials

4.1.1. Chemicals and reagents

Unless otherwise mentioned, chemicals and reagents were purchased from Amersham-Pharmacia, Applied Biosystems, Biomol, Biorad, Difco, Fluka, Invitrogen, Kodak, Merck, New England Biolabs, Promega, Roth, Roche, Riedel de Haen, Serva or Sigma. For all methods described, de-ionized sterile water, sterile solutions and sterile flasks were used.

4.1.2. Antibodies

Antibodies were used in this study for detection of proteins by immunoblotting, for studying protein-protein interactions by immunoprecipitation and intracellular localization of proteins by immunofluorescence microscopy.

Table 4-1. Antibodies used in this study

Primary antibodies:	Source
Monoclonal anti-c-myc (9E10)	Santa Cruz
Polyclonal anti-c-myc (A-14)	Santa Cruz
Monoclonal anti-HA (F-7)	Santa Cruz
Polyclonal anti-HA (Y-11)	Santa Cruz
Monoclonal anti-ubiquitin (P4D1)	Santa Cruz
Monoclonal anti-Dpm1	Molecular Probes
Monoclonal anti-Pgk1	Molecular Probes
Polyclonal anti-Kar2	M. Rose (Princeton University)
Secondary antibodies:	
HRP-coupled anti-rabbit IgG	Dianova
HRP-coupled anti-mouse IgG	Dianova
Alexa Fluor 546 anti-mouse IgG	Molecular Probes

4.1.3. *E. coli* strains

XL1-Blue: *hsdR17 recA1 endA1 gyrA46 thi-1 supE44 relA1 lac* [F' *proAB lacI*^{q}*ZΔM15 Tn10* (Tet^{r})] (Stratagene)

TG1: *supE thi-1* Δ(*lac-proAB*) Δ(*mcrB-hsdSM*)*5* (r_k^- m_k^-) [F' *traD36 proAB lacI*^{q} *ZΔM15*] (Stratagene)

4.1.4. *E. coli* media

LB-medium/plates:

1% (w/v)	tryptone (Difco)
0.5% (w/v)	yeast extract (Difco)
1% (w/v)	NaCl
1.5% (w/v)	agar (plates)
	sterilized by autoclaving

4.1.5. *S. cerevisiae* strains

Most yeast strains used in this study are isogenic to DF5. In experiments with the *cim3-1* proteasomal mutant the CMY826 strain was used as WT control. For Yeast-Two-Hybrid assays the strain PJ69-4a was used.

Table 4-2. Yeast strains

S. cerevisiae strains derived from DF5 WT background

Name	Genotype	Source
DF5 (WT)	*his3Δ200, leu2-3,2-112, lys2-801, trp1-1(am), ura3-52*	(Finley et al., 1987)
pre1-1	*pre1::TRP1, pTX49pre1-1*	(Mayer et al., 1998)
Δspt23 Δmga2	*spt23::hisG, mga2::LEU2*	(Hoppe et al., 2000)
Δspt23	*spt23::kanMX*	this study
Δmga2	*mga2::kanMX*	this study
ufd1-2	*ufd1-2*	(Hoppe et al., 2000)
Δrsp5	*rsp5::HIS3*	(Hoppe et al., 2000)

Other *S. cerevisiae* strains

Name	Genotype	Source
CMY826	*ura3-52, leu2Δ1, his3Δ-200, trp1Δ63, lys2-801, ade2-101, bar1::HIS3*	(Mayer et al., 1998)
cim3-1	*cim3-1, ura3-52, leu2Δ1*	(Mayer et al., 1998)
cim3-1Δhrd1	*ura3-52, leu2Δ1, his3Δ-200, trp1Δ63, lys2-801, ade2-101, bar1::HIS3, hrd1::kanMX*	this study
Δhrd1	*cim3-1, ura3-52, leu2Δ1, hrd1::kanMX*	this study
rsp5-1	*his4-912 ΔR5, lys2-128Δ, ura3-52, rsp5-1*	(Huibregtse et al., 1997)
PJ69-4a	*trp901-, leu2-3,112, ura3-53, his3-200, gal4, gal80, GAL1::HIS3, GAL2-ADE2, met2::GAL7-lacZ*	(James et al., 1996)

4.1.6. *S. cerevisiae* vectors

CEN plasmids: pYCplac33 (URA3), pYCplac22 (TRP1), pYCplac111 (LEU2)
2*μ* plasmids: pYEplac195 (URA3), pYEplac112 (TRP1), pYEplac181 (LEU2)
integrative plasmids: pYIplac211 (URA3),pYIplac204 (TRP1), pYIplac128 (LEU2)
(Gietz and Sugino, 1988)
pUG36 (URA3, CEN, *MET25* promoter) (Niedenthal et al., 1996)
pSE362 (HIS3, CEN) (Elledge and Davis, 1988)
Yeast-Two-Hybrid vectors: pGAD-C1, pGBD-C1 (James et al., 1996)

4.1.7. *S. cerevisiae* plasmids

Mga2 constructs are derivatives of previously described ^{myc}Mga2 version containing triple myc epitopes introduced directly after the start codon (Hoppe et al., 2000). ^{myc}Mga2^{HA} was created by introducing an 3HA tag to the C-terminus of the protein. ^{HA}Mga2 protein contained triple HA epitopes inserted at the N-terminus. For the expression under the control of *MET25* promoter, Mga2 constructs were cloned into the low copy vector pUG36 from which the GFP-encoding fragment was removed (pUG36ΔGFP). ^{myc}Mga2ΔTM encodes a truncated protein encompassing amino acids 1-1037. The entire sequence of *Mus musculus* DHFR (tagged C-terminally with a 3HA cassette) was fused to the C-terminus of ^{myc}Mga2 (^{myc}Mga2-DHFR^{HA}) or ^{myc}Mga2ΔTM (^{myc}Mga2ΔTM-DHFR^{HA}). DHFR was PCR-amplified from construct XVI, described previously (Bachmair and Varshavsky, 1989). Plasmids for expression of Mga2 constructs under the control of *GAL1-10* promoter were cloned into an integrative vector YIplac211. ^{myc}Mga2(TEV)^{HA} protein is an Mga2 variant with amino

acids 671-678 replaced with the ENLYFQG sequence (the TEV protease cleavage site). Truncated Mga2 variants containing ankyrin repeats shown in Figure 2-12 were tagged with triple HA epitopes at their N-termini and expressed under the control of the *ADH1* promoter from YCplac22 vector. To express Mga2 constructs under the control of endogenous promoter the 5.1kb HindIII genomic DNA fragment containing *MGA2* locus was subcloned from YEplac181-mycMga2 (Hoppe et al., 2000) into the integrative YIplac211 or centromeric YCplac22 and YCplac111 vectors. Mutations: ΔANK (amino acids 719-781 of Mga2), *ANK** (mutation of residues 757-761 LHLA to AAFP) and ΔIPT (amino acids 529-625 of Mga2) were introduced into Mga2 constructs by a PCR-based strategy (see 4.5.3). Mga2 constructs for Yeast-Two-Hybrid assays (Figure 2-11) were amplified by PCR and cloned into pGAD-C1 or pGBD-C1 vectors to obtain in frame N-terminal fusions with the activating or binding domain of Gal4, respectively. In all of the created YTH-constructs, the transactivation domain, the TM span and the ER lumen domain of Mga2 were omitted.

^{myc}Spt23^{HA} under the control of its own promoter (Hoppe et al., 2000) was subcloned into the centromeric vector YCplac111. Spt23ΔIPT and ΔANK constructs lack amino acids 507-598 (encoding the IPT domain) and 709-771 (the ankyrin repeat domain), respectively. Spt23 deletions shown in Figure 2-5 were created by a PCR-based strategy. DHFR^{HA} encoding sequence was fused to the C-terminus of the TM span lacking form of ^{myc}Spt23 (residues 1-1005 of Spt23) by a PCR-based strategy. This construct (^{myc}Spt23ΔTM-DHFR^{HA}) was expressed under the control of *MET25* promoter from pUG36ΔGFP.

^{6myc}Hmg2 was subcloned from pRH244 (provided by R.Y. Hampton, University of California, San Diego; (Hampton et al., 1996) into pUG36ΔGFP and expressed under the control of the *MET25* promoter. Insertion of a 3HA cassette at the C-terminus resulted in ^{6myc}Hmg2^{HA}.

The reporter construct used in Figure 2-13 was subcloned from plasmid D1557 (provided by M. Kalocay, Max Planck Institute of Biochemistry). The XbaI-NsiI fragment containing the *LacZ* gene under the control of the *OLE1* promoter was subcloned to XbaI and PstI-partially digested pSE362 vector.

To rescue the Δ*spt23* Δ*mga2* strain the plasmid for heterologous expression of *OLE1* was created. The *OLE1* ORF was amplified by PCR from yeast genomic DNA and placed under the control of the *ADH1* promoter in YCplac33 or YCplac111.

4.1.8. *S. cerevisiae* media and solutions

YPD/YPGal:	1%	(10 g/l)	yeast extract (Difco)
	2%	(20 g/l)	bacto-peptone (Difco)
	2%	(20 g/l)	D-(+)-glucose or galactose
	2%	(20 g/l)	agar (for plates)
			sterilized by autoclaving
SC-media/plates:	0.67%	(6,7 g/l)	yeast nitrogen base (Difco)
	0.2%	(2 g/l)	drop out amino acid mix
	2%	(20 g/l)	glucose, raffinose, or galactose
	2%	(20 g/l)	agar (for plates)
			sterilized by autoclaving

drop out amino acid mix:	20 mg	Ade, Ura, Trp, His
	30 mg	Arg, Tyr, Leu, Lys
	50 mg	Phe
	100 mg	Glu, Asp
	150 mg	Val
	200 mg	Thr
	400 mg	Ser

UFAs-containing media were supplemented with oleic, linoleic or palmitoleic acids (Sigma) resuspended in equal volumes of Nonidet P40 (final concentration of 0.2% (v/v) each).

Growth media used for experiments with MTX (Sigma) were supplemented with 5mg/ml sulfanilamide (Sigma). MTX was added to a final concentration of 10 μM from a 55 mM stock solution in 0.1 M NaOH.

Sporulation medium:	1%	(w/v)	potassium acetate
	0.05%	(w/v)	raffinose
SORB:	100 mM		CH_3COOLi
	10 mM		Tris-HCl, pH 8.0
	1 mM		EDTA, pH 8.0
	1 M		sorbitol
			sterilized by filtration
PEG:	100 mM		CH_3COOLi
	10 mM		Tris-HCl, pH 8.0
	1 mM		EDTA, pH 8.0
	40% (w/v)		PEG-3350
			sterilized by filtration
Zymolase 20T solution:	0.9 M		sorbitol
	0.1 M		Tris-HCl, pH 8.0
	0.1 M		EDTA, pH 8.0
	50 mM		DTT (added freshly)
	0.5 mg/ml		zymolase 20T (ICN Biochemicals)

4.2. Computer-based analyses

For database searches (sequence search and comparison) electronic services were used provided by the Saccharomyces Genome Database (http://www.yeastgenome.org/) and the National Center for Biotechnology Information (http://www.ncbi.nlm.nih.gov/). Most of the protein sequence analyses were done with software programs from ExPASy Proteomics Server (http://www.expasy.org/). For assessment of protein domain composition and protein folding, the programs SMART (http://www.smart.embl-heidelberg.de) and FoldIndex (http://bip.weizmann.ac.il/fldbin/findex) were used, respectively. DNA sequence analyses (DNA restriction enzyme maps, DNA sequencing analyses, DNA primer design) were done with DNA-Star (DNA Star Inc.).

Chemiluminescence signals of immunoblots were detected by a CCD camera (LAS 3000, Fujifilm), quantified with the software program Image Gauge V4.1 (Fujifilm) and processed with Adobe Photoshop (Adobe Systems Inc.). Digitalized

immunoblot films were processed with Adobe Photoshop (Adobe Systems Inc.). For the presentation of text, tables, graphs and figures, software programs of the Microsoft Office package (Microsoft Corp.) were used.

4.3. *E. coli* techniques

4.3.1. Cultivation and storage of *E. coli*

Liquid cultures were grown in LB media shaking at 200 rpm at 37 °C. Cultures on agar plates were incubated at 37 °C. For the selection of transformed bacteria, ampicillin (50μg/ml) was used. The culture density was determined by measuring the absorbance at a wavelength of 600 nm (OD600). Cultures on solid media were stored at 4 °C up to 7 days. For long-term storages, stationary cultures were frozen in 15% (v/v) glycerol solutions at –80 °C.

4.3.2. Preparation of competent *E. coli* cells

DNA plasmids were transformed into *E. coli* competent cells by calcium chloride or by electroporation methods. For the preparation of competent cells, 1 l liquid LB medium was inoculated with 10 ml of an overnight culture derived from a single *E. coli* colony and grown to OD600 of 0.6-0.8 at 37 °C. After chilling the culture flask on ice for 0.5 h, cells were harvested by centrifugation (10 min, 5000 *g*, 4 °C). All following steps were performed with pre-chilled sterile materials and solutions at 4 °C. For the preparation of chemically competent cells, the pellets were carefully resuspended in 200 ml $MgCl_2$ solution (100 mM). The resuspended cells were sedimented by centrifugation, resuspended in 400 ml $CaCl_2$ solution (100 mM) and after incubation on ice for 20 min centrifuged again. Finally, the competent cells were resuspended in 20 ml $CaCl_2$ solution (100 mM) containing 10% (v/v) glycerol and stored in 100 μl aliquots at –80 °C. For the preparation of electrocompetent bacteria, the pellets were washed once with 1 l ice-cold water and once with 0.5 l ice-cold 10% (v/v) glycerol. Then the cells were resuspended in 3 ml 10% (v/v) glycerol and stored in 100 μl aliquots at –80 °C.

4.3.3. Transformation of plasmid DNA into *E. coli* cells

Competent cells were thawed on ice. For the chemical transformation, 50 μl competent cells were mixed with 10 ng plasmid DNA and incubated on ice for 30 min. Subsequently cells were incubated at 42 °C for 90 s. After the heat shock the cell suspension was resuspended in 1 ml LB medium without antibiotics and incubated on a shaker at 37 °C for 1 h. Transformed cells were selected by streaking out the cell suspension on LB agar plates containing ampicillin and incubated over night at 37 °C.

For the electroporation, 40 μl competent cells were mixed with 2 μl ligation sample. The suspension was electroporated in a pre-chilled Gene pulser cuvette, 0.1 cm (Biorad) with a pulse of 1.8 kV and 25 μF at the resistance of 200 Ω. After adding 1 ml LB medium without antibiotics, the suspension was incubated for 1 h on a shaker at 37 °C. Selection of transformants was carried out on ampicillin-containing LB agar plates over night at 37 °C.

4.4. *S. cerevisiae* techniques

4.4.1. Cultivation and storage of *S. cerevisiae*

Cultivation of yeast cells was performed according to standard protocols (Ausubel et al., 1987; Sambrook et al., 1989). Liquid pre-cultures were inoculated with a single colony-derived yeast from a plate and grew with shaking over night at 30 °C or 23 °C (thermosensitive mutants). The culture density was determined by measuring the absorbance at the wavelength of 600 nm (OD600), where OD600 equal 1 corresponds to $1.5x10^7$ cells/ml. The main culture was inoculated with the pre-culture to OD600 0.1-0.2 and incubated at appropriate temperature with shaking at 150-200 rpm until the culture had reached the mid-log phase of growth ($1–5x10^7$ cells/ml). When UFAs containing growth media were used, cells were washed three times with water before OD600 measurement. Cultures on solid media were stored at 4 °C up to 1-2 months. For long-term storages, stationary cultures were frozen in 15% (v/v) glycerol solutions at –80 °C.

4.4.2. Preparation of competent yeast cells

50 ml-culture of yeast cells was inoculated from a fresh pre-culture and grown to a density of 0.5–0.7 OD600. The cells were pelleted by centrifugation (500 *g*, 5 min), washed once with 25 ml sterile water, then with 10 ml volume SORB solution and resuspended in 360 µl SORB solution. After adding of 40 µl carrier DNA (salmon sperm DNA, 10 mg/ml, Invitrogen), competent cells were stored in 50 µl aliquots at –80 °C.

4.4.3. Transformation of yeast cells

For transformation of yeast ~ 0.2 µg of circular or ~ 2 µg linearized plasmid DNA (or PCR products) was mixed with 10 µl or 50 µl competent cells, respectively. After addition of 6 volumes of PEG solution, the cell suspension was incubated at RT for 30 min. Subsequently, DMSO was added to a final concentration of 10% and a heat shock was performed at 42 °C for 15 min. Cells were sedimented by centrifugation (400 *g* for 3 min), resuspended in 100 µl sterile water and plated on the respective SC medium plates. After 2-3 days of incubation at RT (in case of temperature sensitive strains) or 30 °C transformants colonies were used for further analysis. When the antibiotic G418 was used for selection, transformed cells were incubated with shaking in YPD medium for 3 h before they were streaked out onto plates containing G418. If necessary, transformants were replica-plated on G418-containing plates to remove false-positive clones.

Genomic integration by homologous recombination

For the stable integration of DNA into yeast genome vectors of the YIplac series (Gietz and Sugino, 1988) were used. Since they do not contain autonomous replication elements, only stably integrated vectors are propagated in yeast. Before transformation, these vectors are linearized by a single cut within the auxotrophy marker gene. The free DNA ends of the marker gene on the linearized plasmid recombine with the homologous DNA sequences at the endogenous locus of the marker gene and enable the vector to integrate.

A similar strategy was applied for creating yeast strains harbouring chromosomal gene deletions. This method employs a PCR-based strategy (Knop et al., 1999; Longtine et al., 1998). PCR product used to transform competent yeast cells contained a selection marker gene flanked by sequences homologous to the target gene, allowing homologous recombination within the endogenous locus. The primers required to target the PCR product to the gene locus were designed to amplify the selection marker cassette and in addition possessed 50 bp extensions at their 5' ends that are complementary to the promoter and terminator sequences of the target gene. After amplification, the PCR product was precipitated with ethanol, transformed into competent yeast cells and plated on the selection medium. The correct recombination was confirmed by PCR analysis.

4.4.4. Analysis of yeast mutants

Mating type analysis of haploid strains

The tester strains RC634a and RC75-7α were used for identification of yeast mating types. These strains are hypersensitive to the pheromone secreted by yeast of the opposite mating type. 50 µl of the tester strain culture was mixed with 10 ml of molten 1% (w/v) agar resuspended in YPD (cooled down to 45 °C) and poured over the YPD plate. Analyzed strains were replica plated on the a- and α-tester agar plates and incubated for 1-2 days. The tester strains cannot grow in proximity of colonies of the replica-plated strain displaying the opposite mating type, therefore a halo of clear agar appears around them, allowing the identification of their mating type. Diploid cells do not secrete any mating type pheromones and give no halo on both mating type tester strains plates.

Mating of haploid *S. cerevisiae* strains

Haploid strains of opposite mating types (MAT**a**, MATα) grown to mid-log growth phase were mixed and incubated in YPD at 30 °C for 3-4 h. Zygotes were streaked after mating onto the respective selection plates to select diploid cells.

Sporulation and tetrad analysis of diploid *S. cerevisiae* strains

Diploid yeast cells were grown to the stationary phase and 500 µl of the culture was harvested by centrifugation (500 g, 3 min). Cells were washed 3 times with sterile water and resuspended in 5 ml sporulation medium. After incubation on a shaker at RT for 3 days, 10 µl of the culture was mixed with 10 µl zymolase-20T solution and incubated at RT for 10 min. The spores were dissected in tetrads with a micromanipulator (Singer MSM Systems) and grown on YPD plates for 2-3 days. Subsequently, tetrads were replica plated and analyzed genotypically on selection plates for specific markers or by their phenotypes.

4.4.5. Analysis of protein-protein interactions with the yeast two-hybrid system

Selected truncated variants of Mga2 were fused to the C-terminus of the DNA-binding ("baits") or activation domain ("preys") of the Gal4 protein by cloning them into pGBD-C1 or pGAD-C1 vectors, respectively. Bait constructs were co-transformed with empty pGAD-C1 vector to investigate their auto-activation. The construct encompassing amino acids 514-796 did not activate reporter genes in this test, whereas constructs 529-1037ΔANK and 514-640 exhibited auto-activation, which could be blocked on SC –Leu –Trp plates supplemented with 10 mM 3-AT or

on SC –Ade plates. Various combinations of baits and preys plasmids were transformed into PJ69-4a cells (James et al., 1996) and plated on SC –Leu –Trp plates. Equal amounts of transformants were spotted on SC –Leu –Trp –His without and with 3-AT supplement or SC –Leu –Trp –Ade plates. Physical interaction between bait and prey proteins leads to reconstitution of the Gal4 transcription factor, which induces expression of *HIS3* and *ADE2* reporter genes and allows yeast cells to grow on the respective selection media.

4.4.6. Phenotype analysis by growth tests

Analysis of the yeast growth phenotype is based on the comparison of growth rates upon various conditions (e.g. different temperature or presence/absence of 18:1) of different yeast strains cells spotted in equal amounts on a solid medium. Yeast cultures grown to mid-log growth phase or collected from fresh plates were diluted with sterile water to an OD600 of 0.2. In the 96-well microtiter plate 4-5 ten-fold serial dilutions were prepared. 5µl of each cells suspension were spotted on respective plates with a 96-pin-stamp and the plates were incubated at different temperatures for several days.

4.4.7. Expression shut-off experiments

The stability of proteins was determined by cycloheximide chase experiments. Cycloheximide is an inhibitor of cellular translation and after addition to the growth medium blocks *de novo* production of proteins, allowing monitoring over time protein levels in yeast cells. In case of proteins expressed under the control of the *GAL1-10* promoter this approach was combined with selective repression of the promoter in the presence of glucose in the growth medium (*GAL* promoter shut-off experiment).

WT and *cim3-1* cells expressing ^{6myc}Hmg2^{HA} (Figure 2-8) were grown in YPD medium at permissive temperature to exponential phase and then shifted to 37°C for 90 min prior to addition of cycloheximide. *cim3-1* cells expressing ^{myc}Spt23^{HA} or ^{myc}Spt23ΔIPT^{HA} (Figure 2-4b and Figure 2-7e) were grown on SC medium supplemented with 0.2% palmitoleic acid at RT for 3h and then shifted to 37°C for 90 min. Cells were centrifuged, washed, and resuspended in palmitoleic acid-free medium prior to addition of cycloheximide. Translation was inhibited by cycloheximide (final concentration 0.5 mg/ml). For each time point, samples corresponding to OD600 of 1 were withdrawn, and protein extracts were prepared (see 4.4.8).

Yeast expressing proteins under the control of the *GAL1-10* promoter were grown on plates containing raffinose and galactose (both 2% w/v) for 2-3 days. Cells were transferred to a liquid medium containing galactose (2% w/v galactose) and grown to saturated pre-culture. For preparation of the main culture, usually 25 ml YPGal or SC-Gal medium was inoculated with the pre-culture to OD600 of 0.05-0.1 and grown several hours to reach log-phase of growth. When the protein turnover was investigated in temperature sensitive mutants *ufd1-2* and *rsp5-1*, these cells (and the WT cells control) were shifted to the non-permissive temperature (37 °C) for 3 h prior to the start of the promoter shut-off experiment. Cells were harvested by centrifugation (500 *g*, 5 min) and resuspended in YPD containing 0.5 mg/ml cycloheximide. The incubation was continued at respective temperatures and equal amounts of cells were withdrawn after indicated times for extracts preparation.

4.4.8. Preparation of cell extracts and microsomal fractions

Preparation of denatured yeast extracts

For analysis of cellular levels of proteins and examination of post-translational modifications of proteins, denatured protein extracts were prepared in order to avoid proteolysis and de-conjugation during the lysis procedure. Usually, 1 ml of mid-log phase yeast cells corresponding to an OD600 of 1 were harvested by centrifugation and resuspended in 1 ml ice-cold water. Subsequently, 150 µl of lysis buffer (1.85 M NaOH, 7.5% β-mercaptoethanol) was added and placed on ice for 15 min. Next, 150 µl 55% (w/v) trichloroacetic acid (TCA) was added and the mixture was incubated for 10 min on ice. The precipitated material was pelleted by centrifugation (20000 *g* at 4° for 10 min) and the supernatant was carefully removed. The pellet was washed once with acetone, air-dried and resuspended in 50 µl HU sample buffer.

Preparation of native yeast extracts and microsomal fractions

Native proteins extracts were prepared to obtain microsomal fractions and to study interaction of proteins by immunoprecipitation under native conditions. Yeast cells of mid-log phase culture were harvested by centrifugation, washed once with ice-cold water and resuspended in 200-400 µl lysis buffer (Tris-HCl, pH 7.4, 150 mM NaCl) containing protease inhibitors (complete inhibitors set from Roche, 2 mM PMSF, 5 mM benzamidine, 20 mM NEM). After addition of glass beads (ø 425-600 µm, Sigma) the cells were lysed by vortexing 4-5 times for 30 s at 4 °C or using a bead beater (Retsch). The sample tube was perforated with a 23-gauge needle and the cell lysate was separated from beads by centrifugation. The cell debris was removed by centrifugation (700 *g,* 5 min, 4 °C). The whole cell extract contains the soluble fraction (cytosolic and nuclear proteins) as well as microsomes (ER, nuclear envelope and other organelles). The cytosolic fraction is partially contaminated with proteins from the lumen of organelles, which upon the lysis with glass bead are partially disrupted. For separation of microsomes from the soluble phase, whole cell extracts were fractionated by high spin centrifugation (20000 *g*, 1 h, 4 °C).

Determination of protein concentration

Protein concentrations were determined by using the Bradford method (BioRad protein assay; BioRad) and compared to a BSA standard dilution series by measuring the OD595.

4.4.9. Investigation of protein localization in cells

Immunofluorescence microscopy

Intracellular localization of proteins was studied by indirect deconvolution immunofluorescence microscopy. Yeast cells were cultured in sterile-filtered (not autoclaved) SC medium to OD600 of 1. To fix proteins 1/9 volume of 1M potassium phosphate buffer, pH 6.5 and 1/9 volume 37% formaldehyde (Sigma) was added to the culture, and the suspension was incubated on a falcon roller at RT for 1 h. Cells were harvested by centrifugation (1500 *g*, 5 min, 4 °C) and the pellet was carefully washed 3 times in 1ml SP-buffer (0.1 M potassium phosphate buffer, pH 6.5, 1.2 M sorbitol). Subsequently, cells were resuspended in 900 µl SPβ-buffer (10 ml SP-buffer, 14 µl β-mercaptoethanol), 100 µl Zymolase 100T solution (2.5 mg/ml in SPβ-buffer) was added and the digestion reaction was performed at 30 °C for 30 min. After a 3-step washing with SP-buffer (1500 *g*, 5 min, 4 °C) cells were resuspended in 100 µl PBSB-buffer (1 mg/ml BSA in PBS) and the suspension was placed on a

polylysine-coated slide. After addition of the primary antibody (anti-myc monoclonal, 9E10) the slide was incubated in the dark, in a moist chamber at 4 °C for 12 h. Next, cells were carefully washed 5 times with PBSB buffer and the fluorophore-coupled secondary antibody (Alexa Fluor 546 anti-mouse IgG) was added for 2 h at RT (in the dark). Subsequently, the slide was washed once with PBST (1% (v/v) Triton X-100 in PBS), 6 times with PBSB-buffer and finally 5 μl DAPI (2.5 μg/ml DAPI in 50% (v/v) glycerol) was added. The slide was covered with a cover slip, sealed with nail polish and examined under the microscope.

Membrane fractionation

To investigate membrane localization of proteins membrane fractions were prepared (see 4.4.8). To analyze whether proteins are peripherally associated with ER, membrane fractions were divided in equal parts and incubated with a lysis buffer containing 1 M Na_2CO_3, pH 11.3, 500 mM NaCl or 0.1% (w/v) SDS for 30 min on ice with occasional vortexing. Subsequently, samples were subjected to centrifugation (20000*g*, 30 min, 4 °C) to separate soluble and membrane-associated fractions, and further analyzed by immunoblotting.

Proteinase K protection assay

To confirm localization of proteins to the ER lumen, the Proteinase K protection assay was performed. Cells were lysed as described above (see 4.4.8), except that the lysis buffer did not contain protease inhibitors. Total lysates were incubated with Proteinase K (0.2 mg/ml) or Proteinase K and 1% Triton X-100 for 30 min on ice. The reaction was stopped with PMSF (2 mM final concentration), and proteins were TCA-precipitated (see 4.4.8) and subjected to Western blot analysis.

4.4.10. Analysis of protein-protein interactions by immunoprecipitation

Immunoprecipitation under native conditions

To examine protein-protein interactions whole cell extracts were subjected to immunoprecipitation under native conditions. Triton X-100 was added to the lysates (to a final concentration of 0.1-0.4%) to avoid unspecific binding. To extract integral membrane proteins (Mga2 p120) 0.2% dodecyl maltoside (Sigma) was added to the lysates. Immunoprecipitation was carried out with 20 μl slurry anti-HA IgG (3F10; Roche) or anti-myc IgG (9E10; Santa Cruz) coupled to agarose beads, rotating on a falcon roller for 2 h at 4 °C. Unspecifically bound material was removed by 4 washing steps with the lysis buffer containing 0.1% Triton X-100, followed by one washing step with lysis buffer without detergent. The specifically bound material was eluted from the beads by incubation with 20 μl HU sample buffer at 65 °C for 15 min.

Cleavage of proteins with the TEV protease

Beads containing immunoprecipitated Mga2(TEV) were washed and resuspended in 600 μl TEV cleavage buffer (Invitrogen). The suspension was divided in two equal parts and to one of them 20 U of recombinant TEV protease (Invitrogen) was added, while the second part served as a control sample without enzyme. Both samples were incubated at 4 °C for 12 h with constant rotating. TEV protease is a site-specific enzyme, which cleaves between Gln and Gly residues in a seven-amino acid recognition sequence: Glu-Asn-Leu-Tyr-Phe-Gln-Gly. After the digestion reaction, the beads were sedimented by centrifugation (1000 *g*, 2 min, 4 °C). The unbound material from supernatants was TCA-precipitated (see 4.4.8) and denatured in 20 μl

HU sample buffer for 10 min at 65 °C. The beads were washed 3 times with a buffer containing 0.1% Triton X-100, once with PBS and then the bound material was eluted from beads by incubation in 20 µl HU sample buffer at 65 °C for 15 min. Soluble and bound proteins were analyzed by immunoblotting.

Microsomes containing Mga2(TEV) were resuspended in 1 ml TEV cleavage buffer and divided in two equal parts. One part was control sample without TEV protease and to the other part 30 U of recombinant TEV protease (Invitrogen) was added. Digestion was performed with constant rolling at 4 °C for 12 h. Membrane bound material was pelleted by centrifugation (20000*g*, 45 min, 4 °C), resuspended in 50 µl HU sample buffer and proteins were denatured at 65 °C for 15 min.

4.4.11. Analysis of protein modification by ubiquitylation

Immunoprecipitation under denaturing conditions

For examination of post-translational modifications of proteins, whole cell extracts were subjected to immunoprecipitation under denaturing conditions. Cell amounts corresponding to OD600 of 10 were harvested by centrifugation and lysed in 300 µl 2 M NaOH/7.5% β-mercaptoethanol for 15 min on ice. Proteins were precipitated by addition of 300 µl 55% TCA and pelleted by centrifugation (20000 *g*, 15 min, 4 °C). The protein pellet was resolved in 100 µl boiling buffer (100 mM Tris, pH 11, 3% SDS) and incubated at 98 °C with shaking for 5 min. After removal of the unsolved material by centrifugation (16000 *g,* 5 min), the protein solution was diluted by addition of 700 µl IP-buffer (50 mM Tris, pH 7.5, 150 mM NaCl, 1% Triton X-100). For the immunoprecipitation 0.4 µg polyclonal anti-myc antibody (A-14; Santa Cruz) was added and the mixture was rotated on a falcon roller for 2 h at 4 °C. After clearing the sample from occasionally precipitated material by centrifugation (20000 *g*, 20 min, 4 °C), 20 µl Protein A agarose beads (Amersham Biosciences) was added to bind antibodies with immunoprecipitated proteins. Unspecifically bound material was removed by 2 washing steps with washing-buffer (50 mM Tris, pH 7.5, 300 mM NaCl, 1% Triton X-100), one with IP-buffer and one with PBS. The specifically bound material was eluted from the column by adding 20 µl HU sample buffer and analyzed by Western blotting.

4.4.12. X-Gal agarose overlay assay

To semi-quantitatively measure *lacZ* reporter activity, X-Gal agarose overlay assays were performed. In the presence of β-galactosidase, which is the product of the *LacZ* gene, X-Gal is hydrolyzed and yields a blue byproduct. Equal amounts of yeast were spotted on solid medium and grown for 36 h at 30 °C. On the top of the plate 10 ml overlay solution was poured (40-45 °C). After the agarose layer became stiffed, the plate was incubated at 30 °C for 90 min. Yeast clones of high activity of the reporter promoter turn blue, while less active become light blue or stay colourless.

Overlay solution:	50	mM	sodium phosphate buffer, pH 7.0
	1%	(w/v)	SDS
	10	mM	KCl
	1	mM	$MgCl_2$
	0.4%	(w/v)	low melting agarose
	0.2%	(v/v)	β-mercaptoethanol
	10	mM	X-Gal
	1%	(v/v)	DMF

4.5. Molecular biology methods

4.5.1. Isolation of DNA

Isolation of plasmid DNA from *E. coli*

LB medium (5 ml) containing the appropriate antibiotic was inoculated with a single *E. coli* colony harbouring the DNA plasmid of interest and incubated with shaking for 8-14 h at 37 °C. Plasmids were isolated using kits from the companies Qiagen (plasmid mini kit) or Macherey-Nagel (nucleospin plasmid quick pure).

Isolation of plasmid DNA from *S. cerevisiae*

Rapid isolation protocol for plasmid DNA isolation from yeast and direct propagation in *E. coli* was used. Saturated yeast culture (1.5 ml) was harvested by centrifugation (16000 *g*, 30 s) and sedimented cells were resuspended in 200 µl breaking buffer. Glass beads (0.3 g; ø 425-600 µm; Sigma) and 200 µl phenol/chloroform/isoamyl alcohol (24:24:1 v/v/v; Roth) were added and cells were lysed by vortexing for 2 min. After centrifugation (16000 *g*, 5 min), 0.5 µl of the aqueous phase containing DNA was used for transformation of *E. coli* for plasmid propagation.

Breaking buffer	2%	(v/v)	Triton X-100
	1%	(w/v)	SDS
	100	mM	NaCl
	10	mM	Tris-HCl, pH 8.0
	1	mM	EDTA, pH 8.0

Isolation of chromosomal DNA from *S. cerevisiae*

Chromosomal yeast DNA was isolated to serve as a template for the amplification of yeast genes via PCR. Cells from a saturated yeast culture (10 ml) were sedimented by centrifugation (1500 g, 5 min, 23 °C), washed once in 0.5 ml water and resuspended in 200 µl breaking buffer. After addition of 0.3 g glass beads (ø 425-600 µm; Sigma) and 200 µl phenol/chloroform/isoamyl alcohol (24:24:1 v/v/v; Roth) cells were lysed by vortexing for 3 min. The lysate was mixed with 200 µl TE buffer, centrifuged for 5 min and then the aqueous layer transferred to a microcentrifuge tube. DNA was precipitated by adding 1 ml ethanol (100%) and centrifugation (16000 *g*, 3 min). The pellet was resuspended in 0.4 ml TE buffer. To remove RNA contamination 30 µl of DNase-free RNase A (1 mg/ml) (Sigma) was added and the samples were incubated for 5 min at 37 °C. DNA was precipitated with 1 ml ethanol (100%) and 10 µl of ammonium acetate (4 M), briefly centrifuged and the pellet resuspended in 100 µl TE buffer. The yield of the isolated DNA was estimated photometrically (see below).

TE buffer	10	mM	Tris-HCl, pH 8.0
	1	mM	EDTA
			sterilized by autoclaving

Precipitation of DNA

For ethanol precipitation 1/10 volume sodium acetate (3 M, pH 4.8) and 2.5 volume ethanol were added to the DNA solution and incubated at –20 °C for 30 min. The mixture was centrifuged at 16000 *g* at 4 °C for 20 min and the pellet was washed

once with 0.5 ml 70% ethanol. The DNA pellet was air-dried and resuspended in TE buffer or sterile water.

Determination of DNA concentration in solution
The DNA concentration was photometrically determined by measuring the absorbance at a wavelength of 260 nm (OD260). An OD260 of 1 equals a concentration of 50 μg/ml double-stranded DNA.

4.5.2. Molecular cloning methods

Digestion of DNA with restriction enzymes
The sequence-specific cleavage of DNA with restriction enzymes was performed according to standard protocols (Sambrook et al., 1989) and the instructions of the manufacturer (New England Biolabs). Usually, 5-10 units of the restriction enzyme was used for the digestion of 1 μg DNA. Reaction samples were incubated in the appropriate buffer at the recommended temperature for 1-2 h. Linearized vectors were incubated at 37 °C for 1 h with the calf alkaline phosphatase (New England Biolabs) to avoid the re-circularization of DNA in the ligation reaction.

Separation of DNA by gel electrophoresis
DNA samples were mixed with 6x DNA loading buffer and subjected to electrophoresis in 0.8-2% agarose gels containing ethidium bromide (final concentration 0.5 μg/ml) at 100 V in TBE buffer. Separated DNA fragments were visualized by using an UV transilluminator (324 nm). The size of the fragments was estimated by standard size markers (1 kb DNA ladder from Gibco and 100 bp DNA ladder from New England Biolabs).

TBE buffer 5x	90	mM	Tris
	90	mM	boric acid
	2.5	mM	EDTA, pH 8.0
			sterilized by autoclaving
DNA loading buffer 10x	0.5%	(w/v)	SDS
	0.25%	(w/v)	bromophenol blue or orange G
	0.25%	(v/v)	glycerol
	25	mM	EDTA, pH 8.0

Isolation of DNA fragments from agarose gels
DNA fragments separated by gel electrophoresis were excised from the agarose gel using a razor blade. The DNA was extracted from the agarose block using kits from Qiagen (QIAExII, QIAquick gel extraction kit) or Macherey-Nagel (Nucleospin Extract II) and eluted with an appropriate volume of sterile water.

Ligation of DNA fragment
The amounts of isolated insert DNA fragments and linearized vectors were estimated by electrophoresis in an agarose gel containing ethidium bromide. For the ligation reaction a vector to insert ratio of 1:3 – 1:10 was used. The reaction sample (10 μl) contained ~ 100 ng of vector DNA and 10 units of T4 DNA ligase (New England Biolabs). The ligation reaction was performed at 23 °C for 1 h or at 6 °C for 6-12 h. Before transformation of electrocompetent *E. coli* cells, the ligation sample was

dialyzed against de-ionized water for 15 min using a nitrocellulose filter (pore size: 0.05 µm, Millipore).

DNA sequencing
Sequencing of DNA was performed by the Microchemistry Core Facility of the Max Planck Institute of Biochemistry on an ABI 3730 sequencer. The sample usually contained 0.5 µg of plasmid DNA and 5 pmol primer. Sample preparation and sequencing reactions were performed with the DYEnamic ET terminator cycle sequencing kit (Amersham-Pharmacia).

4.5.3. Polymerase chain reaction (PCR)

PCR is an easy and quick method to specifically amplify DNA fragments from small amounts of DNA template. This technique was applied for cloning, amplification of cassettes for chromosomal gene disruptions, and analysis of recombination events after chromosomal integration into yeast strains or of cloned inserts. All PCR reactions were prepared in 0.2 ml tubes (Biozym) on ice, in a volume of 15 µl or 50 µl for preparative PCR. A typical reaction was set up as follows:

50 ng plasmid DNA or 0.2 µg genomic DNA	
10x PCR buffer	1.5 µl
50 mM $MgCl_2$ (optional)	0.6 µl
10 mM dNTPs mix	0.6 µl
10 µM forward primer	0.75 µl
10 µM reverse primer	0.75 µl
Taq DNA polymerase	0.6 µl
sterile de-ionized water	to 15 µl

For amplification of fragments used for cloning, Vent or Phusion DNA polymerases (New England Biolabs) were used, as they are characterized by lower error rates than the *Taq* polymerase. The reaction samples amplified with the Phusion polymerase were prepared according to the manufacturers' instructions.

To pre-select *E. coli* transformants containing desired plasmids, a colony form a plate was transferred directly into a reaction sample with a pipette tip. During an initial denaturation step, bacterial cells are lysed and their released DNA serves as a template for the amplification via PCR.

For the verification of chromosomal gene disruptions, the yeast colony-PCR method was applied. Cells from a single yeast colony were resuspended in 40 µl 20 mM NaOH, to which a small amount of glass beads (ø 425-600 nm, Sigma) was added and shaken in a thermomixer at 100 °C at maximum speed for 5 min. After brief centrifugation 4 µl of the supernatant was used as a template DNA for the PCR reaction carried out in a 50 µl volume. For amplification PCRs a Mastercycler (Eppendorf) was used.

The reaction profile (e.g. annealing temperature or elongation time) was adjusted according to the quantity and quality of the template DNA, the length and G/C content of the oligonucleotides and the length of the amplified sequence. In general, the following program was used:

initial denaturation	94 °C	3	min
	94 °C	45	s
30 amplification cycles	50 °C	45	s
	72 °C	2	min
	72 °C	10	min
cooling	4 °C		

Site-directed mutagenesis

To introduce point mutations or deletions in DNA sequences, a PCR-based strategy was developed according to the Quikchange method (Stratagene). This method uses two complementary oligonucleotide primers with the codon to be mutated in the middle flanked by at least 15 additional base pairs, each corresponding to the target sequence. The reaction was performed in a volume of 50 µl and prepared as follows:

50 ng plasmid DNA		
10x *Pfu* Buffer (Stratagene)	5	µl
10 mM dNTPs mix	1.25	µl
10 µM forward primer	1.25	µl
10 µM reverse primer	1.25	µl
Pfu Turbo DNA polymerase (Stratagene)	1	µl
sterile de-ionized water	to 50	µl

Cycling parameters:

initial denaturation	95 °C	30	s
	95 °C	30	s
18 amplification cycles	55 °C	60	s
	68 °C	2	min / kb of plasmid
cooling	4 °C		

In the PCR, both strands of the plasmid with the desired mutation are fully amplified. To eliminate the template DNA, the reaction was digested with *Dpn*I at 37 °C for 1.5 h. This restriction enzyme cleaves specifically methylated template DNA. After dialysis, the PCR product can be directly used for transformation. The mutagenesis was verified by DNA sequencing.

Fusion of DNA fragments by PCR

For direct fusion of DNA fragments, a two-step PCR method was used. The first step involves two conventional PCR reactions, in which oligonucleotide primers are partially complementary at their 5' ends to the adjacent fragments that are fused to create the chimeric product. The second PCR step leads to the fusion of the PCR fragments generated in the first step and their amplification using the complementary sites and flanking primers. The final PCR product is a direct fusion of two fragments of DNA without introducing any additional sequences (e.g. restriction enzymes sites). For these reactions the highly accurate and processive Phusion DNA polymerase (New England Biolabs) was used.

4.5.4. Protein analysis

SDS polyacrylamide gel electrophoresis (SDS-PAGE)

For separation of proteins, SDS-PAGE was preformed in Mighty Small or Tall electrophoresis chambers (Hoefer) using 4-12% gradient Bis-Tris polyacrylamide gels (Invitrogen or self-poured; see below). These gels allow good resolution of proteins over a large range of different molecular weights (10-200 kDa) and do not require stacking gels. Electrophoresis was carried out at a constant voltage of 100 V in the MOPS running buffer. Protein samples were prepared in Laemmli or HU sample buffer by boiling for 10 min at 95 °C or 65 °C, respectively. For denaturation of the ^{6myc}Hmg2^{HA} protein (in Figure 2-8) which possess a large TM domain, denaturation of samples was performed by incubation at 37 °C for 15 min, to avoid formation of high molecular weight aggregates. Finally, gels were removed from the electrophoresis chamber and the separated proteins were transferred to PVDF membranes (see below). Alternatively, gels were incubated for 30 min in the Coomassie brilliant blue solution, which stains non-specifically virtually all proteins. To remove the non-bound day, gels were destained for 12 h in destaining solution and photographed.

Solutions for pouring 4-12% Bis-Tris SDS-PAGE gradient gels:

	4% solution	12% solution
30% acrylamide/0.8% bis-acrylamide (ProtoGel; National diagnostics)	5.9 ml	17.8 ml
2.5 M Bis-Tris-HCl pH 7.5	6.5 ml	6.5 ml
65% (w/v) sucrose	-	3.4 ml
10% (w/v) SDS	225 µl	225 µl
10% (w/v) ammonium peroxidisulphate	225 µl	225 µl
TEMED (Sigma)	45 µl	22.5 µl
H_2O	32.1 ml	17 ml

HU sample buffer:	200	mM	Tris, pH 6.8
	8	M	urea
	5%	(w/v)	SDS
	1	mM	EDTA
	1.5%	(w/v)	DTT
	0.1%	(w/v)	bromophenol blue
Laemmli sample buffer:	2%	(w/v)	SDS
	20%	(v/v)	glycerol
	100	mM	Tris base
	60	mM	EDTA
	0.1%	(w/v)	bromophenol blue
MOPS running buffer:	50	mM	MOPS
	50	mM	Tris base
	3.5	mM	SDS
	1	mM	EDTA
Coomassie brilliant blue solution:	20%	(v/v)	methanol
	10%	(v/v)	acetic acid
	0.1%	(w/v)	Coomassie Brilliant Blue R-250

Destaining solution	20%	(v/v)	methanol
	10%	(v/v)	acetic acid

Immunoblotting

Western blotting enables for specific detection of proteins separated according to their sizes by the SDS-PAGE technique (see above). Proteins were transferred by electrophoresis form the polyacrylamide gel to a PVDF membrane (Immobilon-P, Millipore) in Mini Transfer Tank (Hoefer) in the blotting buffer at a constant voltage of 80 V for 1.5 h at 4 °C. The PVDF membrane was blocked with 5% (w/v) skim milk powder (Fluka) solution in TBST for 1 h. After addition of the primary antibody, blots were incubated for 1 h at RT or overnight at 4 °C. Subsequently, the membrane was washed 3 times for 5 min in TBST and incubated for 1 h with the solution of secondary antibody coupled to horseradish peroxidase (Dianova) dissolved in 1:5000 ratio in 5% milk in TBST. The blot was washed 5 times in TBST and detection was carried out with the chemiluminescence kit (ECL or ECL plus, Amersham) followed by exposure to ECL hyperfilm (Amersham) or to a CCD (charged-coupled device) camera (LAS 3000, Fujifilm). Digitalized images acquired by a CCD camera were quantified with the software program Image Gauge V4.1 (Fujifilm).

Blotting buffer:	250	mM	Tris base
	1.92	M	glycine
	0.1%	(w/v)	SDS
	20%	(v/v)	methanol
TBST:	25	mM	Tris-HCl, pH 7.5
	137	mM	NaCl
	2.6	mM	KCl
	0.1%	(v/v)	Tween 20

References

Amerik, A. Y., and Hochstrasser, M. (2004). Mechanism and function of deubiquitinating enzymes. Biochim Biophys Acta *1695*, 189-207.

Amir, R. E., Haecker, H., Karin, M., and Ciechanover, A. (2004). Mechanism of processing of the NF-kappa B2 p100 precursor: identification of the specific polyubiquitin chain-anchoring lysine residue and analysis of the role of NEDD8-modification on the SCF(beta-TrCP) ubiquitin ligase. Oncogene *23*, 2540-2547.

Auld, K. L., Brown, C. R., Casolari, J. M., Komili, S., and Silver, P. A. (2006). Genomic association of the proteasome demonstrates overlapping gene regulatory activity with transcription factor substrates. Mol Cell *21*, 861-871.

Ausubel, F. M., Brent, R., Kingston, R. E., Moore, D. D., Seidman, J. G., Smith, J. A., and Struhl, K. (1987). Current Protocols in Molecular Biology, Greene Publishing Associates and Wiley-Interscience, New York).

Baboshina, O. V., and Haas, A. L. (1996). Novel multiubiquitin chain linkages catalyzed by the conjugating enzymes E2EPF and RAD6 are recognized by 26 S proteasome subunit 5. J Biol Chem *271*, 2823-2831.

Bachmair, A., Finley, D., and Varshavsky, A. (1986). In vivo half-life of a protein is a function of its amino-terminal residue. Science *234*, 179-186.

Bachmair, A., and Varshavsky, A. (1989). The degradation signal in a short-lived protein. Cell *56*, 1019-1032.

Bajorek, M., and Glickman, M. H. (2004). Keepers at the final gates: regulatory complexes and gating of the proteasome channel. Cell Mol Life Sci *61*, 1579-1588.

Baldwin, A. S., Jr. (1996). The NF-kappa B and I kappa B proteins: new discoveries and insights. Annu Rev Immunol *14*, 649-683.

Baumeister, W., Walz, J., Zuhl, F., and Seemuller, E. (1998). The proteasome: paradigm of a self-compartmentalizing protease. Cell *92*, 367-380.

Bays, N. W., Wilhovsky, S. K., Goradia, A., Hodgkiss-Harlow, K., and Hampton, R. Y. (2001). HRD4/NPL4 is required for the proteasomal processing of ubiquitinated ER proteins. Mol Biol Cell *12*, 4114-4128.

Borden, K. L. (2000). RING domains: master builders of molecular scaffolds? J Mol Biol *295*, 1103-1112.

Braun, B. C., Glickman, M., Kraft, R., Dahlmann, B., Kloetzel, P. M., Finley, D., and Schmidt, M. (1999). The base of the proteasome regulatory particle exhibits chaperone-like activity. Nat Cell Biol *1*, 221-226.

Braun, S., Matuschewski, K., Rape, M., Thoms, S., and Jentsch, S. (2002). Role of the ubiquitin-selective CDC48(UFD1/NPL4)chaperone (segregase) in ERAD of OLE1 and other substrates. Embo J *21*, 615-621.

Brown, M. S., Ye, J., Rawson, R. B., and Goldstein, J. L. (2000). Regulated intramembrane proteolysis: a control mechanism conserved from bacteria to humans. Cell *100*, 391-398.

Burton, J. L., and Solomon, M. J. (2000). Hsl1p, a Swe1p inhibitor, is degraded via the anaphase-promoting complex. Mol Cell Biol *20*, 4614-4625.

Carvalho, P., Goder, V., and Rapoport, T. A. (2006). Distinct ubiquitin-ligase complexes define convergent pathways for the degradation of ER proteins. Cell *126*, 361-373.

Chang, A., Cheang, S., Espanel, X., and Sudol, M. (2000). Rsp5 WW domains interact directly with the carboxyl-terminal domain of RNA polymerase II. J Biol Chem *275*, 20562-20571.

Chang, H. Y., and Yang, X. (2000). Proteases for cell suicide: functions and regulation of caspases. Microbiol Mol Biol Rev *64*, 821-846.

Chellappa, R., Kandasamy, P., Oh, C. S., Jiang, Y., Vemula, M., and Martin, C. E. (2001). The membrane proteins, Spt23p and Mga2p, play distinct roles in the activation of Saccharomyces cerevisiae OLE1 gene expression. Fatty acid-mediated regulation of Mga2p activity is independent of its proteolytic processing into a soluble transcription activator. J Biol Chem *276*, 43548-43556.

Choi, J. Y., Stukey, J., Hwang, S. Y., and Martin, C. E. (1996). Regulatory elements that control transcription activation and unsaturated fatty acid-mediated repression of the Saccharomyces cerevisiae OLE1 gene. J Biol Chem *271*, 3581-3589.

Ciechanover, A., Gonen, H., Bercovich, B., Cohen, S., Fajerman, I., Israel, A., Mercurio, F., Kahana, C., Schwartz, A. L., Iwai, K., and Orian, A. (2001). Mechanisms of ubiquitin-mediated, limited processing of the NF-kappaB1 precursor protein p105. Biochimie *83*, 341-349.

Cohen, S., Orian, A., and Ciechanover, A. (2001). Processing of p105 is inhibited by docking of p50 active subunits to the ankyrin repeat domain, and inhibition is alleviated by signaling via the carboxyl-terminal phosphorylation/ ubiquitin-ligase binding domain. J Biol Chem *276*, 26769-26776.

Crosas, B., Hanna, J., Kirkpatrick, D. S., Zhang, D. P., Tone, Y., Hathaway, N. A., Buecker, C., Leggett, D. S., Schmidt, M., King, R. W.*, et al.* (2006). Ubiquitin chains are remodeled at the proteasome by opposing ubiquitin ligase and deubiquitinating activities. Cell *127*, 1401-1413.

Denic, V., Quan, E. M., and Weissman, J. S. (2006). A luminal surveillance complex that selects misfolded glycoproteins for ER-associated degradation. Cell *126*, 349-359.

Desterro, J. M., Rodriguez, M. S., and Hay, R. T. (1998). SUMO-1 modification of IkappaBalpha inhibits NF-kappaB activation. Mol Cell *2*, 233-239.

Deveraux, Q., Ustrell, V., Pickart, C., and Rechsteiner, M. (1994). A 26 S protease subunit that binds ubiquitin conjugates. J Biol Chem *269*, 7059-7061.

Dunn, B. M., Goodenow, M. M., Gustchina, A., and Wlodawer, A. (2002). Retroviral proteases. Genome Biol *3*, REVIEWS3006.

Dunn, R., Klos, D. A., Adler, A. S., and Hicke, L. (2004). The C2 domain of the Rsp5 ubiquitin ligase binds membrane phosphoinositides and directs ubiquitination of endosomal cargo. J Cell Biol *165*, 135-144.

Eilers, M., and Schatz, G. (1986). Binding of a specific ligand inhibits import of a purified precursor protein into mitochondria. Nature *322*, 228-232.

Elledge, S. J., and Davis, R. W. (1988). A family of versatile centromeric vectors designed for use in the sectoring-shuffle mutagenesis assay in Saccharomyces cerevisiae. Gene *70*, 303-312.

Elsasser, S., and Finley, D. (2005). Delivery of ubiquitinated substrates to protein-unfolding machines. Nat Cell Biol *7*, 742-749.

Esser, C., Alberti, S., and Hohfeld, J. (2004). Cooperation of molecular chaperones with the ubiquitin/proteasome system. Biochim Biophys Acta *1695*, 171-188.

Fan, C. M., and Maniatis, T. (1991). Generation of p50 subunit of NF-kappa B by processing of p105 through an ATP-dependent pathway. Nature *354*, 395-398.

Finley, D., Ozkaynak, E., and Varshavsky, A. (1987). The yeast polyubiquitin gene is essential for resistance to high temperatures, starvation, and other stresses. Cell *48*, 1035-1046.

Finley, D., Sadis, S., Monia, B. P., Boucher, P., Ecker, D. J., Crooke, S. T., and Chau, V. (1994). Inhibition of proteolysis and cell cycle progression in a multiubiquitination-deficient yeast mutant. Mol Cell Biol *14*, 5501-5509.

Fortini, M. E. (2002). Gamma-secretase-mediated proteolysis in cell-surface-receptor signalling. Nat Rev Mol Cell Biol *3*, 673-684.

Froeschke, M., Basler, M., Groettrup, M., and Dobberstein, B. (2003). Long-lived signal peptide of lymphocytic choriomeningitis virus glycoprotein pGP-C. J Biol Chem *278*, 41914-41920.

Fu, D., Kobayashi, M., and Lin, L. (2004). A p105-based inhibitor broadly represses NF-kappa B activities. J Biol Chem *279*, 12819-12826.

Gauss, R., Jarosch, E., Sommer, T., and Hirsch, C. (2006). A complex of Yos9p and the HRD ligase integrates endoplasmic reticulum quality control into the degradation machinery. Nat Cell Biol *8*, 849-854.

Ghislain, M., Udvardy, A., and Mann, C. (1993). S. cerevisiae 26S protease mutants arrest cell division in G2/metaphase. Nature *366*, 358-362.

Ghosh, G., van Duyne, G., Ghosh, S., and Sigler, P. B. (1995). Structure of NF-kappa B p50 homodimer bound to a kappa B site. Nature *373*, 303-310.

Gietz, R. D., and Sugino, A. (1988). New yeast-Escherichia coli shuttle vectors constructed with in vitro mutagenized yeast genes lacking six-base pair restriction sites. Gene *74*, 527-534.

Glickman, M. H., Rubin, D. M., Coux, O., Wefes, I., Pfeifer, G., Cjeka, Z., Baumeister, W., Fried, V. A., and Finley, D. (1998). A subcomplex of the proteasome regulatory particle required for ubiquitin-conjugate degradation and related to the COP9-signalosome and eIF3. Cell *94*, 615-623.

Groll, M., Bajorek, M., Kohler, A., Moroder, L., Rubin, D. M., Huber, R., Glickman, M. H., and Finley, D. (2000). A gated channel into the proteasome core particle. Nat Struct Biol *7*, 1062-1067.

Groll, M., Ditzel, L., Lowe, J., Stock, D., Bochtler, M., Bartunik, H. D., and Huber, R. (1997). Structure of 20S proteasome from yeast at 2.4 A resolution. Nature *386*, 463-471.

Hampton, R. Y., Gardner, R. G., and Rine, J. (1996). Role of 26S proteasome and HRD genes in the degradation of 3-hydroxy-3-methylglutaryl-CoA reductase, an integral endoplasmic reticulum membrane protein. Mol Biol Cell *7*, 2029-2044.

Hampton, R. Y., and Rine, J. (1994). Regulated degradation of HMG-CoA reductase, an integral membrane protein of the endoplasmic reticulum, in yeast. J Cell Biol *125*, 299-312.

Hanna, J., Hathaway, N. A., Tone, Y., Crosas, B., Elsasser, S., Kirkpatrick, D. S., Leggett, D. S., Gygi, S. P., King, R. W., and Finley, D. (2006). Deubiquitinating enzyme Ubp6 functions noncatalytically to delay proteasomal degradation. Cell *127*, 99-111.

Heinemeyer, W., Simeon, A., Hirsch, H. H., Schiffer, H. H., Teichert, U., and Wolf, D. H. (1991). Lysosomal and non-lysosomal proteolysis in the eukaryotic cell: studies on yeast. Biochem Soc Trans *19*, 724-725.

Hicke, L., Schubert, H. L., and Hill, C. P. (2005). Ubiquitin-binding domains. Nat Rev Mol Cell Biol *6*, 610-621.

Hilioti, Z., Chung, Y. S., Mochizuki, Y., Hardy, C. F., and Cohen-Fix, O. (2001). The anaphase inhibitor Pds1 binds to the APC/C-associated protein Cdc20 in a destruction box-dependent manner. Curr Biol *11*, 1347-1352.

Hochstrasser, M., Johnson, P. R., Arendt, C. S., Amerik, A., Swaminathan, S., Swanson, R., Li, S. J., Laney, J., Pals-Rylaarsdam, R., Nowak, J., and Connerly, P. L. (1999). The Saccharomyces cerevisiae ubiquitin-proteasome system. Philos Trans R Soc Lond B Biol Sci *354*, 1513-1522.

Hoege, C., Pfander, B., Moldovan, G. L., Pyrowolakis, G., and Jentsch, S. (2002). RAD6-dependent DNA repair is linked to modification of PCNA by ubiquitin and SUMO. Nature *419*, 135-141.

Hoppe, T., Matuschewski, K., Rape, M., Schlenker, S., Ulrich, H. D., and Jentsch, S. (2000). Activation of a membrane-bound transcription factor by regulated ubiquitin/proteasome-dependent processing. Cell *102*, 577-586.

Hoppe, T., Rape, M., and Jentsch, S. (2001). Membrane-bound transcription factors: regulated release by RIP or RUP. Curr Opin Cell Biol *13*, 344-348.

Huang, D. B., Huxford, T., Chen, Y. Q., and Ghosh, G. (1997). The role of DNA in the mechanism of NFkappaB dimer formation: crystal structures of the dimerization domains of the p50 and p65 subunits. Structure *5*, 1427-1436.

Huibregtse, J. M., Scheffner, M., Beaudenon, S., and Howley, P. M. (1995). A family of proteins structurally and functionally related to the E6-AP ubiquitin-protein ligase. Proc Natl Acad Sci U S A *92*, 2563-2567.

Huibregtse, J. M., Yang, J. C., and Beaudenon, S. L. (1997). The large subunit of RNA polymerase II is a substrate of the Rsp5 ubiquitin-protein ligase. Proc Natl Acad Sci U S A *94*, 3656-3661.

Huxford, T., Huang, D. B., Malek, S., and Ghosh, G. (1998). The crystal structure of the IkappaBalpha/NF-kappaB complex reveals mechanisms of NF-kappaB inactivation. Cell *95*, 759-770.

Ismail, N., and Ng, D. T. (2006). Have you HRD? Understanding ERAD is DOAble! Cell *126*, 237-239.

Jacobs, M. D., and Harrison, S. C. (1998). Structure of an IkappaBalpha/NF-kappaB complex. Cell *95*, 749-758.

James, P., Halladay, J., and Craig, E. A. (1996). Genomic libraries and a host strain designed for highly efficient two-hybrid selection in yeast. Genetics *144*, 1425-1436.

Jarosch, E., Taxis, C., Volkwein, C., Bordallo, J., Finley, D., Wolf, D. H., and Sommer, T. (2002). Protein dislocation from the ER requires polyubiquitination and the AAA-ATPase Cdc48. Nat Cell Biol *4*, 134-139.

Jentsch, S., and Rumpf, S. (2007). Cdc48 (p97): a 'molecular gearbox' in the ubiquitin pathway? Trends Biochem Sci *32*, 6-11.

Jiang, J., and Struhl, G. (1998). Regulation of the Hedgehog and Wingless signalling pathways by the F-box/WD40-repeat protein Slimb. Nature *391*, 493-496.

Jiang, Y., Vasconcelles, M. J., Wretzel, S., Light, A., Gilooly, L., McDaid, K., Oh, C. S., Martin, C. E., and Goldberg, M. A. (2002). Mga2p processing by hypoxia and unsaturated fatty acids in Saccharomyces cerevisiae: impact on LORE-dependent gene expression. Eukaryot Cell *1*, 481-490.

Jiang, Y., Vasconcelles, M. J., Wretzel, S., Light, A., Martin, C. E., and Goldberg, M. A. (2001). MGA2 is involved in the low-oxygen response element-dependent hypoxic induction of genes in Saccharomyces cerevisiae. Mol Cell Biol *21*, 6161-6169.

Johnson, E. S., Ma, P. C., Ota, I. M., and Varshavsky, A. (1995). A proteolytic pathway that recognizes ubiquitin as a degradation signal. J Biol Chem *270*, 17442-17456.

Johnson, P. R., Swanson, R., Rakhilina, L., and Hochstrasser, M. (1998). Degradation signal masking by heterodimerization of MATalpha2 and MATa1 blocks their mutual destruction by the ubiquitin-proteasome pathway. Cell *94*, 217-227.

Johnston, J. A., Johnson, E. S., Waller, P. R., and Varshavsky, A. (1995). Methotrexate inhibits proteolysis of dihydrofolate reductase by the N-end rule pathway. J Biol Chem *270*, 8172-8178.

Kanayama, A., Seth, R. B., Sun, L., Ea, C. K., Hong, M., Shaito, A., Chiu, Y. H., Deng, L., and Chen, Z. J. (2004). TAB2 and TAB3 activate the NF-kappaB pathway through binding to polyubiquitin chains. Mol Cell *15*, 535-548.

Kee, Y., Lyon, N., and Huibregtse, J. M. (2005). The Rsp5 ubiquitin ligase is coupled to and antagonized by the Ubp2 deubiquitinating enzyme. Embo J *24*, 2414-2424.

Kee, Y., Munoz, W., Lyon, N., and Huibregtse, J. M. (2006). The Ubp2 deubiquitinating enzyme modulates Rsp5-dependent K63-linked polyubiquitin conjugates in Saccharomyces cerevisiae. J Biol Chem.

Kenniston, J. A., Baker, T. A., and Sauer, R. T. (2005). Partitioning between unfolding and release of native domains during ClpXP degradation determines substrate selectivity and partial processing. Proc Natl Acad Sci U S A *102*, 1390-1395.

Kisselev, A. F., Kaganovich, D., and Goldberg, A. L. (2002). Binding of hydrophobic peptides to several non-catalytic sites promotes peptide hydrolysis by all active sites of 20 S proteasomes. Evidence for peptide-induced channel opening in the alpha-rings. J Biol Chem *277*, 22260-22270.

Kloetzel, P. M. (2004). The proteasome and MHC class I antigen processing. Biochim Biophys Acta *1695*, 225-233.

Knop, M., Siegers, K., Pereira, G., Zachariae, W., Winsor, B., Nasmyth, K., and Schiebel, E. (1999). Epitope tagging of yeast genes using a PCR-based strategy: more tags and improved practical routines. Yeast *15*, 963-972.

Koegl, M., Hoppe, T., Schlenker, S., Ulrich, H. D., Mayer, T. U., and Jentsch, S. (1999). A novel ubiquitination factor, E4, is involved in multiubiquitin chain assembly. Cell *96*, 635-644.

Kohler, A., Cascio, P., Leggett, D. S., Woo, K. M., Goldberg, A. L., and Finley, D. (2001). The axial channel of the proteasome core particle is gated by the Rpt2 ATPase and controls both substrate entry and product release. Mol Cell *7*, 1143-1152.

Lam, Y. A., Lawson, T. G., Velayutham, M., Zweier, J. L., and Pickart, C. M. (2002). A proteasomal ATPase subunit recognizes the polyubiquitin degradation signal. Nature *416*, 763-767.

Lederkremer, G. Z., and Glickman, M. H. (2005). A window of opportunity: timing protein degradation by trimming of sugars and ubiquitins. Trends Biochem Sci *30*, 297-303.

Lee, C., Prakash, S., and Matouschek, A. (2002). Concurrent translocation of multiple polypeptide chains through the proteasomal degradation channel. J Biol Chem *277*, 34760-34765.

Lee, C., Schwartz, M. P., Prakash, S., Iwakura, M., and Matouschek, A. (2001). ATP-dependent proteases degrade their substrates by processively unraveling them from the degradation signal. Mol Cell *7*, 627-637.

Letunic, I., Copley, R. R., Pils, B., Pinkert, S., Schultz, J., and Bork, P. (2006). SMART 5: domains in the context of genomes and networks. Nucleic Acids Res *34*, D257-260.

Li, X., and Coffino, P. (1992). Regulated degradation of ornithine decarboxylase requires interaction with the polyamine-inducible protein antizyme. Mol Cell Biol *12*, 3556-3562.

Lin, L., DeMartino, G. N., and Greene, W. C. (1998). Cotranslational biogenesis of NF-kappaB p50 by the 26S proteasome. Cell *92*, 819-828.

Lin, L., DeMartino, G. N., and Greene, W. C. (2000). Cotranslational dimerization of the Rel homology domain of NF-kappaB1 generates p50-p105 heterodimers and is required for effective p50 production. Embo J *19*, 4712-4722.

Lin, L., and Ghosh, S. (1996). A glycine-rich region in NF-kappaB p105 functions as a processing signal for the generation of the p50 subunit. Mol Cell Biol *16*, 2248-2254.

Lin, L., and Kobayashi, M. (2003). Stability of the Rel homology domain is critical for generation of NF-kappa B p50 subunit. J Biol Chem *278*, 31479-31485.

Liu, C. W., Corboy, M. J., DeMartino, G. N., and Thomas, P. J. (2003). Endoproteolytic activity of the proteasome. Science *299*, 408-411.

Longtine, M. S., McKenzie, A., 3rd, Demarini, D. J., Shah, N. G., Wach, A., Brachat, A., Philippsen, P., and Pringle, J. R. (1998). Additional modules for versatile and economical PCR-based gene deletion and modification in Saccharomyces cerevisiae. Yeast *14*, 953-961.

Marsh, L., Neiman, A. M., and Herskowitz, I. (1991). Signal transduction during pheromone response in yeast. Annu Rev Cell Biol *7*, 699-728.

Martoglio, B., and Dobberstein, B. (1998). Signal sequences: more than just greasy peptides. Trends Cell Biol *8*, 410-415.

Mayer, T. U., Braun, T., and Jentsch, S. (1998). Role of the proteasome in membrane extraction of a short-lived ER-transmembrane protein. Embo J *17*, 3251-3257.

McConnell, S. J., Stewart, L. C., Talin, A., and Yaffe, M. P. (1990). Temperature-sensitive yeast mutants defective in mitochondrial inheritance. J Cell Biol *111*, 967-976.

McGrath, J. P., Jentsch, S., and Varshavsky, A. (1991). UBA 1: an essential yeast gene encoding ubiquitin-activating enzyme. Embo J *10*, 227-236.

Moorthy, A. K., and Ghosh, G. (2003). p105.Ikappa Bgamma and prototypical Ikappa Bs use a similar mechanism to bind but a different mechanism to regulate the subcellular localization of NF-kappa B. J Biol Chem *278*, 556-566.

Moorthy, A. K., Savinova, O. V., Ho, J. Q., Wang, V. Y., Vu, D., and Ghosh, G. (2006). The 20S proteasome processes NF-kappaB1 p105 into p50 in a translation-independent manner. Embo J *25*, 1945-1956.

Morris, J. R., and Solomon, E. (2004). BRCA1 : BARD1 induces the formation of conjugated ubiquitin structures, dependent on K6 of ubiquitin, in cells during DNA replication and repair. Hum Mol Genet *13*, 807-817.

Mosavi, L. K., Cammett, T. J., Desrosiers, D. C., and Peng, Z. Y. (2004). The ankyrin repeat as molecular architecture for protein recognition. Protein Sci *13*, 1435-1448.

Mosavi, L. K., Minor, D. L., Jr., and Peng, Z. Y. (2002). Consensus-derived structural determinants of the ankyrin repeat motif. Proc Natl Acad Sci U S A *99*, 16029-16034.

Muller, C. W., Rey, F. A., Sodeoka, M., Verdine, G. L., and Harrison, S. C. (1995). Structure of the NF-kappa B p50 homodimer bound to DNA. Nature *373*, 311-317.

Murakami, Y., Matsufuji, S., Kameji, T., Hayashi, S., Igarashi, K., Tamura, T., Tanaka, K., and Ichihara, A. (1992). Ornithine decarboxylase is degraded by the 26S proteasome without ubiquitination. Nature *360*, 597-599.

Muratani, M., and Tansey, W. P. (2003). How the ubiquitin-proteasome system controls transcription. Nat Rev Mol Cell Biol *4*, 192-201.

Neurath, H. (1989). Proteolytic processing and physiological regulation. Trends Biochem Sci *14*, 268-271.

Niedenthal, R. K., Riles, L., Johnston, M., and Hegemann, J. H. (1996). Green fluorescent protein as a marker for gene expression and subcellular localization in budding yeast. Yeast *12*, 773-786.

Nishikawa, H., Ooka, S., Sato, K., Arima, K., Okamoto, J., Klevit, R. E., Fukuda, M., and Ohta, T. (2004). Mass spectrometric and mutational analyses reveal Lys-6-linked polyubiquitin chains catalyzed by BRCA1-BARD1 ubiquitin ligase. J Biol Chem *279*, 3916-3924.

Orian, A., Gonen, H., Bercovich, B., Fajerman, I., Eytan, E., Israel, A., Mercurio, F., Iwai, K., Schwartz, A. L., and Ciechanover, A. (2000). SCF(beta)(-TrCP) ubiquitin ligase-mediated processing of NF-kappaB p105 requires phosphorylation of its C-terminus by IkappaB kinase. Embo J *19*, 2580-2591.

Orian, A., Schwartz, A. L., Israel, A., Whiteside, S., Kahana, C., and Ciechanover, A. (1999). Structural motifs involved in ubiquitin-mediated processing of the NF-kappaB precursor p105: roles of the glycine-rich region and a downstream ubiquitination domain. Mol Cell Biol *19*, 3664-3673.

Palombella, V. J., Rando, O. J., Goldberg, A. L., and Maniatis, T. (1994). The ubiquitin-proteasome pathway is required for processing the NF-kappa B1 precursor protein and the activation of NF-kappa B. Cell *78*, 773-785.

Pan, Y., Bai, C. B., Joyner, A. L., and Wang, B. (2006). Sonic hedgehog signaling regulates Gli2 transcriptional activity by suppressing its processing and degradation. Mol Cell Biol *26*, 3365-3377.

Peters, J. M. (2006). The anaphase promoting complex/cyclosome: a machine designed to destroy. Nat Rev Mol Cell Biol *7*, 644-656.

Petroski, M. D., and Deshaies, R. J. (2003). Context of multiubiquitin chain attachment influences the rate of Sic1 degradation. Mol Cell *11*, 1435-1444.

Petroski, M. D., and Deshaies, R. J. (2005). Function and regulation of cullin-RING ubiquitin ligases. Nat Rev Mol Cell Biol *6*, 9-20.

Pfleger, C. M., and Kirschner, M. W. (2000). The KEN box: an APC recognition signal distinct from the D box targeted by Cdh1. Genes Dev *14*, 655-665.

Pickart, C. M. (2001). Mechanisms underlying ubiquitination. Annu Rev Biochem *70*, 503-533.

Pickart, C. M., and Cohen, R. E. (2004). Proteasomes and their kin: proteases in the machine age. Nat Rev Mol Cell Biol *5*, 177-187.

Pickart, C. M., and Fushman, D. (2004). Polyubiquitin chains: polymeric protein signals. Curr Opin Chem Biol *8*, 610-616.

Podust, V. N., Brownell, J. E., Gladysheva, T. B., Luo, R. S., Wang, C., Coggins, M. B., Pierce, J. W., Lightcap, E. S., and Chau, V. (2000). A Nedd8 conjugation pathway is essential for proteolytic targeting of p27Kip1 by ubiquitination. Proc Natl Acad Sci U S A *97*, 4579-4584.

Prakash, S., Tian, L., Ratliff, K. S., Lehotzky, R. E., and Matouschek, A. (2004). An unstructured initiation site is required for efficient proteasome-mediated degradation. Nat Struct Mol Biol *11*, 830-837.

Prilusky, J., Felder, C. E., Zeev-Ben-Mordehai, T., Rydberg, E. H., Man, O., Beckmann, J. S., Silman, I., and Sussman, J. L. (2005). FoldIndex: a simple tool to predict whether a given protein sequence is intrinsically unfolded. Bioinformatics *21*, 3435-3438.

Rape, M., Hoppe, T., Gorr, I., Kalocay, M., Richly, H., and Jentsch, S. (2001). Mobilization of processed, membrane-tethered SPT23 transcription factor by CDC48(UFD1/NPL4), a ubiquitin-selective chaperone. Cell *107*, 667-677.

Rape, M., and Jentsch, S. (2002). Taking a bite: proteasomal protein processing. Nat Cell Biol *4*, E113-116.

Rice, N. R., MacKichan, M. L., and Israel, A. (1992). The precursor of NF-kappa B p50 has I kappa B-like functions. Cell *71*, 243-253.

Richly, H., Rape, M., Braun, S., Rumpf, S., Hoege, C., and Jentsch, S. (2005). A series of ubiquitin binding factors connects CDC48/p97 to substrate multiubiquitylation and proteasomal targeting. Cell *120*, 73-84.

Rumpf, S., and Jentsch, S. (2006). Functional division of substrate processing cofactors of the ubiquitin-selective Cdc48 chaperone. Mol Cell *21*, 261-269.

Saeki, Y., Tayama, Y., Toh-e, A., and Yokosawa, H. (2004). Definitive evidence for Ufd2-catalyzed elongation of the ubiquitin chain through Lys48 linkage. Biochem Biophys Res Commun *320*, 840-845.

Sambrook, J., Fritsch, E. F., and Maniatis, T. (1989). Molecular Cloning, Cold Spring Harbor Laboratory Press, NY).

Scheffner, M., Huibregtse, J. M., Vierstra, R. D., and Howley, P. M. (1993). The HPV-16 E6 and E6-AP complex functions as a ubiquitin-protein ligase in the ubiquitination of p53. Cell *75*, 495-505.

Scheffner, M., Nuber, U., and Huibregtse, J. M. (1995). Protein ubiquitination involving an E1-E2-E3 enzyme ubiquitin thioester cascade. Nature *373*, 81-83.

Scherer, D. C., Brockman, J. A., Chen, Z., Maniatis, T., and Ballard, D. W. (1995). Signal-induced degradation of I kappa B alpha requires site-specific ubiquitination. Proc Natl Acad Sci U S A *92*, 11259-11263.

Searle, J. S., Schollaert, K. L., Wilkins, B. J., and Sanchez, Y. (2004). The DNA damage checkpoint and PKA pathways converge on APC substrates and Cdc20 to regulate mitotic progression. Nat Cell Biol *6*, 138-145.

Sears, C., Olesen, J., Rubin, D., Finley, D., and Maniatis, T. (1998). NF-kappa B p105 processing via the ubiquitin-proteasome pathway. J Biol Chem *273*, 1409-1419.

Sedgwick, S. G., and Smerdon, S. J. (1999). The ankyrin repeat: a diversity of interactions on a common structural framework. Trends Biochem Sci *24*, 311-316.

Seufert, W., and Jentsch, S. (1992). In vivo function of the proteasome in the ubiquitin pathway. Embo J *11*, 3077-3080.

Sharipo, A., Imreh, M., Leonchiks, A., Imreh, S., and Masucci, M. G. (1998). A minimal glycine-alanine repeat prevents the interaction of ubiquitinated I kappaB alpha with the proteasome: a new mechanism for selective inhibition of proteolysis. Nat Med *4*, 939-944.

Sharon, M., Witt, S., Felderer, K., Rockel, B., Baumeister, W., and Robinson, C. V. (2006). 20S proteasomes have the potential to keep substrates in store for continual degradation. J Biol Chem *281*, 9569-9575.

Shcherbik, N., and Haines, D. S. (2007). Cdc48p(Npl4p/Ufd1p) Binds and Segregates Membrane-Anchored/Tethered Complexes via a Polyubiquitin Signal Present on the Anchors. Mol Cell *25*, 385-397.

Shcherbik, N., Kee, Y., Lyon, N., Huibregtse, J. M., and Haines, D. S. (2004). A single PXY motif located within the carboxyl terminus of Spt23p and Mga2p mediates a physical and functional interaction with ubiquitin ligase Rsp5p. J Biol Chem *279*, 53892-53898.

Shcherbik, N., Kumar, S., and Haines, D. S. (2002). Substrate proteolysis is inhibited by dominant-negative Nedd4 and Rsp5 mutants harboring alterations in WW domain 1. J Cell Sci *115*, 1041-1048.

Shcherbik, N., Zoladek, T., Nickels, J. T., and Haines, D. S. (2003). Rsp5p is required for ER bound Mga2p120 polyubiquitination and release of the processed/tethered transactivator Mga2p90. Curr Biol *13*, 1227-1233.

Shearer, A. G., and Hampton, R. Y. (2005). Lipid-mediated, reversible misfolding of a sterol-sensing domain protein. Embo J *24*, 149-159.

Spellman, P. T., Sherlock, G., Zhang, M. Q., Iyer, V. R., Anders, K., Eisen, M. B., Brown, P. O., Botstein, D., and Futcher, B. (1998). Comprehensive identification of cell cycle-regulated genes of the yeast Saccharomyces cerevisiae by microarray hybridization. Mol Biol Cell *9*, 3273-3297.

Steiner, D. F. (1998). The proprotein convertases. Curr Opin Chem Biol *2*, 31-39.

Stukey, J. E., McDonough, V. M., and Martin, C. E. (1989). Isolation and characterization of OLE1, a gene affecting fatty acid desaturation from Saccharomyces cerevisiae. J Biol Chem *264*, 16537-16544.

Su, K., Roos, M. D., Yang, X., Han, I., Paterson, A. J., and Kudlow, J. E. (1999). An N-terminal region of Sp1 targets its proteasome-dependent degradation in vitro. J Biol Chem *274*, 15194-15202.

Sun, Z. W., and Allis, C. D. (2002). Ubiquitination of histone H2B regulates H3 methylation and gene silencing in yeast. Nature *418*, 104-108.

Swanson, R., Locher, M., and Hochstrasser, M. (2001). A conserved ubiquitin ligase of the nuclear envelope/endoplasmic reticulum that functions in both ER-associated and Matalpha2 repressor degradation. Genes Dev *15*, 2660-2674.

Thrower, J. S., Hoffman, L., Rechsteiner, M., and Pickart, C. M. (2000). Recognition of the polyubiquitin proteolytic signal. Embo J *19*, 94-102.

Tian, L., Holmgren, R. A., and Matouschek, A. (2005). A conserved processing mechanism regulates the activity of transcription factors Cubitus interruptus and NF-kappaB. Nat Struct Mol Biol *12*, 1045-1053.

Urban, M. B., and Baeuerle, P. A. (1990). The 65-kD subunit of NF-kappa B is a receptor for I kappa B and a modulator of DNA-binding specificity. Genes Dev *4*, 1975-1984.

Welchman, R. L., Gordon, C., and Mayer, R. J. (2005). Ubiquitin and ubiquitin-like proteins as multifunctional signals. Nat Rev Mol Cell Biol *6*, 599-609.

Willems, A. R., Schwab, M., and Tyers, M. (2004). A hitchhiker's guide to the cullin ubiquitin ligases: SCF and its kin. Biochim Biophys Acta *1695*, 133-170.

Wolfe, M. S., and Kopan, R. (2004). Intramembrane proteolysis: theme and variations. Science *305*, 1119-1123.

Yao, T., and Cohen, R. E. (2002). A cryptic protease couples deubiquitination and degradation by the proteasome. Nature *419*, 403-407.

Zhang, S., Burkett, T. J., Yamashita, I., and Garfinkel, D. J. (1997). Genetic redundancy between SPT23 and MGA2: regulators of Ty-induced mutations and Ty1 transcription in Saccharomyces cerevisiae. Mol Cell Biol *17*, 4718-4729.

Zhang, S., Skalsky, Y., and Garfinkel, D. J. (1999). MGA2 or SPT23 is required for transcription of the delta9 fatty acid desaturase gene, OLE1, and nuclear membrane integrity in Saccharomyces cerevisiae. Genetics *151*, 473-483.

Zheng, N., Wang, P., Jeffrey, P. D., and Pavletich, N. P. (2000). Structure of a c-Cbl-UbcH7 complex: RING domain function in ubiquitin-protein ligases. Cell *102*, 533-539.

Abbreviations

μ	micro (x10-6)
2*μ*	multi-copy vectors
3-AT	3-aminotriazole
AAA	ATPases associated with various cellular activities
AD	Gal4 activation domain
ANK	ankyrin repeat domain
APC/C	anaphase promoting complex/cyclosome
ARS	autonomous replicating sequence
ATP	adenosine 5-triphosphate
BD	Gal4 DNA binding domain
bp	base pairs
BSA	bovine serum albumin
CCD	camera charged-coupled device camera
cDNA	complimentary DNA
CEN	centromeric (low copy vectors)
CHX	cycloheximide
C-terminal	carboxyl-terminal
C-terminus	carboxyl terminus
CUE	coupling of ubiquitin conjugation to endoplasmic reticulum degradation
DAPI	4',6-diamidino-2-phenylindole
DMF	N,N-dimethylformamide
DMSO	dimethylsulfoxide
DNA	deoxyribonucleic acid
dNTP	deoxy nucleoside triphosphate
DTT	dithiothreitol
DUB	deubiquitylating
E1	ubiquitin activation enzyme
E2	ubiquitin conjugation enzyme
E3	ubiquitin ligase
E4	polyubiquitylation factor
EDTA	ethylenediaminetetraacidic acid
ER	endoplasmic reticulum
ERAD	ER-associated degradation
F	farad
g	gram
g	gravitational constant (6.6742×10^{-11} N m^2 kg^{-2})
Gal	galactosidase
GRR	glycine-rich region
h	hours
HECT	homologous to E6AP C-terminus
Ig	immunoglobulin
IP	immunoprecipitation
IPT	immunoglobulin-like/plexins/transcription factors
k	kilo ($x10^3$)
kan	kanamycine
kb	kilo base pairs

kDa	kilo dalton
LB	Luria-Bertani
M	molar
m	milli ($x10^{-3}$)
MAT	mating type
MHC	major histocompatibility complex
min	minutes
MOPS	3-N-Morpholinopropane sulfonic acid
mRNA	messenger RNA
MTX	methotrexate
MW	molecular weight
n	nano ($x10^{-9}$)
NEM	N-ethylmaleimide ADP adenosine 5-diphosphate
N-terminal	amino-terminal
N-terminus	amino terminus
OD	optical density
ORF	open reading frame
PAGE	polyacrylamide gel electrophoresis
PBS	phosphate-buffered saline
PCNA	proliferating cell nuclear antigen
PCR	polymerase chain reaction
PEG	polyethylene glycol
PMSF	phenylmethylsulphonyl fluoride
PVDF	polyvinylidene fluoride
RING	really interesting new gene
RIP	regulated intramembrane proteolysis
RNA	ribonucleic acid
rpm	rounds per minute
RT	room temperature
RUP	ubiquitin/proteasome-dependent processing
s	seconds
S	sedimentation coefficient (Svedberg)
SC	synthetic complete medium
SCF	Skp1-Cul1-F-box complex
SDS	sodium dodecylsulfate
TAD	transactivation domain
TBE	Tris/borate/EDTA buffer
TBS	Tris-buffered saline
TCA	trichloro acidic acid
TEMED	N,N,N',N'-tetramethylethylenediamin
TM	transmembrane
Tris	Tris(hydroxymethyl)aminomethane
U	unit
Ub	ubiquitin
UBA	ubiquitin associated
UBC	ubiquitin conjugating enzyme
UFA	unsaturated fatty acid
UFD	ubiquitin fusion degradation
UIM	ubiquitin interacting motif
UPS	ubiquitin/proteasome system

UV	ultraviolet light
V	volt
v/v	volume per volume
w/v	weight per volume
WT	wild type
YPD	yeast bactopeptone dextrose medium
Ω	ohm

Acknowledgements

I would like to thank Stefan Jentsch who gave me the opportunity to do my doctoral research in his laboratory. His interest in my research, his continuous support and the scientific freedom he offered me during my studies allowed me to enjoy the time spent in his lab. His scientific expertise and our fruitful discussions were precious source of suggestions and ideas, which put my work on the right track and made this thesis possible.

I would like to acknowledge the members of the thesis committee of the Ludwig Maximilian University for kindly accepting to review this work. In particular, I thank Prof. Dr. Peter B. Becker who agreed to be the co-referee of this thesis.

I am grateful to Michael Rape and Sigurd Braun for their help during my first days in the Jentsch lab. I want to thank Alex Buchberger, Boris Pfander, Sebastian Rumpf and Christian Schuberth for useful technical advises and discussions, which helped me to solve many problems encountered during my research. I am grateful to Aleksandra Piwko-Czuchra and Lucian Moldovan for careful reading and correcting this thesis.

Many thanks to all the people of the Jentsch department for constantly offering me help, advices and for the friendly working atmosphere. I am also grateful to all of them for the time spent together outside the institute, lots of fun and activities. I want to thank Sandrine Creton, Michael Schwarz and Zeuzera Pyrina for many helpful discussions not always related to science, for spreading their good mood and for making the lab a funny place. I greatly appreciate the help from Klara Schwander in all kinds of Formulare and organization things, especially at the beginning of my stay in Munich.

I want to thank all my friends from inside and outside the institute for making the “Munich times” good times!

Special thanks go to my parents, brothers and my sister, who all supported me continuously and trusted in me.

Finally, I thank you Ola for so much! Particularly for your care, understanding and patience, and most importantly for making my life so happy.

Curriculum vitae

Name:	Wojciech Piwko
Adresse:	Am Klopferspitz 18 82152 Martinsried
Geburtsdatum:	14. August 1977
Geburtsort:	Kielce, Polen
Nationalität:	Polnisch

Schulbindung

1984 – 1992	Grundschule Nr. 31, Kielce, Polen
1992 – 1996	Hanka Sawicka Allgemeinbildendes Lyzeum Nr. 4, Kielce, Polen

Studium

1997 – 2001	Jagiellonen-Universität Krakau, Polen Studiengang: Biotechnologie Diplomarbeit: “ Spektroskopische Analyse der Interaktion zwischen cAMP und dem CRP-Rezeptorprotein aus *Escherichia coli*“ Institut für Molekulare Biologie, Abteilung für Physikalische Biochemie, (Arbeitsgruppe Prof. Dr. Zygmunt Wasylewski) Abschluss mit Diplom in Biotechnologie im Juni 2001

Doktorarbeit

Seit Dezember 2001	Max-Planck-Institut für Biochemie, Martinsried Abteilung für Molekulare Zellbiologie (Arbeitsgruppe Prof. Stefan Jentsch)